School of Geography, Archaeology and Environmental Studies
University of the Witwatersrand, Johannesburg

THE SPATIAL DISTRIBUTION OF HAZE OVER THE BOJANALA DISTRICT

Beverley Cindy Barnes
Student Number: 0407219N

Supervisor: Prof. Stuart J. Piketh
Co-Supervisor: Prof. Stefan Grab

A dissertation submitted to the Faculty of Science, University of the Witwatersrand, in fulfilment of the requirements for the degree of Master of Science

Johannesburg,

DECLARATION

I declare that this dissertation is my own unaided work. It is being submitted for the degree of Master of Science in the School of Geography, Archaeology and Environmental Studies at the University of the Witwatersrand, Johannesburg. It has not been submitted previously for any degree or examination in any other university.

_____

(Beverley Barnes)

26th day of June 2015

ABSTRACT

The air quality over the Bojanala District has been identified as an area of concern. The Bojanala Platinum District falls within the Waterberg Priority Area, which was declared as a priority area for air quality in 2012. This study was conducted in the southern part of the Bojanala district to identify the spatial and temporal distribution of aerosols over the district. Aerosol optical thickness and Ångstrom exponent were derived using data retrieved from direct solar radiation measurements using hazemeters during winter 2008, early winter 2009 and late winter 2010. Results of the study reveal that aerosol loadings differ significantly as winter progresses. AOT levels are found to be considerably higher during winter and late winter, compared with the early winter campaign. Diurnal variation during the late winter campaign is found to be very similar to that of the early winter campaign, with little variation in aerosol loadings and characteristics during the day; while the winter 2008 campaign reveals a significant decreasing trend in AOT and Ångstrom exponent as the day progresses. The AOT and Ångstrom exponent levels for the different campaigns, local sources and the diurnal trends identified assist in the attribution of domestic fuel burning practices; and the concentration of pollutants emitted in the area by inversion layers to the characteristics of the aerosol loadings during winter. The high AOT and contribution of fine mode particles during late winter is attributed to the onset of the biomass burning season. The importance of industrial sources to the aerosol loadings is clear during all three campaigns; however, it is clear that aerosols at different levels in the atmosphere have a significant impact on AOT over the district. The vertical distribution of aerosols is explored through the use of trajectories and associated surface wind roses which indicate that foreign airmasses from the Mpumalanga Highveld and the Atlantic Ocean clearly have a significant impact on the aerosol loadings over the Bojanala District and are associated with extremes in AOT levels. Further, spatial analysis reveals that the highest concentrations of aerosols (associated with larger particles) are identified toward the eastern side of the district except during late winter. It is probable that the aerosols in the Bojanala District may have a significant regional climatic impact which requires further investigation.

PREFACE

Understanding the impact of human activities on climate remains a difficult task, with substantial uncertainties. The presence of aerosols in the atmosphere creates considerable concern with regard to their impact on solar radiation, the hydrological cycle and human health. Studies have been carried out across the globe to understand and attempt to ascertain the impact which these particles have on the global climate, as well as regional climates.

For this project research into the atmospheric aerosol loadings over the Bojanala District in the North-West province was conducted. The aims of the project included an investigation into the temporal and spatial properties of aerosols over the district; and secondly, to identify the relative contribution of combustion and non-combustion sources to the aerosol loadings. Volunteers from eight schools in the district assisted in taking solar radiation readings using hazemeters. The Bojanala Platinum District, as its name reveals, is home to some of the largest platinum mines in the world. According to the Bojanala Platinum District Municipality Air Quality Management Plan (BPDM AQMP) the area is under significant pressure from increased mining activities and the associated traffic, human movement and other industrial activities (BPDM AQMP, 2011). The district is also home to many agricultural activities and various industries. Domestic fuel burning adds to the air pollution loading in and around the informal settlements in the area which is exacerbated by poor dispersion potential during winter.

This dissertation is divided into six chapters. **Chapter One** provides a simple introduction to the field of aerosol science and the aims and objectives of this study. **Chapter Two** provides a summary of the literature on aerosols. The chapter comprises information regarding aerosol sources, composition and particle sizes; aerosol climatology and the importance of particle size; the impact of various meteorological conditions on the concentrations of aerosols in South Africa; and finally a brief look into aerosol studies conducted in southern Africa. **Chapter Three** explores the methodology used in the collection of data and the derivation of aerosol optical thickness and the Ångstrom exponent. Further, the chapter describes the Bojanala District and provides a brief understanding of the aerosol sources which are significant in the area. In **Chapter Four** the results of the study are analysed. A temporal analysis of aerosol optical thickness and Ångstrom exponent is presented. Data analysis includes an investigation into the impact of foreign airmasses on the district; as well as a

comparison with traffic and particulate matter concentration data. Further analysis includes a brief description of the aerosol vertical profiles over the nearby town of Rustenburg. **Chapter Five** presents a spatial analysis of the aerosol concentrations in the area as well as an understanding of the meteorological conditions which may have impacted on the aerosol loadings in the area. **Chapter Six** provides the conclusions drawn from this study.

ACKNOWLEDGEMENTS

The author wishes to thank the following people/institutions:

- Firstly the students and educators from the schools who assisted in taking readings are thanked as without their assistance this research would not exist
- Lonmin Platinum for sponsoring the project
- The South African Weather Service for providing meteorological data, as well as for the bursary provided for this MSc
- Paul Beukes and his team from North-West University for the use of their particulate matter data
- Prof. Stuart Piketh (supervisor), for his guidance, wisdom, patience, understanding and wealth of knowledge; and Prof. Stefan Grab (Co-supervisor) for his kindness and willingness to help at all times
- Roelof Burger and Thomas Bigala for their assistance in many aspects of the project
- Dr. Thierry Elias (Centre National de Recherche Meteorologique/Groupe de Me´te´orologie a` Moyenne E ´ chelle, Me´te´oFrance, Toulouse, France) and Dr. David Giles (NASA) for their assistance in the derivation of AOT and Ångstrom exponent.
- Timothy Kriel and Phumudzo Tharaga who have been kind and generous in their assistance with certain aspects of the project
- Michael Weston for his valuable and kind assistance in the creation of the spatial maps
- My husband, Kent Vertue for your unending patience, love and understanding.
- To my father and mother, Eric and Yvonne Barnes for your love and the sacrifices you have made to get me to where I am today. To my sisters, Charlene Mouski and Deirdre Barnes for your support and to my brother, Eric Barnes, I wish you were here.
- To Kirsten Collett and Seneca Naidoo for pushing me and believing in me.
- To my loving father God, to Jesus Christ for all you are to me. Forgive me for doubting myself and in doing so, doubting you. You wrote this scripture on my heart so many years ago and you have never failed me:

  "No eye has seen, nor ear heard, nor the heart of man imagined, what God has prepared for those who love him" – 1 Corinthians 2:9;

CONTENTS

LIST OF FIGURES

LIST OF TABLES

ABBREVIATIONS AND ACRONYMS

AE	Ångstrom Exponent
AERONET	Aerosol Robotic Network
AFIS	Advanced Fire Information System
AGL	Above Ground Level
AOT	Aerosol Optical Thickness
AQMP	Air Quality Management Plan
AVHRR	Advanced Very High Resolution Radiometer
BPDM	Bojanala Platinum District Municipality
CCN	Cloud Condensation Nuclei
CoVar	Coefficient of Variance
CRG	Climatology Research Group
DEAT	Department of Environmental Affairs and Tourism
ENSO	El Nino-Southern Oscillation
FSSP	Forward Scattering Spectrometer Probe
GMT	Greenwich Mean Time
HM	Hazemeter
hPa	Hectopascal
HYSPLIT	Hybrid Single-Particle Lagrangian Integrated Trajectory
INDOEX	Indian Ocean Experiment
IPCC	Intergovernmental Panel on Climate Change
Km	Kilometer
LED	Light-emitting Diode

MAGL	Meters Above Ground Level
MISR	Multi-angle Imaging SpectroRadiometer
MODIS	Moderate Resolution Imaging SpectroRadiometer
m/s	meters per second
NASA	National Aeronautics and Space Administration
NIR	Near-Infrared
nm	Nanometer
NOAA	National Ocean and Atmospheric Administration
OTG	Gaseous Optical Thickness
PCASP	Passive Cavity Aerosol Spectromoter Probe
PM1	Particulate Matter Concentrations (<1µm)
PM2.5	Particulate Matter Concentrations (<2.5µm)
PM10	Particulate Matter Concentrations (<10µm)
SAFARI	Southern Africa Fire Atmosphere Research Initiative
SANRAL	South African National Roads Agency Limited
SHARP	Synchronized Hybrid Ambient Real-time Particulate Monitor
TEOM	Tapered Element Oscillating Microbalance
TOMS	Total Ozone Mapping Spectrometer
Vo	Extraterrestrial Voltage
W/m2	Watts per meter squared
µg/m^3	Microgram per meter cubed
µm	Micrometer

CHAPTER 1: INTRODUCTION

A brief background to aerosol science is discussed. The key research objectives are outlined.

1.1. Background

One of the most common and visible impacts of human activities is the brownish haze which can be seen over many industrial regions and regions exposed to heavy biomass burning (Ramanathan, 2001). This haze is a common site on a cold South African winter morning and is an aerosol which is made up of water droplets, various pollutants such as NO_2 and dust (Seinfeld and Pandis, 2006). Our atmosphere is stratified into various layers which have numerous properties. The troposphere, which is one of the least stable of these layers, contains the highest concentration of aerosols (Tesfaye, 2011). Aerosols play a significant role in ambient air quality and the related human health risks; and are important climate forcing agents. It is for this reason that understanding these particles is essential. An aerosol is defined as a suspension of fine, solid or liquid particles in a gas (Seinfeld and Pandis, 2006) and may be classified into two categories according to their origin, namely anthropogenic and natural sources. Human activities such as quarrying and mining, industrial processes, energy consumption, agriculture and transportation result in the injection of anthropogenic aerosols into the atmosphere (Kemp, 1994). Anthropogenic aerosol sources include emissions from fossil fuel and biofuel combustion, industrial processes, agricultural practices, biomass burning and vehicular emissions (Charlson *et al*., 1992; Kaufman *et al.*, 1997). A number of different natural sources of aerosols have been identified which make a significant contribution to aerosol loading, these include: windblown mineral dust, precursor gases from volcanic eruptions, wild fires, vegetation and oceans. These sources are highly unpredictable and their impact on aerosol concentrations may be severe (Tesfaye, 2011).

Aerosols are classified according to the extent to which their properties have changed since emission as primary and secondary aerosols. Primary aerosols are those which have retained their properties from their source. Secondary aerosols such as nitrates, sulphates and organic carbon (Piketh *et al.*, 1996) are primary aerosols which have been transformed by physical and chemical reactions in the atmosphere (Kemp, 1994).

The properties of aerosol are highly dynamic and depend on their atmospheric lifetimes and interactions. It is for this reason that characterising aerosols globally is highly difficult and complex (Levy, 2007). Further complexities arise as aerosols come into contact with one another. Anthropogenic and natural aerosols are not easily distinguishable from one another as individual particles may exist as a mixture of both of different particles (Kaufman *et al.*, 2002). An aerosol may exist as a chemically distinct species such as sulphates, organics, black carbon or dust, however, composite mixtures of a core material (black carbon, dust, sea salt) with a coating of organics, sulphates and nitrates frequently occur (Levy, 2007).

Over the past decade, the science of aerosols has become increasingly more important, particularly with regard to their climate forcing properties. A significant level of uncertainty still exists with regard to the extent to which the concentrations of atmospheric aerosols have increased, and the impact which they have had on solar radiation over the past century (Wang *et al*., 2009).

Remote sensing data requires improvement on spatial and temporal scales in order to reduce the degree of uncertainty inherent in aerosol sciences (Nakajima and Higurashi, 1998; Ignatov *et al.*, 2004). Aerosol properties are currently determined through ground-based and satellite remote-sensing measurements. While ground-based measurements are more accurate, they are limited in spatial coverage (Guoyong *et al*., 1999) Research on atmospheric aerosol properties with regard to their spatial and temporal distributions is crucial to fully ascertain the connections between aerosols and the earth's radiation budget (Wilson, 2011), as well as related forcing mechanisms within the earth-atmosphere system.

Aerosol research in South Africa has been conducted during the various SAFARI campaigns. Continuous monitoring of aerosols takes place as part of the Aerosol Robotic Network (AERONET) programme in South Africa and across the world. Satellites can measure aerosol properties at large spatial scales, but lack the temporal advantages of ground-based instruments. It is for this reason that fully understanding and predicting aerosol properties requires that satellite and ground-based observations work hand-in-hand.

1.2 **Aims and Objectives**

The core objective of this research project is to gain an understanding of the spatial and temporal distribution of aerosols over the Bojanala District in the North-West province of South Africa. The Bojanala District, in which the towns of Rustenburg and Brits are located, is home to some of the largest platinum mines in the world, namely, Anglo Platinum, Impala Platinum and Lonmin Platinum. According to the Rustenburg Air Quality Management Plan, the air quality in the Rustenburg area represents an area of concern (AQMP, 2005). The area has now been declared an air quality priority area. The problem with regard to air pollution concentrations in the area is compounded by the impact of intense valley inversions which trap pollutants and form as a direct result of the local topography and overlying meteorology. Aerosols in the district are emitted from sources such as mining and industrial activities, agricultural practices, domestic fuel burning and motor vehicles. This project aims to investigate the spatial and temporal distribution of the tropospheric aerosol burden over a portion of the Bojanala District, situated in north-eastern corner of the North-West Province. In order to achieve the aforementioned, aerosol optical thickness and Ångstrom exponent are retrieved using signals measured by handheld sun photometers (hazemeters).

Hazemeters were placed at schools within the district as part of a hazemeter network. This research will give the first comprehensive look at aerosol loading in an integrated manner over the area. The purpose of this project is to assess the distribution and nature of atmospheric aerosols over the Bojanala District during the winter periods of 2008, 2009 and 2010; with the following specific objectives:

1. Establish the spatial and temporal distribution of the tropospheric aerosol burden over the Bojanla Distict in the North-West Province of South Africa
2. Establish whether the optical properties of the aerosols over the region may be used to quantify the relative importance of combustion and non-combustion sources to the aerosol loading.

In order to achieve these objectives, aerosol optical thickness and Ångstrom exponent are retrieved using data collected from the hazemeters.

An added benefit of the project is that students from eight schools involved in the project were introduced to scientific investigation within the atmospheric sciences field. Students were asked to take readings with the hazemeters, thus gaining hands-on experience in measurements and a practical understanding of their physical science and geography curriculums.

****

With the background to aerosol science, as well as the aims and objectives of this study presented above, the aerosol literature is examined in the following chapter. The importance of aerosols is outlined with regard to their impacts on radiative forcing. Further, aerosol studies in southern Africa are reviewed.

CHAPTER 2: LITERATURE REVIEW

This chapter outlines the importance and complexity inherent in aerosols and gives a basic understanding of aerosol radiative forcing. Aerosol research in southern Africa is explored.

2.1. Aerosols – A background

The vertical profile of aerosols is significantly complex (Sullivan *et al*., 2015). Two dominant layers of aerosols are common, one near the earth's surface (0-3km) and a stratospheric layer at approximately 15-25km. The concentrations of particles are found to decrease with altitude as particles fall out due to gravity or precipitation scavenging. It is for this reason that aerosol residence times in the troposphere are generally low, however, within the stratosphere residence times may be up to seven years as a result of the stability of this atmospheric layer (Power, 2003). The concentrations of aerosols have increased over all continental regions except over Europe from 1979 to 2006 (Wang *et al.*, 2009). Aerosols are constantly monitored as they may impose serious health risks for human beings and animals, plants etc. These particles, however, are extremely important to the hydrological cycle and may counteract the warming resulting from greenhouse gases. Unfortunately, aerosols present major uncertainties when considering the impact of these particles on climate (Kahn, 2011; IPCC, 2014). Aerosols are removed from the atmosphere by wet deposition (cloud and precipitation scavenging) (Yum and Hudson, 2001), or through dry deposition (gravitational processes), which decreases the atmospheric lifetime of aerosols (Seinfeld and Pandis, 2006). Studies have found that wet deposition effectively cleanses the atmosphere (Croft *et al.*, 2009). The amount of time which aerosols spend in residence in the atmosphere depends on various removal processes and on the size of the aerosol particles.

2.2. Aerosol Particle Sizes and Atmospheric Lifetimes

One of the most important properties of aerosols, particularly with regard to their impact on solar radiation, is their aerodynamic diameter. Aerosol size distribution is largely a factor of primary and secondary production mechanisms, as well as aerosol removal processes (Power, 2003). Aerosols can be divided into two groups based on their size, namely, fine and coarse mode aerosols. Fine mode aerosols may be related to combustion processes, whereas coarse mode aerosols originate from non-combustion processes. There are exceptions to this rule, however, where natural aeolian desert dust particles are fine and fossil fuel combustion

particles are coarse (Eck *et al.*, 2005). Natural aerosols are produced through processes such as the wave actions of oceans or wind erosion in deserts.

2.2.1. Aerosol Atmospheric Lifetimes

The size of the atmospheric particles has a direct impact on the lifetime of that aerosol in the troposphere and, as a result, aerosol concentrations are highly variable (Annegarn *et al.*, 1983, 1993; Garstang *et al*., 1996a). The stability of the atmosphere in which the particles reside is also a significant factor to consider in this regard (Piketh *et al*., 1996). Large particles fall close to their sources as a result of gravity, while smaller particles will remain in the atmosphere for greater amounts of time (Kemp, 2004). The residence times of particles <2.5μm is approximately 7 days, while particles between 2.5 and 10μm will remain in the atmosphere for approximately 4 days. Very coarse particles, >20μm, will fall out within minutes to hours (Piketh, 1996). The fine-mode classification is then further sub-divided (as indicated in the figure) into Aitken Mode, accumulation mode and nucleation mode particles. Aitken nuclei are particles with diameters between 10 and 100nm and have a short residence time as they are removed by diffusion. Nucleation mode particles are created in situ from the gas phase by nucleation. These particles constitute very little mass, whilst the Aitken nuclei form the accumulation mode in particle mass distribution.

The largest concentrations of particles in the atmosphere are usually particles smaller than 0.1μm. These, however, constitute the smallest mass, and coagulate very quickly resulting in relatively short atmospheric lifetimes (Seinfeld and Pandis, 2006). Aerosols between 0.1 and 1μm are known as Accumulation mode aerosols and are removed by nucleation scavenging or may be washed out of the atmosphere through precipitation. Accumulation mode particles are not large enough to be removed due to gravitational settling and are too large to be scavenged through diffusion processes. Particles of this size therefore have the longest atmospheric lifetimes ranging from days to several weeks, and are known to accumulate in the Greenfield Gap (Greenfield, 1957; Shaw, 1987). The Greenfield Gap coincides with the peak wavelength of solar radiation (the visible wavelengths) and it is in this region where accumulation mode aerosols attenuate sunlight very efficiently (Power, 2003). The Greenfield Gap is also defined as the region where particles are least likely to be scavenged by precipitation (Paramonov *et al.*, 2011).

The significance of fine mode aerosols becomes clear when comparing the volume and number of aerosols in each size mode classification (Figure 2.1.). Particles with a diameter larger than 0.1µm contribute practically all the aerosol mass. These particles are, however, negligible in number compared to that of particles smaller than 0.1µm (Seinfeld and Pandis, 2006).

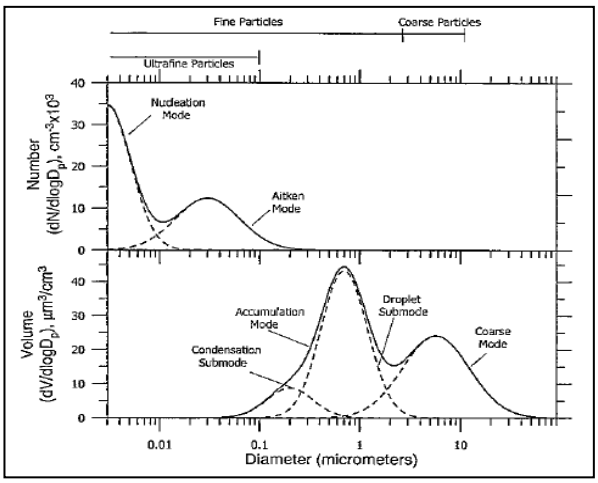

Figure 2.1. Typical number and volume distributions of atmospheric particles within different modes idicating the greater abundance of particles <1µm (after Seinfeld and Pandis, 2006, 369).

Although the atmospheric lifetimes of aerosols are short, during this time aerosols may travel thousands of kilometres and undergo many physical and chemical changes (Sato *et al.*, 2003). One of the important changes which occur in the atmosphere is that the size of particles increases over time, especially where aerosols have remained in a highly stable atmosphere. This occurs because, after emission, particles undergo condensational growth and coagulation (Formenti *et al.*, 2003), resulting in larger particles (Haywood *et al.*, 2003). Processes of scattering and absorption, which cause the perturbation of solar radiation, are affected by the size of the particles (Van de Hulst, 1957). It is for this reason that understanding the nature and size, as well as the spatial and temporal distribution of aerosols is critical to understanding climate change.

2.3. Aerosol Climatology

Anthropogenic activities have had a substantial and irreversible impact on the climate of the earth throughout history. Radiative forcing due to aerosols is widely recognised as one of the greatest sources of uncertainty in the prediction of climate change. Studies have revealed that

aerosols have an overall cooling effect on the climate, and have offset a significant amount of warming resulting from greenhouse gases (IPCC, 2014).

Measuring and understanding aerosol changes, both spatially and temporally, are essential in the prediction of climate (Tesfaye, 2011). Aerosol changes which affect the impact which aerosols have on climate including composition, size and number (among others) are highly uncertain. The difficulty in understanding the environmental impacts of aerosols lies in their relationship with dynamic atmospheric conditions. The relationship between aerosols, climate and human beings is complicated. While aerosols have a significantly negative impact on ambient air quality and human health, certain aerosols are found to counteract the warming induced by greenhouse gases and also act as cloud condensation nuclei; therefore playing an essential part in the hydrological cycle. Aerosol particles provide sites for atmospheric reactions, and in turn, the trace gas chemistry of the atmosphere affects aerosol growth rates and formation (Jacob *et al*., 1995). Aerosols affect the radiative exchanges of the atmosphere, and therefore have both climatological and meteorological impacts. These solid or liquid atmospheric particles have impacts on atmospheric turbidity; while on a micro-scale, higher levels of humidity result in enhanced hygroscopic growth of aerosols (Kay and Box, 2000; Pilinis *et al.,* 1995; Ramaswamy *et al*., 2001; Power, 2003).

The understanding of the temporal and spatial distribution of various aerosols remains challenging (Tesfaye, 2011). The impacts of aerosols on climate, therefore requires a regional scale understanding and quantification, rather than an overall global understanding (Piketh *et al.,* 2002).

2.3.1. Aerosol Radiative Forcing

The impact which particulate matter may have on the radiative balance of the atmosphere is uncertain. Tropospheric aerosols may influence climate directly by processes of radiative scattering and absorption (Wang *et al.,* 2009), or indirectly by impacting on cloud formation processes, cloud lifetimes and cloud radiative forcings (Charlson *et al.,* 1992; Croft *et al*., 2009), by acting as cloud condensation nuclei or ice nuclei (Lohmann and Feichter, 2005).

2.3.1.1. Direct Radiative Forcing

According to Ramanathan (2001), anthropogenic activities are making our planet more absorptive in the infra-red wavelengths, and therefore, darker with time. Alternatively, in the visible wavelengths our planet is brightening. Studies by Folini and Wild (2011) indicate that the surface solar radiation decreased between 1950 and 1980, and increased again thereafter. These two time periods are referred to as global dimming and global brightening, respectively. This dimming has been associated with the interactions of aerosols with solar radiation. The highly unpredictable nature of aerosols and their impacts on solar radiative forcing has made the task of predicting their impacts extremely difficult. Aerosols result in significant reduction in visibility. Reduction in visibility is a direct result of the presence of aerosols, whose nature and concentrations have a large impact on the amount of solar radiation which reaches the surface of the earth (Wang *et al.,* 2009). Three radiative forcing agents play pivotal roles in the nature of our climate, namely: changes in solar radiation, changes in planetary albedo and changes in atmospheric aerosol concentrations (Kemp, 1994).

According to Kemp (1994), ideally the amount of incoming energy should balance the amount of outgoing energy. This balance is upset by the presence of greenhouse gases and aerosols. The magnitude of radiative forcing resulting from the presence of a perturbing particle, is calculated as the change in the net irradiance at the tropopause (Haywood and Boucher, 2000). Aerosols are only minor constituents of the atmosphere but are highly efficient at interacting with the visible and near-infrared portions of the electromagnetic spectrum (Queface, 2002). This interaction is referred to as the direct radiative forcing effect. Direct radiative forcing is the result of a process of the scattering of sunlight, which results in an increase in the amount of light reflected by the planet and hence a decrease in the amount of solar radiation reaching the surface (Seinfeld and Pandis, 2006). Two terms address the effect of aerosol on the earth's radiation budget; firstly, the direct radiative effect refers to the instantaneous impact of all particles, whereas direct radiative forcing refers to the change in the direct radiative effect from pre-industrial times (Heald *et al.*, 2014). Aerosol direct radiative forcing is of a significant magnitude and studies have revealed that radiative forcing resulting from aerosols is usually negative, except when considering the radiative forcing resulting from black carbon (IPCC, 2014). When estimating radiative forcing, warming is referred to as positive radiative forcing, whereas cooling would result in a negative forcing.

The nature and composition of certain aerosol species may result in the warming of the atmosphere due to their absorptive properties. Figure 2.2., below, illustrates the types of interactions which occur between a particle and the incoming solar radiation. The processes of scattering and absorption are clearly indicated in the figure and are dependent on the wavelength of incident radiation, aerosol size and composition.

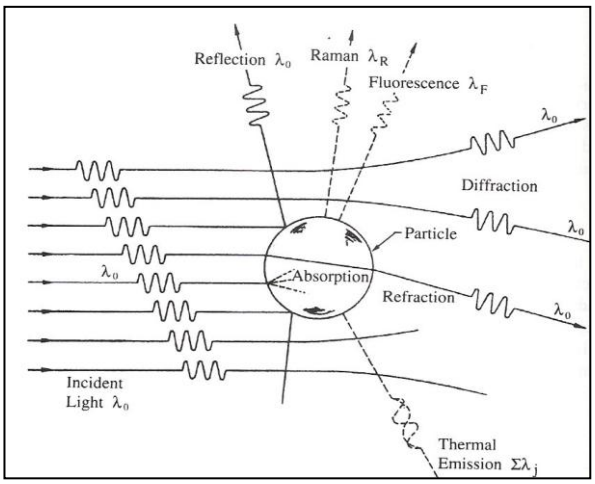

Figure 2.2: The mechanisms of interaction between a particle and incident radiation (after Seinfeld and Pandis, 2006, 692).

The extinction of light by aerosol particles and gases occurs as a result of two processes (Queface, 2002):

- Elastic Scattering: Part of the radiation beam is deflected in other directions as it comes into contact with a particle in the atmosphere, conserving light energy.
- Absorption: Photons transfer their energy to the particle, increasing the internal energy of the particle and causing the heating of the particles and eventually the surrounding medium.

The impact of all aerosols is to decrease the amount of sunlight which reaches the earth's surface (Ocko et al., 2012). When a beam of light on entering the earth's atmosphere comes into contact with an aerosol, electrical charges in the particle are agitated into oscillatory motion. The excited electric charges re-radiate energy in all directions (scattering) and may convert a part of the incident radiation into thermal energy (absorption) (Seinfeld and Pandis, 2006), thus keeping the energy in the climate system (Ocko et al., 2012). The key parameters that govern the scattering and absorption of light by a particle are the wavelength of incident

radiation, and the size of the particle (Seinfeld and Pandis, 2006). In this regard, aerosol size distribution is an important field of research (Elias *et al.*, 2003). According to Watson and Chow (1994), fine particulate matter (<2.5μm) is the most important category of aerosols with regard to radiative forcing, with particles with a radius below 1μm being highly efficient at scattering incoming solar radiation (Seinfeld and Pandis, 2006). Larger particles (coarse particles) may also contribute significantly at some of the locations, however, they are less effective as a result of their size and residence times in the atmosphere. Scattering occurs more readily at shorter wavelengths because the impenetrability of aerosols increases at longer wavelengths (Charlson, 1992; Queface, 2002). Diffraction of solar radiation by aerosol particles results when the particle size lies between 1/10 and 10 times that of the wavelength of incident radiation (Tyson and Preston-Whyte, 2000). According to Campbell *et al*.(2003), these interactions also result in a reduction of visibility.

Studies of direct radiative forcing over the south Atlantic, to the west of southern Africa, reveal that aerosol radiative forcing is highly variable, with periods of extreme aerosol forcings and other periods of more prolonged, consistent forcings (de Graaf, 2014). The absorption of solar radiation by aerosols containing black carbon may result in reduced cloud cover due to the modification of the atmospheric temperature profiles, as well as the evaporation of clouds (Hansen *et al.*, 1997; Ackerman *et al.*, 2000; Eck *et al*., 2003). Further, fire smoke plumes (Rosenfeld, 2000), air pollution (Rosenfeld, 2000; Rosenfeld and Woodley, 2001) and dust storms have been found to significantly suppress precipitation (Xin *et al*., 2005).

The Electromagnetic Spectrum

The electromagnetic spectrum reveals the importance of aerosols with regard to incoming solar radiation. As previously stated, studies have revealed that aerosols have a much larger impact in the visible, shorter wavelengths (Fallah-ADL *et al*., 1997). Aerosols interact predominantly with visible light, but also slightly with the infrared and ultraviolet wavelengths through processes of scattering and absorption. The electromagnetic spectrum classifies different wavelengths of solar radiation into various categories. The 380 to 770 nanometer wavelength range is classified as visible light**.** As can be seen in Figure 2.3., the increasing solar radiation flux is highest at visible wavelengths, where the impacts of aerosols are the most significant**.** The importance of aerosols with regard to their impact on solar

radiation is therefore realised. The principle of operation of many instruments relies on the interaction of aerosols with light.

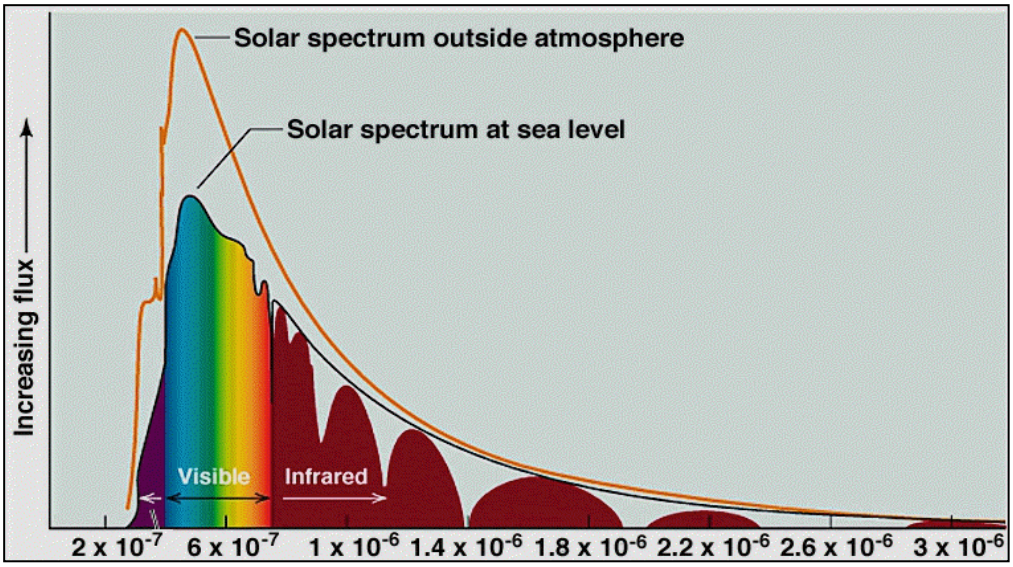

Figure 2.3: The relationship between the energy flux and wavelength indicating the highest increasing flux over the visible wavelength range (http://csep10.phys.utk.edu/astr162/lect/light/spectrum.html).

2.3.1.2. Indirect Radiative Forcing

Aerosols are an essential component of the hydrological cycle and without these particles clouds would not form (Seinfeld and Pandis, 2006). Indirect Radiative forcing involves interactions between aerosols and clouds. The interaction between clouds and aerosols and the resulting effects on the radiation budget of the earth remain one of the greatest uncertainties in aerosol climatology and the modelling of future climate (IPCC, 2014; Regayre et al., 2014). Aerosols act as cloud condensation nuclei, forcing the climate indirectly through the Twomey effects, which are referred to as the first and second indirect effects. The first indirect effect (Figure 2.4.) involves aerosols acting as cloud condensation nuclei. Studies show that as aerosol concentrations increase, cloud droplet concentrations increase (eg. Ross et al., 2003). This results in a decrease in the size of water droplets in the atmosphere (Twomey, 1974). The second indirect effect occurs as a direct result of the first, where reduction in cloud droplet size results in a reduction in precipitation efficiency, an increase in liquid water content, cloud lifetime (Albrecht, 1989), cloud thickness (Pincus and Barker, 1994), cloud amount (Ramanathan, 2001) and cloud albedo (Twomey, 1977, Boucher et al., 2013). Reviews on the aerosol effects on the hydrological cycle by Lohmann and

Feichter (2005) reveal that aerosols may alter convection processes and so may simultaneously have an impact on drought and flooding events. Further, cooling in the Northern Hemisphere as a result of aerosols may have resulted in a shift in the intertropical convergence zone, thus playing a role in Sahelian droughts.

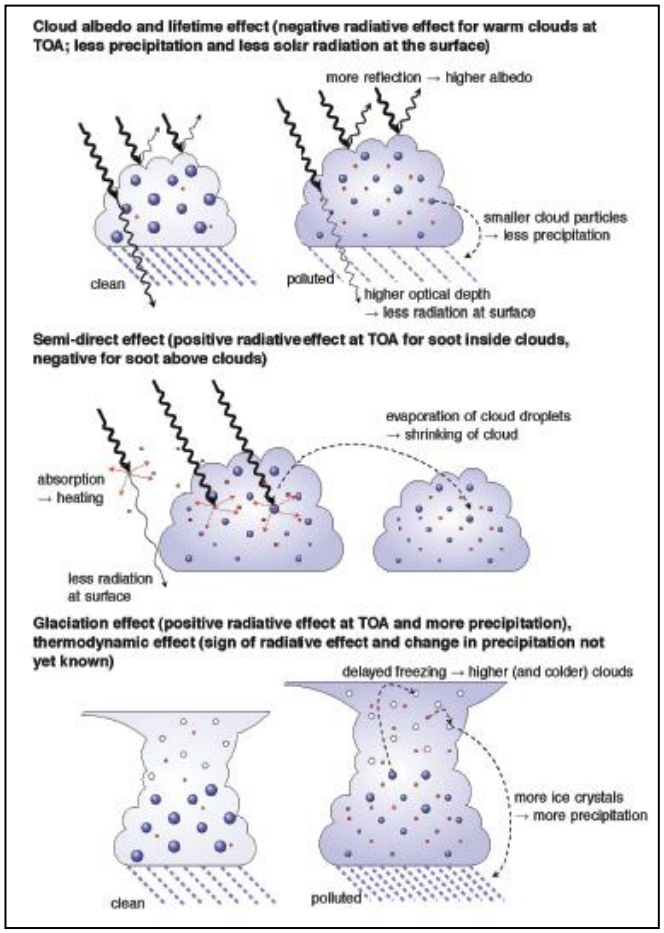

Figure 2.4: The various effects of aerosols on clouds is indicated. These include the cloud-albedo, lifetime and semi-direct effects (http://www.ipcc.ch/publications_and_data/ar4/wg1/en/ch7s7-5-2.html).

The Indian Ocean Experiment (INDOEX) results reveal that at the top of the atmosphere, the cooling effect of the first indirect effect is more significant than that of the direct effect, whereas at the surface the opposite is true (Ramanathan,2001).

2.3.1.3. Global Impacts of Aerosol Radiative Forcing

Evidence suggests that aerosols may have an impact on the radiative balance on a local and regional scale, and even globally (Charlson *et al.*, 1989). An estimation of the magnitude of

the radiative forcing exerted by significant aerosol species is presented in Table 2.1. Sulphate is found to be the most important aerosol causing cooling, whereas black carbon aerosols from industry and biomass burning aerosols result in significant warming. Research has revealed that aerosols emitted from biomass burning and industrial emissions have significant potential to induce climate change (Charlson *et al.,* 1990; Andreae, 1991; Schimel *et al.,* 1996). Figure 2.5 gives a short summary of the estimated radiative forcing of climate between 1750 and 2011 through natural and anthropogenic processes. The figure indicates the various positive and negative radiative forcing agents divided into anthropogenic and natural forcing agents. Positive forcing results in warming, whereas negative forcing results in cooling. It is clear that direct radiative forcing resulting from aerosols has offset warming significantly.

Table 2.1. The global mean radiative forcing as estimated by the IPCC fourth assessment report (2014). The direct radiative forcing for each aerosol is indicated in W/m^2 (watts per meter square) and the error for each estimation is given. A positive direct radiative forcing value indicates heating, whereas a negative value indicates cooling (Bergstrom et al.,2003).

Aerosol Species	**Direct Radiative Forcing (W/m^2)**	**Error (W/m^2)**
Sulfate	-0.4	-0.6 to -0.2
Fossil Fuel Organic Carbon	-0.09	-0.16 to -0.03
Fossil Fuel Black Carbon	0.4	0.05 to 0.8
Biomass Burning	-0.0	±0.2
Nitrate	-0.11	-0.3 to -0.03
Mineral Dust	-0.1	-0.3 to 0.1
Secondary Organic Aerosol	-0.35	-0.85 to 0.15

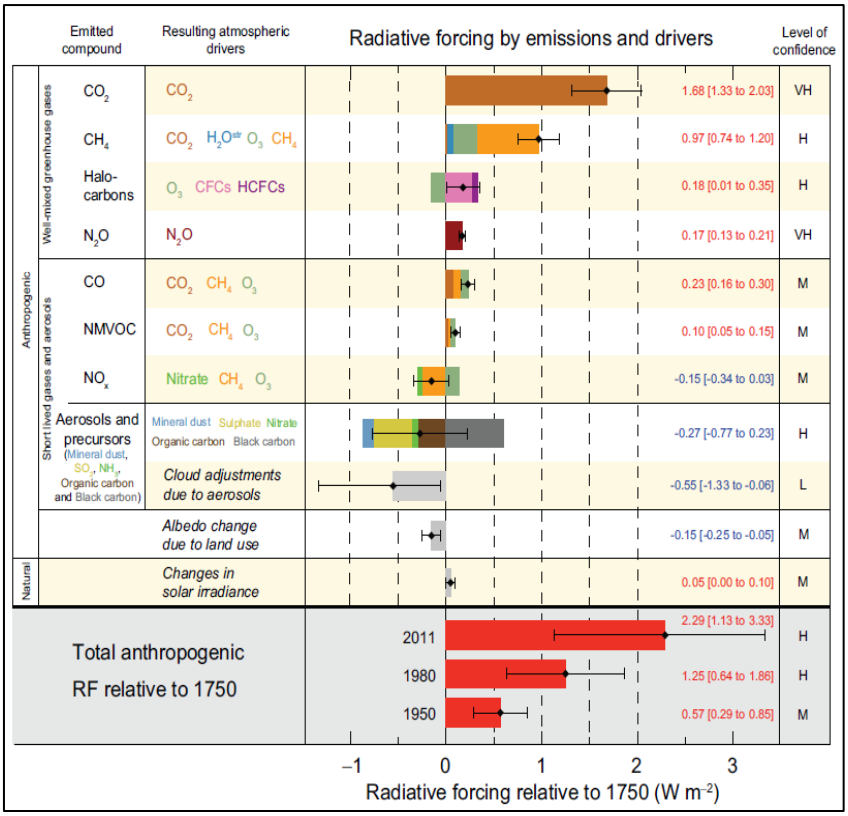

Figure 2.5: Radiative forcing due to various natural processes and human activities (after IPCC,2014, 14).

An understanding of the optical properties of aerosols is important to determine the effects which these particles may have on climate.

2.4.Aerosol Optical Properties

In order to estimate and predict the radiative forcing impacts of aerosols, it is important to have an understanding of the optical properties of aerosols (Chylek and Wong, 1995). The optical thickness and size distribution of aerosols are important parameters defining the optical state of the atmosphere (King *et al.*, 1999). Both the aerosol optical depth and the Ångstrom exponent are dependent on the amount of aerosols of different sizes and concentrations, their chemical compositions and the wavelength of incident radiation (Eck *et al.*, 1999, 2003; O'Neill *et al.*, 2003).

2.4.1. Aerosol Optical Thickness

Studies reveal that anthropogenic and natural aerosols contribute almost equally to the global aerosol optical thickness (AOT) (Ramanathan, 2001). The spectral aerosol optical depth is

the most detailed and accurate way of describing atmospheric turbidity (Power, 2003). AOT is a measure of the aerosol concentrations in the total atmospheric column and is estimated by the resultant attenuation of incoming solar radiation at specific wavelengths which results from the presence of atmospheric aerosols (Gobbi *et al.*, 2007). AOT is dependent on the concentration and nature (particle size and composition) of aerosols (Elias *et al.*, 2006). Aerosol optical depth is the most important parameter to consider when estimating radiative forcing as its magnitude is directly proportional to the magnitude of aerosol radiative forcing (Elias *et al.*, 2006). Aerosol optical thickness can be derived from measurements of attenuated direct solar radiation, the aerosol size distribution and the single-scattering albedo, which are key parameters in defining the optical state of the atmosphere (King *et al.*, 1999). AOT data is a standard product of satellite retrievals and is commonly measured in field experiments (Chin *et al.*, 2002).

The AOT is usually reported at or close to the 500nm wavelength band, depending on the spectral range measured by the instrument. Reporting AOT at 500nm is due to the fact that this wavelength lies within the visible range (photopic curve) of the solar spectrum, where minimum absorption by atmospheric gases occurs (Power, 2003). In principle, the AOT over a 50km squared domain should not vary significantly, except over regions near major emission sources. AOT measured in remote areas should exhibit little spatial variation (Li *et al.*, 2007).

The aerosol optical thickness may be derived at the specific wavelength of interest, based on Beer-Lambert-Bouguer Law. This law states that the attenuation or extinction of light which has travelled through a medium is proportional to the distance which this light has travelled and is subject to local fluctuations of radiation (Iqbal, 1983), and is presented in the following equation

$$V(\lambda) = V_0(\lambda)D(-\tau^{\lambda M}) \text{.....1}$$

Where the instrument signal, $V(\lambda)$, exo-atmospheric voltage, $V_0(\lambda)$, earth-sun distance, D, and optical airmass, M, are used to calculate the total optical thickness, τ_λ.
$V(\lambda)$ = the signal detected by the instrument
$V_0(\lambda)$ = the exo-atmospheric voltage
D = the earth-sun distance at the time of the observations, in astronomical units
τ_λ = Optical Thickness
M = Optical Airmass

Optical thickness is one of the most accurate and widely measured parameters when estimating aerosol radiative forcing (Charlson *et al*., 1989). The optical thickness is a total value comprising the magnitude of optical thickness resulting from Rayleigh, aerosol and ozone scattering. As the optical thickness increases, the upwelling flux at the top of the atmosphere is found to increase and more sunlight is scattered back to space (Ichoku *et al*., 2002). Twomey(1974) has found that a 10 per cent increase in aerosol nuclei will result in a 2.5 per cent increase in optical thickness. Furthermore, as aerosol concentrations increase, and as a result, AOT increases, the atmospheric turbidity too will increase (Reck, 1975). The natural background aerosol optical depth is estimated at 0.12, although AOT's in the southern hemisphere have been measured at 0.05 (Charlson, 1992). According to Queface (2002), an AOT of 0.4 or above is considered to be representative of high aerosol concentrations. According to Globe (2002), values of AOT > 0.5 indicate extremely hazy conditions. AOT is a vitally important component in understanding the size distribution of aerosols as the wavelength dependence of AOT is used to derive the Ångstrom exponent.

2.4.2. Ångstrom Exponent

Ångstrom exponent (AE) is an accurate way of deriving aerosol size distribution characteristics (Gobbi *et al*., 2007). The Ångstrom exponent is a representation of the gradient of the wavelength dependence of AOT in logarithmic coordinates (Angström, 1929) and is used to give an approximate indication of the size of aerosol particles determining AOT (Kaufman *et al*., 1994; Barenbrug, 2003). The Ångstrom exponent (α) is usually computed over a large wavelength range (eg. 440-1020nm), which provides information that is sensitive to both fine and coarse mode particles. If α is computed over a short wavelength range (eg. 440-675nm) then the AE is sensitive to fine mode particles only (Eck *et al*., 1999). A direct relationship exists between the wavelength of incident radiation and the size of the aerosol particle. It is for this reason that shorter wavelengths are used to identify events dominated by fine or accumulation mode aerosols, while longer wavelengths are used to determine events dominated by larger coarse mode particles (Elias *et al*., 2006).

According to Queface (2002), $\alpha > 1$ indicates the dominance of fine mode aerosols; whereas $\alpha < 1$ indicates the dominance of coarse mode particles. The typical values of α range from $\alpha > 2$ for fresh smoke particles (dominated by accumulation mode particles) (Kaufman *et al*.,

1992), to nearly zero for high optical thickness Sahelian/Saharan desert dust where coarse mode particles are dominant (Holben *et al.*, 1991). According to Tesfaye (2011), values of Ångstrom exponent which are above 1.5 indicate fine mode aerosols, with radii of approximately 0.35μm or below. These values of the Ångstrom exponent are indicative of combustion particles such as those which originate from urban pollution (particularly sulphate) and biomass burning (carbonaceous aerosols). Where the Ångstrom exponent lies between 1 and 1.5, the aerosol loading may be dominated by accumulation-mode particles. An Ångstrom exponent which lies below 1 indicates that non-combustion particles dominate the aerosol loading, with particles being greater than 0.75μm (Tesfaye, 2011).

Ångstrom exponent values varying from below 1 to greater than 1 indicate that aerosol particles in the area range from fine to coarse in size. This further indicates that the particles are derived from a range of different sources (Queface, 2002). The aging and humidification of pollution aerosols, as well as cloud contamination both decrease α. During stable meteorological conditions, the size of fine-mode aerosols increases, as pollution stagnates and OT increases. An increase in radius with AOT may occur as a result of the aging of the particle due to coagulation, condensation and gas-to-particle conversion (Reid *et al.*, 1998). Under humid conditions hygroscopic particle growth may contribute. Cloud contamination will enhance the weighting of coarse mode particles while humidification will increase the fine mode weighting (Gobbi *et al.*, 2007). According to O'Neill *et al* (2001a) the separation of coarse particles from fine particles using the Ångstrom exponent is feasible as the coarse mode AOT spectral variation is approximately neutral. The uncertainty of α increases as the AOT decreases (Elias *et al*., 2006). It is important to understand that the Ångstrom exponent alone does not provide unambiguous information about the relative weight of coarse and fine mode aerosols in determining AOT (Gobbi *et al*., 2007).

2.5.Aerosol Properties over Southern Africa

2.5.1. Factors affecting aerosol concentrations over southern Africa

The climatological characteristics of southern Africa play an important role in the concentrations of pollutants over the area. The focus on atmospheric transport over southern Africa has shifted over the years from research into mesoscale circulations, prior to 1990, to macro-scale transport studies (Tyson *et al*., 1988; Tyson, 1997). Mesoscale factors such as

regionally induced topographic winds, urban heat island effects and atmospheric stability are important factors controlling air pollution dispersion over the country (Held and Snyman, 1994). Aeolian dust remains a major contributor to aerosol loading over South African throughout the year, reaching a maximum during winter (Piketh, 2000).

Many factors affect the concentrations of aerosols over South Africa. Thunderstorms, common over the Highveld in summer serve to cleanse the air of aerosols significantly. These, and other meteorological parameters such as relative humidity and wind speed may have significant impacts on aerosol concentrations and physical and chemical compositions (Mallet *et al*., 2003).

Synoptic conditions have the most direct control on the horizontal and vertical distribution of aerosols (Stein *et al.,* 2003; Myhre *et al.,* 2003). In order to assess the atmospheric distribution of pollution, information about the climate, terrain characteristics and the nature of seasonal and diurnal variations of the study area are required (Tyson *et al*., 1998). Vertical mixing in the atmosphere is one of the critical processes determining pollution dispersion and is closely linked to the stability structure of the atmosphere (Piketh, 2000). Three persistent absolutely stable layers have been identified over southern Africa (Cosijn and Tyson, 1996). These exist at the 700hPa, 500hPa and 850hPa atmospheric pressure layers (Figure 2.6.). These stable layers serve as boundaries for the vertical distribution of pollution (Garstang *et al*., 1996a; Elias *et al*., 2003) and a significant portion of pollutants are transported below these layers (Piketh *et al*., 1996). Pollutants are dispersed poorly during these conditions and boundary layer concentrations build up (Elsom, 1987), especially as these stable layers may persist for a number of days. Trace gas and aerosol emissions become trapped below these stable layers where they are subject to accumulation and photochemical reactions. During stable meteorological conditions fine aerosols may become larger and optical thickness may increase (Gobbi *et al*., 2007).

A common occurrence over South Africa during winter is the presence of surface radiative inversions. These inversions frequently occur as the clear, calm and dry conditions over the South African Highveld are favourable to their formation. Surface inversions reaching depths of between 400 and 600 metres deep are common over Johannesburg and Tshwane. Surface inversions occurring over flat terrain and usually develop as a result of the ground cooling rapidly and radiating the heat to the air above the ground. Inversions occurring in hilly

topography often form as a result of cold air accumulation at the bottom of slopes (katabatic flow) (Tyson, 2000). These inversions trap pollutants and prevent the vertical movement and hence, dilution.

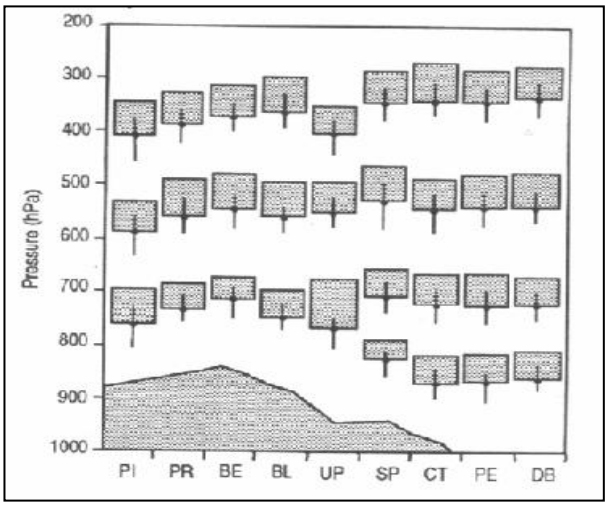

Figure 2.6: Absolutely stable layers over southern Africa on days where no rain is recorded. Stable layers are common at the 850, 700, 500 and 300hPa levels. (PI – Pietersburg; PR-Pretoria; BE – Bethlehem; BL – Bloemfontein; UP – Upington; SP – Springs; CT – Cape Town; PE – Port Elizabeth; DB – Durban) (after Tyson and Preston-Whyte, 2000, 287).

Occasionally, particularly during winter, these stable layers may be disrupted by westerly low pressure systems (cold fronts), which essentially pick up accumulated particles and transport them eastwards over the Indian Ocean (Kirkman, 1998). Air pollution moving over southern Africa may either exit directly off the continent in the Angolan or Natal plume or be recirculated by the Continental High Pressure. Anticyclonic circulation and westerly disturbances tend to result in air being transported from Africa and eastward over the adjacent Indian Ocean through the Natal plume. Easterly wave conditions result in transport to the west over the tropical Atlantic Ocean in the Angolan Plume (Garstang and Tyson, 1997). The anticyclonic circulation of the Continental High Pressure, prevalent over southern Africa results in the recirculation of pollutants. An eight year trajectory climatology of the southern African Highveld (Frieman and Piketh, 2003) confirmed the prevalence of recirculation over the subcontinent. Studies have found that 44 per cent of the aerosol flux transported over the region is recirculated (Figure 2.7.). Airmasses commonly recirculate over southern Africa for approximately two to three weeks before exiting off the continent toward the two adjacent oceans (Tyson *et al*., 1996b). The various SAFARI campaigns have revealed that particles

are being recirculated from the industrial Highveld over the Indian Ocean and back toward the subcontinent as a result of this system (Piketh *et al*. 1996). Stability and the recirculation of particles as a result of the high pressure system, is found to prolong aerosol residence times (Garstang *et al*., 1996a), resulting in the aforementioned impacts on aerosol size and distribution.

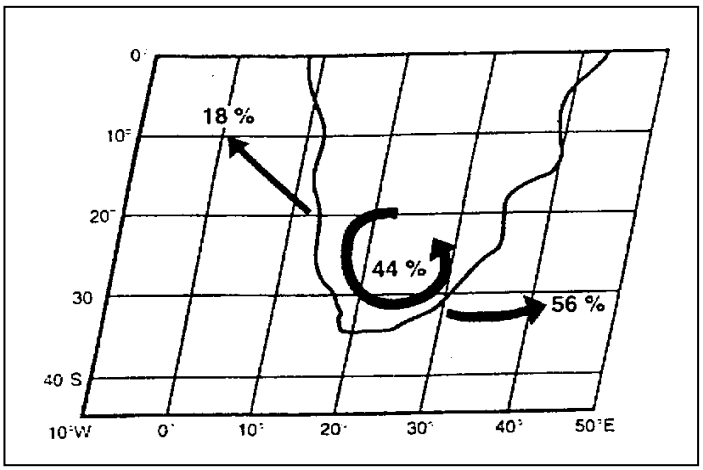

Figure 2.7: The average transport for all synoptic circulation types between the surface and 500hPa indicating that 44 % of all air parcels are recirculated over the interior of South Africa (after Piketh et al., 1996).

The aerosol loading, dispersion, removal processes and aging processes such as physiochemical changes are all affected by the various synoptic and meteorological conditions specified above.

During winter in South Africa and many other countries around the world, domestic fuel burning practices are intensified. While the use of fuel burning for cooking and lighting purposes occurs throughout the year, these practices are enhanced during winter. As temperatures drop the need for space heating, particularly in low income settlements is enhanced and the burning of coal, wood etc. becomes more frequent and intense. Studies into the importance of, and emissions from, these practices were carried out by Mdluli (2007) and Terblanche et al. (1993a) among others.

Satellite and ground-based remote sensing experiments have become the most popular and practical methods of measuring aerosol loading and making aerosol observations (Ichoku *et al*., 2002).

2.5.2. Field Experiments

Field campaigns are used to verify our understanding of aerosol optical properties and radiative transfer and are extremely important inputs for modelling research. Field campaigns such as the SAFARI2000 (Southern African Fire Atmosphere Resaerch Initiatives) campaigns in southern Africa, as well as the global AERONET campaigns have supplied important information regarding the chemical, physical and optical properties of aerosols (Ross *et al*., 1998; Ross *et al*., 2003; Holben *et al*., 1998; Haywood and Boucher, 2000).

The Haze over the Highveld Project (Bigala, 2008) which was conducted during 2002 and 2003 provides an understanding of the aerosol burden over the Highveld region. The project aimed to investigate the spatial distribution of aerosols, as well as the aerosol burden over the South African Highveld during the winter and summer periods of 2002 and 2003. Hazemeters were placed at selected sites in industrial, urban, township and agricultural areas during this period. These areas are all significant emitters of sulphur, carbon, nitrogen and their oxides. The results of the project revealed that the highest AOT was recorded during the summer 2002 campaign at the township sites ($\geq$0.6). This high AOT was attributed to high atmospheric dust levels. The aerosol optical thickness did not exceed 0.5 for all sites during winter. The AOT for industrial/urban sites was found to be higher during winter rather than summer due to meteorological conditions concentrating pollutants in the area. AOT values over agricultural sites are significantly variable during summer. Factors such as easterly waves, continental anticyclones, ridging highs and cut-off lows played a significant role in concentrating pollutants over the Highveld. Higher wind speeds enhanced the concentration of dust in the atmosphere. Cold fronts were found to significantly affect AOT concentrations over the entire research area, resulting in distinct increases and decreases in AOT. Fine weather occurred over the area, significantly concentrating pollutants.

The Ångstrom exponent for the entire Highveld area varied between 1.6 and 2 indicating the dominance of combustion aerosols to the aerosol burden. During summer these values were found to decrease to between 0.8 and 1. This is attributed to the high atmospheric dust levels, especially in township areas. Industrial and urban sites were found to have the highest Ångstrom exponent values due to presence of fine mode secondary aerosols such as sulphates.

A study was carried out to investigate the atmospheric aerosol loading off the east coast of southern Africa (Queface, 2002). Solar radiation measurements were made using CIMEL Sun Photometers which were placed at Inhaca Island Biological Station which lies 32km east of Maputo, Mozambique. As a comparison, the aerosol loadings were compared to that of AERONET CIMEL Sun Photometer sites located in Mongu (Zambia) and Bethelehem (South Africa). The CIMEL at Inhaca Island was placed 10km from the local village. Aerosol sources common to the area include cooking fires, industry, fossil fuel combustion and dust originating from the city of Maputo. Air masses, originating from the South African Highveld, carrying anthropogenic aerosols often move over Inhaca Island. A major contributor to the aerosol loading at Mongu is biomass burning; while the site at Bethlehem has no biomass burning activities in the area.

Results indicate that between April and November of 2000, daily average AOT varied from 0.05 to 1.12. The overall average was found to be 0.26. Two distinct periods were identified during 2000; one in which AOT was low (April to July), and another period where AOT was high (August to November). These months of high AOT were found to be the months when biomass burning activities had increased and intensified significantly.

Monthly averages of AOT at Mongu, Inhaca Island and Bethlehem all indicate similar seasonal trends. The AOT at all of these sites increases significantly during the biomass burning season. The biomass burning signature is seen in Mongu during September, and during October at Inhaca Island and Bethlehem.

The daily average Ångstrom exponent for Inhaca Island was found to lie between 0.12 and 1.96, with the overall average at 1.22. The great variation in Ångstrom exponent indicates that a diversity of aerosol sources contribute to the aerosol loading of the area. Of all of the observations recorded, 71% of the indicated an Ångstrom exponent above 1. This indicates that fine mode particles are most dominant at the site.

The aerosol loading over Bethlehem is found to be made up of low concentrations of fine mode particles which were found to be a mixture of dust and industrial aerosols. At Inhaca Island the aerosol loading is found to be a mixture of combustion particles and sea salt aerosols. Between April and June, biomass burning is not significant and the reason for the

existence of fine mode aerosols is that these particles, originating from Maputo or the South African Highveld were being transported into the area, as was found to occur by Freiman and Piketh, (2003).

Days were identified when AOT was significantly higher than normal. HYSPLIT trajectories indicated that recirculation and westerlies played a significant role in aerosol concentration levels. Recirculation results in prolonged aerosol atmospheric lifetimes (Tyson *et al.,* 1996; Freiman and Piketh, 2003). Of the 6 days identified with abnormally high AOT, five of these days exhibited an Ångstrom exponent above 1. On the other day, high aerosol loadings were attributed to coarse mode particles.

2.5.2.1. The Southern African Regional Science Initiative (SAFARI)

As part of an investigation into the aerosol burden over southern Africa, the SAFARI 92, 94 and 2000 campaigns were initiated. The extremely well-known and successful SAFARI studies started in 1992, bringing together international scientists to investigate the nature of aerosols and trace substances which have an impact on the southern African atmosphere. The nature, spatial and temporal distributions of biomass burning and industrial and biogenic aerosols were investigated. Satellite, airborne and ground-based observations were brought together in order to verify the data which was collected, and gain as much knowledge as possible. SAFARI 92 was conducted during an El Nino Southern Oscillation (ENSO) phase and as a result, extremely dry conditions were encountered in southern Africa. During this research campaign unusual synoptic airflows created a large plume of smoke (the river of smoke) which moved southward from equatorial Africa, exiting off the east coast toward the Indian Ocean (Swap *et al.,* 2003).

SAFARI 92 and SA'ARI94 differ in that the 1992 campaign sought to investigate biomass burning and its impacts on the atmosphere, whereas the 1994 campaign sought to establish the aerosol characteristics of the area during the non-burning season (Helas *et al*., 1995). The SAFARI campaign was once again initiated during 2000. SAFARI 2000 integrated surface, airborne and space-borne field research campaigns in southern Africa during 2000 and 2001. Aerosol optical properties were investigated using AERONET sun-sky radiometers at several sites during August and September 2000. Results from SAFARI 2000 provide information

collected during the La Nina phase of southern African climatic conditions. Wetter cycles such as the La Nina phase of the ENSO significantly increase fuel loading and therefore biomass burning emissions (Swap *et al.*, 2003).

The results of the SAFARI campaigns have established spatial and temporal aerosol climatologies for southern Africa. A significant fraction of the total particulate matter over South Africa is comprised of anthropogenic aerosols (Piketh *et al*., 1999). Aerosol sources identified as important during these campaigns are: soil (largest contributor to the aerosol loading), wave activity, industry and biomass burning (Held *et al*., 1996). Other important sources include mineral and marine emissions, and plant and soil microbial action. One of the major atmospheric features during the dry season campaign included a massive, thick layer of aerosols which covered much of southern Africa (Schmid *et al*., 2003; Swap *et al*., 2003). These include smoke and haze originating from countries to the north of South Africa. The characteristics of these emission sources are still poorly understood (Swap *et al*., 2003). Biomass burning is considered a significant source of trace gases, as well as various aerosol species, specifically organic and black carbon in southern Africa (Andreae et al., 1996a; Andreae *et al*., 1998).

Atmospheric aerosols over the plateau indicate a significant continental signature, with a large contribution of industrial particles. Aerosol concentrations are lower near the coast due to a constant inflow of clean marine air and are mostly contained within the surface mixing layer (Ross, 2003). The South African Highveld is the heart of industrial complexes and power plants between 25.5˚ South, 27.5˚ East, and 27˚ South, 30.5˚ East. Low-level easterly airflow and southerly airflow above 1000m above ground level commonly transport emissions from power plants and industries on the eastern Highveld. The highest concentrations of aerosols were recorded directly downwind of the industrialized region. The surprisingly low average aerosol concentrations over the industrialized Highveld are attributed to thunderstorms and the advection of cleaner air from the east. In the clean air north and south of the industrialized region, a broader range of accumulation mode particles were found, indicating an aged air mass with few fresh inputs. Fresh smoke particles were found to be larger than aged particles and are deposited quickly (Ross, 2003). Aerosol concentrations close to sources are a lot higher than further away along transport routes due to

dispersion, diffusion and dry deposition. Further results for the 2000 campaign indicate that as AOT increases the particle radius of aerosols increases proportionally (Eck *et al*., 2001).

Seasonal fires in southern Africa have a significant impact on the concentrations of aerosols. Industrial emissions are static throughout the year, however, their signature is more visible during the fire-free season. Aerosol concentrations during spring were found to be much higher than for autumn due to the smaller impact of fires during the autumn period. Industrial emissions prevail throughout the year as significant contributors to the aerosol loading. Aerosol concentrations are significantly lower due to industrial pollution than as a result of biomass burning (Kirkman, 1998).

2.5.2.2. Indirect Radiative Forcing over southern Africa

Aerosols have a significant impact on the cloud droplet concentration, as well as the physical and chemical properties of cloud droplets. The effects of aerosols on the radiative properties of clouds presents the highest uncertainty in the understanding of the impact of aerosols on climate (Regayre, 2014). Studies on the aerosol indirect effect have revealed that elevated levels of hygroscopic cloud condensation nuclei (CCN) result in an increase in the number of cloud droplets formed (Leaitch *et al.*, 1986; Ross et al., 2003). This in turn has a significant effect on clouds, not only increasing their lifetime and spatial extent, but impacting on the albedo of clouds, as well as the amount of time which clouds reflect solar radiation (Twomey *et al*., 1984; Albrecht, 1989, Boucher *et al*., 2013). Elevated aerosol concentrations are expected to contribute to direct radiative forcing during the dry season, and indirect radiative forcing during the wet season (Ross *et al*, 2003).

It is important to note that field campaigns are limited in spatial extent and distinguishing between anthropogenic and natural sources remains difficult. Where ground-level field campaigns are lacking, satellite remote sensing of aerosols becomes a key factor.

2.5.3. The Observation of Aerosols from Satellite Platforms

Satellite platforms offer the greatest potential for the global monitoring of aerosols. Satellites can sense the amount of solar radiation scattered back to space due to the presence of aerosols in our atmosphere, but this is not without extensive difficulties and error (King *et al.*, 1999;

Power, 2003). To date, several satellite platforms have been developed and tested to derive aerosol properties. Advanced Very High Resolution Radiometer (AVHRR) and Total Ozone Mapping Spectrometer (TOMS) are the longest-standing of all these sensors (Power, 2003). Aerosol distribution is spatially and temporally inhomogeneous (Li *et al*., 2007). It is for this reason that satellite retrievals of aerosol properties are vital. Satellite measurements of aerosols and their properties will help in the estimation of the aerosol direct radiative forcing effect, and so, help to validate model predictions of future global aerosol cycles (Levy *et al*., 2007).

Research conducted by Tesfaye (2011) over South Africa using aerosol loading data from the MISR (Multiangle Imaging Spectroradiometer) established a ten year aerosol climatology in which the country was divided into three sections: the lower, central and upper parts (Figure 2.8.). This classification is based on the aerosol loading observed over the country and illustrates low, medium and high aerosol concentrations respectively.

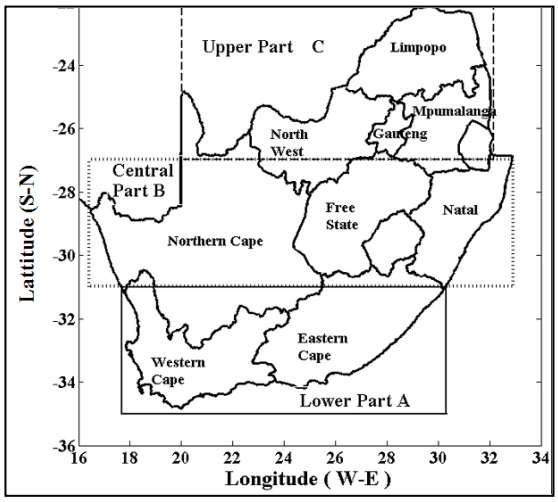

Figure 2.8: South Africa has been divided into three parts according to a ten-year aerosol climatology of the area (after Tesfaye, 2011, D20216, 2).

Aerosol optical thickness over South Africa appears to be low during summer and early winter. The possible reason for the low concentrations during summer is due to thunderstorms and precipitation scavenging which are common over the central and upper parts. The upper part however indicates a slightly higher AOT than the other two parts. AOT increases from June, as South Africa goes through its winter season, reaching a maximum during September (spring). Biomass burning activities are common as the country approaches the spring season (Magi *et al*., 2009), especially in the north-eastern and eastern

regions of South Arica. Biomass burning aerosols originating from Namibia, Zimbabwe and Botswana also significantly add to the aerosol loading over the country at this time (Tesfaye, 2011).

According to Myhre et al., (2013) the certainty in the aerosol direct radiative effect is the lowest over the south Atlantic near southern African than anywhere in the world. Studies by de Graaf *et al.,* (2012 and 2014) focused on the direct radiative effect of biomass burning aerosols which are advected westward over the south Atlantic from southern Africa. The maximum direct radiative effect measured during August 2006 focusing on an extensive biomass burning plume was as high as 132 $W.m^{-2}$ (error of $8W.m^{-2}$). Further, research from 2006 to 2009 (de Graaf et al., 2014) found that the temporal variation of the direct radiative effect may vary considerably. Results revealed that during some of the years short periods of high aerosol loadings dominated, whereas, during other years aerosol loadings were lower but prolonged. Monthly averaged climate models are found to be unable to represent these high aerosol loading events.

2.5.3.1. The Importance of the integration of various aerosol observation methods

Ground-based observations enable the retrieval of data as many times as possible during the day, but only at individual locations. Networks of ground-based observational instruments should be set-up to gather more information on the spatial distribution of aerosols in a particular region. Satellite observations, on the other hand, cover extensive areas of the earth in one day, making observations only once or twice at a given position per day. Ground-based and satellite observations are therefore vital in cross-validating one another and act as a compliment to one another (Ichoku *et al*., 2002). Data collected from the Aerosol Robotic Network (AERONET) is specifically used for the validation of aerosol data retrieved by the Moderate Resolution Imaging Spectroradiometer (MODIS) (Chu *et al*., 2002; Remer *et al*., 2002). Overall, MODIS and AERONET have high correlation coefficients and are in good agreement (Chu *et al.,* 2002).

While ground-based and satellite measurement techniques are very important and their accuracy improves daily, global models remain necessary in the estimation of global radiative forcing (Haywood and Boucher, 2000).

****

The nature and distribution of aerosols makes the understanding of these particles difficult. Aerosols are emitted from both natural and anthropogenic sources and may undergo changes in the atmosphere. Extensive uncertainty exists with regard to the impacts aerosols will have on climate. The meteorological conditions in South Africa during winter are conducive to the build-up of aerosols at this time of year. Now that the literature has been explored the methodology involved in this research project is presented in the following chapter.

CHAPTER 3: METHODOLOGY

This chapter provides a description of the research site, as well as the methodology involved in data collection. The instrument used to measure direct solar radiation is discussed and the algorithms used to calculate aerosol optical thickness and Ångstrom exponent are presented.

The Bojanala District lies within the North-West province of South Africa. The District is often referred to as the Bojanala Platinum District as it is home to some of the largest platinum mines in the world. Data collection for this research project has taken place over the South-Eastern sector of the Bojanala District near Rustenburg and Brits in the North-West province during the various stages of winter: winter 2008, early winter 2009, and late winter 2010. Data collection has taken place during the winter period of July and early August 2008 when domestic fuel burning activities are enhanced and the concentrations of pollutants as a result of the presence of intense inversions are increased significantly. As a comparison, data collection during the 2009 period occurred during the early winter month of May and early June. The reason for this is to establish a comparison between the spatial and temporal aerosol distributions before the onset and intensification of domestic fuel burning and inversions. Further, the late winter campaign (Late July and August) investigates the onset of the biomass burning season. Forestry Service handheld sun photometers (hazemeters) were placed at eight selected schools situated within the district. Students at the selected schools were asked to take direct sun measurements on behalf of the Climatology Research Group from the University of the Witwatersrand. Measurements were taken every half hour from 7am to 5pm for approximately four weeks per season.

3.1. Site Description

The research site is located in the eastern region of the North-West Province at the foothills of the Magaliesberg Mountain range. The site is approximately 120km from Johannesburg and Tshwane at approximately 1200m above sea level. Situated on the edge of the Bushveld Igneous Complex, this region is home to some of the most mineral-rich areas in the world. According to the Strategic Environmental Management Plan report the air quality in the Rustenburg area is rated poor to very poor as a result of mining and industrial activities, domestic fuel burning and the topography of the area (AQMP, 2005). Mines in the area are located along the Merensky Reef which stretches from Pilansberg to Marikana and further

eastward toward Brits (BPDM AQMP, 2011). The topography of the area contributes to episodes of high atmospheric pollutant concentrations under stable conditions, and as a result the area has been designated as a major priority area in the field of ambient air quality. Pollutants are concentrated under stable atmospheric conditions as a result of the presence of intense inversions. The slopes of the Magaliesberg Mountain Range which lie to the south of the research site create anabatic and katabatic winds, which dominate the airflow in the area. Air flow is therefore reversible as a result and the recirculation of pollution is common.

Aerosols are found to originate from sources such as processing of minerals and smelting operations, mine tailings, landfills, transportation along dirt roads and the N4 highway, domestic fuel burning, smaller industrial sources and agriculture. Investigations have found that most of the traffic within the Bojanala Platinum Districts is between Rustenburg and Brits. The Bojanala Platinum District's Air Quality Management Plan found that a large portion of emissions in the area originate from mining activities such as opencast mining, quarrying, materials handling, vehicle entrainment from haul roads, wind erosion in open areas, drilling and blasting. Dust entrainment by vehicles specifically associated with mining activities result in elevated dust levels throughout the day. Further emissions include domestic fuel burning, transportation and veld fires. Domestic fuel burning is found to be an area of concern in the district as fuel burning is increased and intensified during winter. Domestic fuel burning practices are characterised by diurnal and seasonal signatures. Solid fuel is burnt during the morning and evening for space heating and cooking. Due to the decrease in temperatures during winter, particularly in June and July these activities increase significantly, specifically as a result of the need for space heating. Traffic, agriculture and biomass burning are also important aerosols emitters. The risk of veld fires has been classified as extreme for all of the local municipalities within the Bojanala District. (BPDM AQMP, 2011). Local aerosol sources are identified indicating overall aerosol sources originating from industry and mining, traffic and domestic fuel burning (Table 3.1).

Table 3.1. Identified aerosol sources at each site.

Site	Significant Sources of Aerosols	Overall impact	Overall location	Overall Locational Sources
Bob Edward	N4; Industrial	Dust from dirt roads and mining activities, domestic fuel burning, burning of waste, mine tailings, landfills, smelters an processing	East	Largely domestic fuel burning - large townships; many dirt roads, mine dump
Johane Mololobatsi	N4; Industrial			
St. Theresa	Industrial, Mine dump			
J. Gotsube	Along major road;Township, mining processes (smelter)		West	Largely within mining areas. Many different mining practices important
Machadam	N4; Industrial			
Marikana	N4, closer to formal residential area			
Thlapi Moruwe	Township			
Rakgatla	Township			

Research by Annegarn et al. (1996) revealed that the progression of the mixing layer throughout the day has an impact on aerosols emitted at the surface. Ambient aerosol concentrations generally reveal two peaks, one in the morning and one at night. This is usually as a result of the enhancement of the activities which generate these aerosols and the presence of nocturnal ground-level inversions. This type of occurrence is usually associated with domestic fuel burning and traffic sources. The mixing layer deepens due to convective mixing as temperatures rise in the morning and aerosol concentrations are reduced. (Annegarn et al., 1996).

Hand-held sun photometers were placed at eight schools in the study region (Figure 3.1). The schools are all close to a number of mining-related aerosol sources; namely those from Anglo Platinum, Lonmin Platinum and Impala Platinum. The activities from these industries contribute significantly to particulate pollution, especially dust. The synoptic scale circulation feature (Figure 3.2) which dominates over most of South Africa during the year is the continental anticyclone. Studies reveal these synoptical scale features dominate for up to

70% of the time during winter (Tyson, 1986), having a significant impact on the dispersion of pollutants over the country.

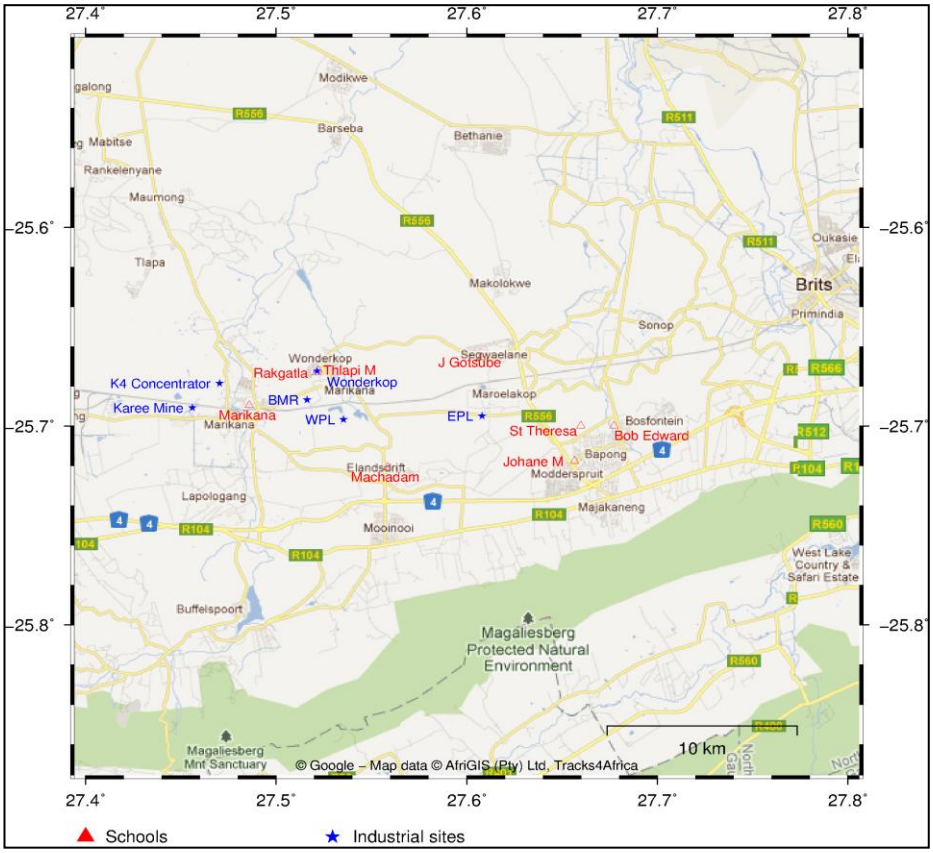

Figure 3.1. Study area indicating the schools where the hazemeters were placed (red triangles) as well as local land-use activities. Industrial sites are marked with blue stars. The green shading represents nature reserves, the yellow lines are roads and the grey shading represents built-up area.

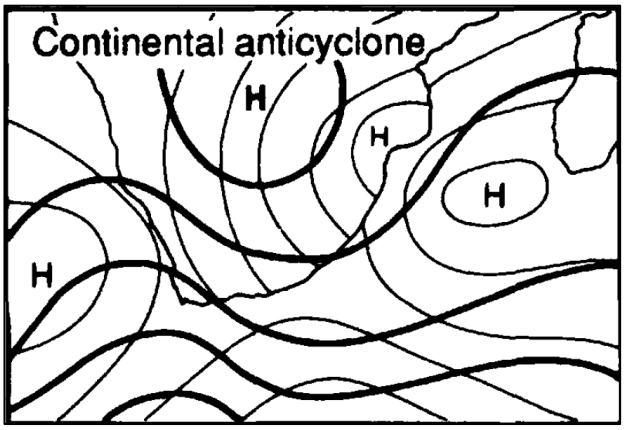

Figure 3.2: The major synoptic scale circulation type dominating over South Africa (up to 70% of the time during winter) (After Tyson, 1986, 220).

3.1.1. Meteorological Overview of the Bojanala District

As part of the Rustenburg Air Quality Management Plan the meteorology of the area was investigated and revealed that the complexity of the terrain has a direct impact on airflow over the district. Temporal wind data for Rustenburg exhibits a distinct oscillation in air flow between day and night. South-westerly flow most commonly occurs at night, reversing during the day to a north-easterly/north-westerly flow. Wind data measured at Lonmin's L2/BMR air quality monitoring station for the period from 2001 to 2004 (Figure 3.3) also has a distinctive split between a north-westerly sector and a south-easterly sector. The slight differences in the dominant wind directions between Lonmin's air quality monitoring station and the station situated in Rustenburg can be explained by the relative change in position of the two stations with respect to topography. Wind speeds were found to be slow to moderate, with calm conditions occurring 17% of the time.

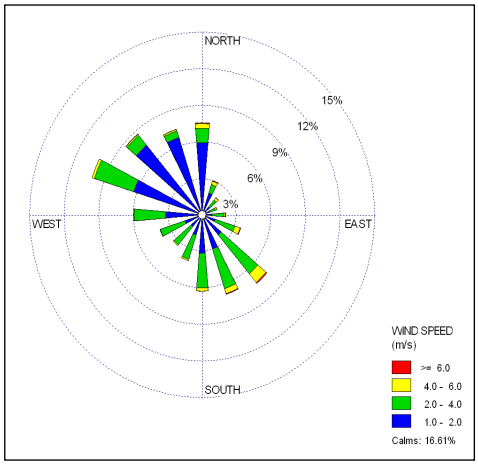

Figure 3.3: The average wind speed and direction at Lonmin's L2/BMR station for the period 2001 – 2004 (after AQMP, 2005, 47).

Diurnal wind roses created for the period from 2001 to 2004 indicate significant variations in flow (Figure 3.4), where winds from the south-east and south-south-east are found to be have greater velocities between 06:00 and 18:00.

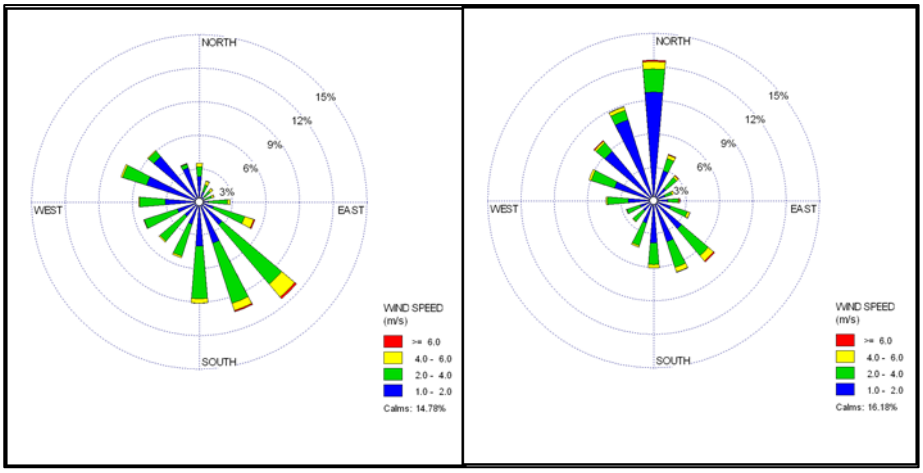

Figure 3.4: Diurnal variation of winds at Lonmin Platinum's L2/BMR station between 06:00 – 18:00 (left) and 18:00 – 24:00 (right), 2001 – 2004 (after AQMP, 2005, 48).

3.1.2. Rainfall and Temperature

Rustenburg lies toward the northern part of South Africa. Cold winters with little rainfall are characteristic of the area. Monthly average rainfall and ambient temperature data from 2003 to 2013 received from the South African Weather Service for Rustenburg indicates that rainfall and temperature are highly variable (Figure 3.5). Rustenburg falls within the summer rainfall region of South Africa, with the greatest amount of precipitation recorded between November and February. Aerosols are removed most effectively through wet deposition during rainfall events (Yum and Hudson, 2001), which are uncommon during winter in the area. During the summer months aerosol concentrations are expected to be reduced as a result of the higher frequency of (and greater amounts of) rainfall. The lowest minimum temperatures are recorded in July.

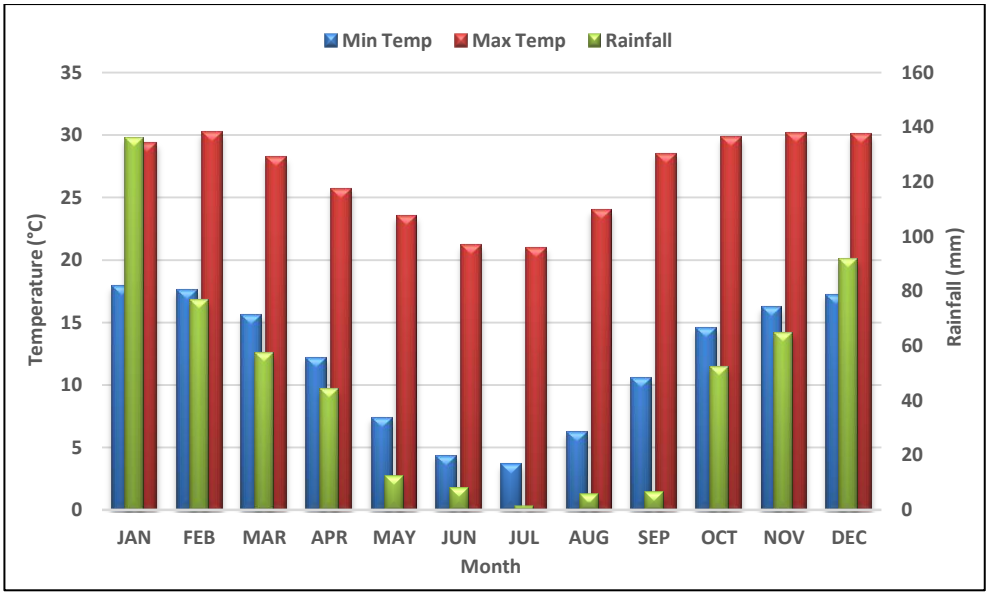

Figure 3.5. Monthly average rainfall and temperature data for Rustenburg for the period from 2003 to 2013.

3.1.3. Transboundary Transport of Airmasses

SAFARI 2000 revealed that airmasses originating in Mpumalanga and Zambia often move directly over the study area (Figure 3.6 and 3.7). The two most important sources of pollutants originating from these regions are biomass burning and industry. Biomass burning is easily identified using satellite imagery and is a highly seasonal source. The biomass burning season starts early in June near the equator in southern Africa. The smoke plume carrying high concentrations of aerosol particles and other pollutants travels southward. The impact of these aerosols reaches its maximum intensity during September in South Africa, as aerosol levels reach their highest concentrations (Tesfaye, 2011). At this time of year, the Bojanala District lies directly in the path of these airmasses as they transport trace-gases and aerosols southward.

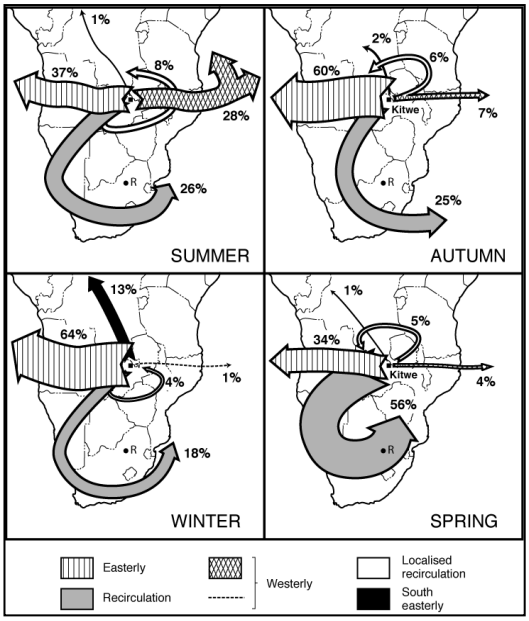

Figure 3.6: Seasonal atmospheric transport from Zambia over the southern Africa subcontinent. The position of Rustenburg is denoted by the R on the map. Atmospheric pollutant concentrations are vastly increased during the biomass burning season (AQMP, 2005, 52).

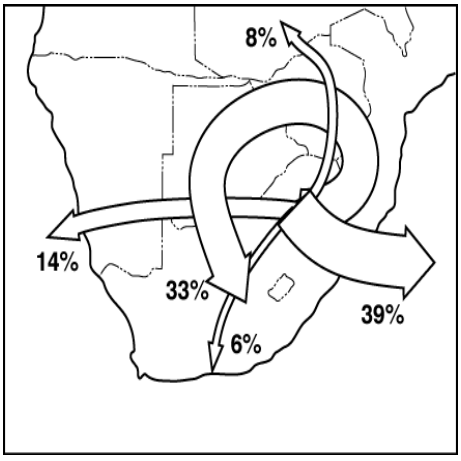

Figure 3.7: Atmospheric transport from the industrial Mpumalanga Highveld based on a five year trajectory climatology (Freiman and Piketh, 2003, 997).

An analysis of transport from Zambia and other southern African countries has shown that pollutants emitted from north of South Africa frequently impact on the Highveld region (Piketh *et al*., 1998). Southward transport of air masses from Zambia occurs throughout the year. The frequency of occurrence is highest during the spring season (Meter *et al*. 1999; Queface, 2002).

3.2.Instrumentation

3.2.1 *Hazemeter*

Hand-held Sun Photometers, known as hazemeters, were obtained from the United States Forestry Service. Scattered light from a particle is an extremely sensitive indicator of particle size and forms the basis for a number of aerosol measuring instruments (Hao, 2005). Hazemeters were developed in 2000 and are low cost and easy to use. The instruments contain automatic signal detectors, an accurate internal clock, and non-volatile storage to minimize the need to record data manually. The hazemeters (Figure 3.8) measure six analogue channels, solar intensity, temperature and battery voltage. Readings are easily taken at remote sites as data from 120 days of measurements may be stored. These characteristics make the instrument ideal for field research.

These instruments measure the amount of solar radiation reaching the surface as opposed to the theoretical amount that would reach the surface if no scattering or absorption by particles were taking place. The instrument measures solar radiation in four wavelengths, namely, 405, 500, 650 and 880nm using photodiode filters.

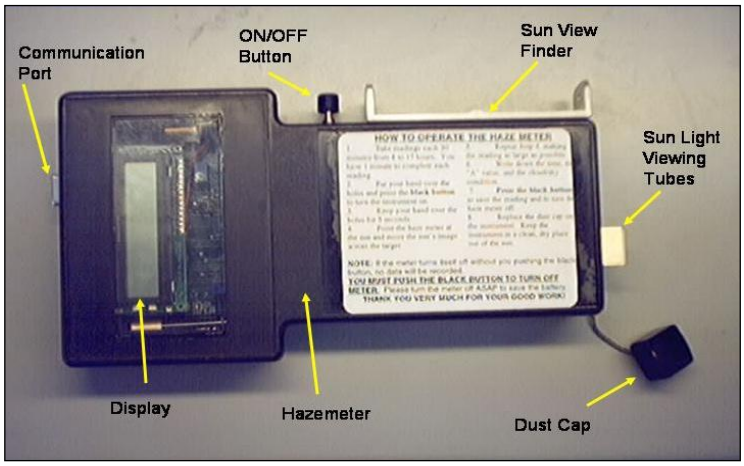

Figure 3.8: The handheld sun photometer (hazemeter) used in the research project. Various components are indicated.

A combination of LED's (Light-emitting diodes) and a phototransistor are used to sense solar energy received. Solar signals are amplified, buffered and converted by an analogue to digital microcontroller to a unipolar 10-bit digital value. Thirty-two readings over about 5s are added and averaged to form a value that reduces random noise for each spectral band. Readings are taken every half hour from 7am to 5pm during periods of full sunshine (Hao,

2005). Comparison to CIMEL Sun Photometers and Microtops instruments have revealed that the instrument is reliable to monitor aerosol optical thickness. The AOT values are within acceptable limits of error when compared to the CIMEL Sun Photometer (Hao, 2005). Hazemeters offer greater spatial and temporal coverage, as they may be easily used in any area. While the instruments are very convenient they, however, can only be used to determine limited optical information (Li, 2007), namely aerosol optical thickness and Ångstrom exponent.

3.2.2 *CIMEL Sun Photometer*

A CIMEL sun photometer is a highly accurate instrument that has been used for calibration of the hazemeters in this project (Figure 3.9). CIMEL sun photometers (CE 318) are used as part of the Aerosol Robotic Network (AERONET), which is a global research project run by the National Aeronautic Space Administration (NASA). Instruments are set up at selected sites around the globe to monitor aerosols, solar radiation and water vapour. These instruments have excellent temporal resolution as measurements are taken every five minutes. The CIMEL is fully automated and set up to track the sun daily throughout the period of sunshine. The sensor head is directed to within 1˚ of the sun using the site coordinates and time. Direct sun measurements are then made at eight various wavelengths within the range of 340-1020 nm (Holben *et al*., 1998). Studies reveal that uncertainties in AOT measured by CIMEL sun photometers range from $< \pm 0.01$ for wavelengths greater than 440nm to $< \pm 0.02$ for shorter wavelengths. (Holben *et al*., 1998; Dubovik *et al*., 2000). The instruments are cross-calibrated regularly against the master Sun Photometer at Mauna Loa Observatory in Hawaii. During the calibration procedure the instrument may be set up to constantly track the sun for the required period.

Figure 3.9: The CIMEL Sun Photometer used as part of AERONET is used in the calibration of the hazemeters (www.arm.gov/instruments/csphot).

3.3.The Calculation of Aerosol Optical Thickness from Direct Solar Radiation Measurements

3.3.1 *Total Optical Thickness*

Aerosol optical thickness is retrieved using the methodology of Knobelspiesse (2004). The Beer-Lambert-Bouguer Law is used to express the spectral extinction of solar radiation and is expressed in the following equation,

$$V(\lambda) = V_0(\lambda)\frac{{d_0}^2}{d}e^{-m\tau_t(\lambda)} \text{.....1}$$

which is used to calculate optical thickness using the voltage data downloaded from the hazemeters.

Solar radiation is measured at centre wavelengths (λ), specific to the instrument as voltages, V. Total optical thickness (τ_t) is calculated through the use of the exo-atmospheric voltage, V_0, and m, the airmass, which is dependent on the solar zenith angle (Knobelspiesse, 2004). The ratio of the average earth-sun distance, d_0, to the earth-sun distance on the day of observation, d, is calculated as follows:

$$\frac{{d_0}^2}{d} = 1 + 0.034cos\frac{2\pi J}{365} \text{.....2}$$

where, J is the Julian day for the day of measurement. The earth sun distance is a parameter which is calculated based on the distance between the earth and the sun at different times of the year, and therefore is a function of the day number (Julian Day).

Airmass is an important parameter which has a significant impact on the optical thickness. The airmass is calculated using the solar zenith angle (θ_0) which is calculated as a function of the latitude and longitude, the day of year and the hour angle (Figure 3.9).

$$m = (cos\theta_0 + 0.50572(96.07995 - \theta_0)^{-1.6364})^{-1} \quad \text{.....3}$$

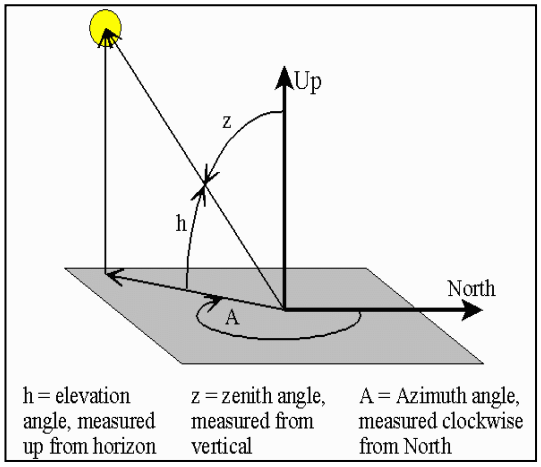

Figure 3.10: The figure indicates the solar zenith angle, as well as the elevation angle and azimuth angle. The solar zenith angle is calculated using latitude, Julian day, elevation and hour angles (http://www.science.smith.edu/~jcardell/Courses/EGR100/protect/slides/L18.pdf).

Once optical thickness is retrieved, a number of corrections are applied to account for ozone absorption and Rayleigh scattering.

3.3.1.1. Optical Thickness Due to Rayleigh Scattering

The optical thickness as a result of Rayleigh scattering is an important value as it has a significant impact on the aerosol optical thickness. The Rayleigh optical thickness is calculated as follows:

$$\tau_R(\lambda) = \frac{P}{P_0} K_{Ray}(\lambda) e^{-\frac{H}{7998.9}} \quad \text{.....4}$$

Where, the Rayleigh constant (K_{Ray}) is calculated for the different wavelengths of the instrument. This combined with the standard pressure, P_0, pressure at the time of measurement, P, and the height above sea level, H, are used to calculate the Rayleigh optical thickness:

K_{Ray} is derived in equation 5, using the specific wavelength of interest:

$$\mathrm{K_{Ray}}(\lambda) = 28773.597886 \times \left[1 \times 10^{-8}\left(8342.13 + \frac{2406030}{130 - \lambda^{-2}} + \frac{15997}{38.9 - \lambda^{-2}}\right)\right]^2 \times \left[1 \times 10^{-8}\left(8342.13 + \frac{2406030}{130 - \lambda^{-2}} + \frac{15997}{38.9 - \lambda^{-2}}\right) + 2\right]^2 \times \lambda^{-4} \quad \text{.....5}$$

Where, K_{Ray}, the Rayleigh constant is derived using the wavelength of interest, λ, in micrometers.

3.3.1.2. Gaseous Optical Thickness (OTG)- Optical Thickness due to Ozone

The gaseous optical thickness due to ozone is calculated at the various wavelengths of the instrument. In the visible to near-infrared (NIR) wavelength range, gaseous absorption, τ_g, is mainly due to ozone (Knobelspiesse, 2004). τ_g is derived using the following equation:

$$\tau_g(\lambda) = K_{Oz}(\lambda) \frac{Z}{1000} \quad \text{.....6}$$

Where, the ozone constant (K_{0z}), as well as the ozone concentration in Dobson units (Z) are used to calculate this value. The K_{Oz} at the various wavelengths were calculated using a plot of wavelength vs K_{Oz}, from Table 3.2 which was derived from Nicolet (1989) and Komhyr *et al*., 1989.

Table 3.2. The ozone constant at specific visible wavelengths, inicating the greater sensitivity between 490 and 675nm (adapted from Nicolet, 1981; Komhyr *et al.*, 1989, after Knobelspiesse, 2004, 90).

Wavelength	440	443	490	500	560	670	675	870
K (Oz)	0.0034	0.0038	0.0223	0.0328	0.1044	0.0449	0.0414	0.0036

3.3.2. Calibration of the Hazemeters

The exo-atmospheric voltage is a value which approximates the amount of solar radiation which would reach the instrument if the instrument were placed outside of our atmosphere. This means that there would be no impact by particles in the atmosphere on solar radiation. Ideally, calibration would be completed at a high altitude site, on cloudless days with low atmospheric turbidity. This type of calibration is usually carried out at the Mauna Loa Observatory in Hawaii by NASA scientists.

The exo-atmospheric voltage conveys the instrument calibration. It is an instrument-specific value which is calculated using the methodology of Knobelspiesse (2004). This value was retrieved through a calibration process with the CIMEL Sun Photometer. Calibration with the CIMEL was performed at Elandsfontein in the Mpumalanga province and at the University of the Witwatersrand in Johannesburg in Gauteng. Measurements were taken from 11am until 1pm. Data was downloaded from the hazemeters and for the CIMEL Sun Photometer from the AERONET website. The reading taken by the hazemeter is matched to the closest CIMEL Sun Photometer reading, ideally within 60 seconds of one another. Once the calibration has been completed, a number of calculations were used to derive the exo-atmospheric voltage of each instrument, for each wavelength of the instrument. If the Hazmeter measures voltages in the same wavelength as that of the CIMEL Sun Photometer the following calculation is used:

$$V_0(\lambda) = \frac{V_0^{'}(\lambda)V(\lambda)}{V'(\lambda)} \quad \text{.....7}$$

Where, $V_0'(\lambda)$ is the exo-atmospheric voltage for the CIMEL Sun Photometer. $V(\lambda)$ and $V'(\lambda)$ are the direct sun voltages measured by the uncalibrated instrument (in this case, the hazemeters) and the sun photometer, respectively. If the uncalibrated instrument and the sun

photometer measure in slightly different wavelengths a correction is applied to the above equation:

$$V_0(\lambda_i) = \left[\frac{V_0\prime(\lambda_j)V(\lambda_i)}{V\prime(\lambda_j)}\right] e^{m\phi} \quad \text{.....8}$$

Where, the closest channel, λ_j to the uncalibrated instruments measurement band, λ_i, is used; m is the airmass and ϕ is computed using the aerosol optical thickness (τ_{a0}) as presented in the following equation:

$$\phi = \tau_R(\lambda_i) - \tau_R(\lambda_j) + \tau_g(\lambda_i) - \tau_g(\lambda_j) + \tau_{a0}(\lambda_i^{-\alpha} - \lambda_j^{-\alpha}) \quad \text{..... 9}$$

Where, Rayleigh optical thickness (τ_R) and ozone optical thickness (τ_g) at the different wavelengths of the respective instruments are used. The aerosol optical thickness at 1µm(τ_{a0}) and the Ångstrom exponent (α) are calculated from data measured by the CIMEL Sun Photometer. τ_{a0} is calculated by extrapolating the shorter wavelength values of τ using the Ångstrom exponent, α.

Exo-atmospheric voltages are calculated using the measurements of the hazemeter which lie within 60 seconds of the voltages measured by the CIMEL Sun Photometer. Measurements where the airmass is less than three are used to minimize long atmospheric pathways, as well as encountering variable aerosol types. Computed values of the exo-atmospheric voltage are averaged and the coefficient of variation is calculated. Values of the coefficient of variation for a highly accurate instrument such as the master sun photometer and CIMEL sun photometer should be below 1% in order for the calibration to be deemed successful.

The exo-atmospheric voltage derived from the above equations is then used to calculate Total Optical Thickness ($\tau_T(\lambda)$) using equation 1.

Finally, with the use of the Rayleigh Optical Thickness and the Gaseous Optical Thickness derived in equation 4 and 6, respectively; as well as the Total Optical Thickness $\tau_T(\lambda)$ derived in equation 1, the aerosol optical thickness (τ_a) is finally calculated using the following equation:

$$\tau_T(\lambda) = \tau_a(\lambda) + \tau_R(\lambda) + \tau_g(\lambda) \quad \text{.....10}$$

Where, the Rayleigh optical thickness (τ_R) and gaseous optical thickness (τ_g) values for each wavelength are subtracted from the total optical thickness (τ_T) to retrieve the aerosol optical thickness, $\tau_a(\lambda)$, at the specific wavelength of interest.

3.3.3. Retrieval of the Ångstrom Exponent

The Ångstrom exponent is calculated as the gradient of the line which connects the aerosol optical thickness measured at each wavelength of the instrument. In order to achieve the above-mentioned straight line, the Ångstrom exponent may be calculated using the slope of a linear fit to the logarithm of wavelength (λ) vs. the logarithm of τ_a (Knobelspiesse,2004). The retrieval of the Ångstrom exponent is achieved using the following equation:

$$\alpha = \frac{\ln[\tau_a(\lambda_2)] - \ln[\tau_a(\lambda_1)]}{\ln(\lambda_1) - \ln(\lambda_2)} \quad \text{…….11}$$

Once the AOT values and Ångstrom exponents have been derived, the temporal variations were plotted. The spatial distribution of the average AOT and Ångstrom exponent were plotted for each research campaign.

3.3.4. HYSPLIT Trajectory Analysis

Backward trajectories were calculated where the daily variation in AOT and Ångstrom exponent was recorded above or below average for all the respective sites. The purpose of the trajectories is to ascertain whether airmasses foreign to the district may have an impact on the aerosol loading of the area. The trajectories were calculated using Hybrid Single-Particle Langrangian Integrated Trajectory (HYSPLIT) model. This model computes simple air parcel trajectories toward a selected position using the following link on the NOAA website: *www.arl.noaa.gov/HYSPLIT.php*. HYSPLIT trajectories are useful for the identification and direction of sources and air parcels. The trajectories created allow for the understanding of the movement of airmasses from their source to a specified location, as well as the variation in altitude with time and space (Wilson, 2011). The HYSPLIT trajectories for the Bojanala District were run to include different starting heights of 500, 1000 and 1500m above ground level, in order to establish whether airmasses at different heights may have been transported from different source regions. The reason for this is that the hazemeters measure the aerosol loading for the entire atmospheric column and do not simply take into account the concentrations of aerosols at ground level. Further, the trajectories were set to run for a 72-hour period prior to the date of interest.

3.3.5. Comparison to Ambient Particulate Data and Flight Profiles

The aerosol optical thickness data will be compared to particulate data received from a study carried out by Paul Beukes and colleagues at the University of Potchefstroom's Unit for Environmental Science and Management in order to identify whether a correlation exists between ambient particulate matter concentrations and AOT at Marikana in the Bojanala District. In 2008 particulate matter concentrations were recorded using a Tapered Element Oscillating Microbalance (TEOM) instrument rotating between PM1, PM2.5 and PM10. Time resolution was limited as readings were only taken every hour, alternating between the three particulate sizes, therefore data for each PM size was only recorded every three hours. During 2009 data was taken with Synchronized Hybrid Ambient Real-time Particulate Monitor (SHARP), model 5030, which replaced the TEOM. Only PM10 data was recorded every 15 minutes.

3.3.6. Analysis of Vertical Aerosol Concentration Profiles over Rustenburg

The aerosol data collected by the hazemeters was also further compared with aerosol flight profile data collected using the SAWS Aero Commander 690A during 2005. The Aero Commander is able to reach heights of 30 000ft. A Passive Cavity Aerosol Spectromoter Probe (PMS PCASP Model 100) and the Forward Scattering Spectrometer Probe (PMS FSSP) instruments were placed on-board the aircraft to measure aerosol concentrations and size distributions in the atmosphere over the Rustenburg and Highveld areas. The flight tracks at 167magl (meters above ground level) over the Rustenburg area are presented in Figure 3.11. Data collected during the winter campaign on the 25th July and 27th July 2005 were used to understand whether the concentrations of aerosols are highest closest to the ground and so may be related to ambient sources.

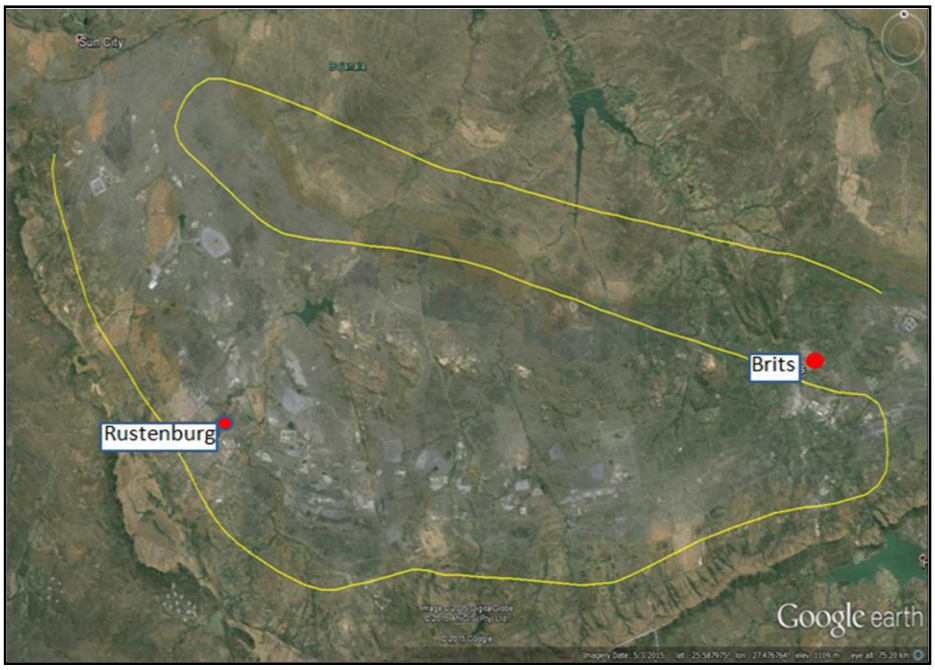

Figure 3.11: The flight tracks of the AERO Commander at 167magl during 2005 over the Rustenburg/Brits area (after Ncipha, 2011, 55)

3.4.Data Recovery and Limitations

3.4.1. Limitations to and the Recovery of the Exo-atmospheric Voltage

A number of problems were identified with regard to data collection and retrieval of the exo-atmospheric voltages. The task of calculating the exo-atmospheric voltage proved to be extremely difficult as direct sun measurements were required during times of extremely clean atmospheric conditions. The hazemeters used for research purposes were calibrated on 11 February 2010 at the University of the Witwatersrand under ideal atmospheric conditions. Exo-atmospheric voltages retrieved from this calibration (Table 3.3) are similar to those calculated for previous calibrations. Once the exo-atmospheric voltage for each wavelength of each instrument is calculated, the standard deviation and coefficient of variance are calculated. The coefficient of variance of the exo-atmospheric voltages retrieved for calibration of the CIMEL Sun Photometers against the Master Sun Photometers at Mauna Loa Observatory should not exceed 1 per cent. These instruments are the most accurate of Sun Photometers. Eck *et al* (1999) have calculated the uncertainty in AOT to be between 0.01 and 0.02, taking uncertainties in calibration, as well as Rayleigh and Ozone optical depth into account. Studies by Hao *et al* (2005) investigated the AOT measured by the haze meters compared to that measured by the CIMEL sun photometer. Results reveal agreement of 0.03 to 0.8 for the 880nm wavelength; and 0.2 to 2.0 for the 500 nm wavelength. The 680/670nm

wavelength (which would apply to the 650nm wavelength) revealed the least agreement, however the R^2 value was still high, at 0.976. Table 3.4 below indicates the coefficient of variance calculated for the exo-atmospheric voltages of each instrument and indicates a successful calibration. The values cannot be expected to be as low as those for the CIMEL Sun Photometers as the hazemeters are less accurate and errors due to the fact that instruments are hand-held should be considered. Values which were found to be slightly high have been highlighted in the table. The 405nm wavelength is found to be the least stable wavelength for all instruments. Instrument 95 is found to be the least stable instrument for all wavelengths of this instrument. Certain instruments were undergoing maintenance during the calibration process and the average exo-atmospheric voltages from previous calibrations were used. The values highlighted in the table may have an impact on the accuracy of the Ångstrom exponents retrieved as the Ångstrom exponent is calculated using all the wavelengths of the instrument.

Table 3.3: Exo-atmospheric voltages calculated from calibration data recorded on 11 February 2010 per instrument per wavelength. (Note: HM is hazemeter)

Instrument No.	880nm	650nm	500nm	405nm
HM 62	16448.07	20740.25	23498.61	50416.62
HM 67	17087.61	20256.29	22803.83	46034.70
HM 79	18294.03	20092.25	22275.07	48252.31
HM 80	18236.43	21940.50	22263.44	46712.97
HM 85	17062.69	19001.42	21799.65	48203.64
HM 94	16837.91	20117.16	23336.64	47969.21
HM 95	18868.89	18270.78	22825.11	46786.68

Table 3.4: The coefficient of variance for each instrument as calculated from the Exo-atmospheric Voltages for 11 February 2011. (Note: CoVar is the Coefficient of Variance, Vo the Extraterrestrial Voltage).

Exo-atmospheric Voltage	CoVar Vo(880)	CoVar Vo(650)	CoVar Vo(500)	CoVar Vo(405)
HM 62	0.947	0.808	0.888	3.031
HM 67	1.122	1.487	1.430	3.662
HM 79	1.624	6.634	2.951	6.297
HM 80	0.914	1.035	1.931	2.703
HM 85	0.932	1.196	1.253	2.845
HM 94	0.838	0.761	1.028	1.319
HM 95	1.566	12.300	7.299	3.954

3.4.2. Data Recovery and Limitations for the retrieval of AOT and the Ångstrom Exponent.

Due to the nature of this project, data recovery is low. Instruments are hand-held and manually operated and so readings are therefore subject to human error. The instruments may only be used when there are little to no clouds, as even high water vapour levels may have an impact on the readings. While water vapour is accounted for in the derivation of AOT, readings are still limited during cloudy conditions. This occurrence was common during the 2009 campaign where a number of cold fronts moved over the area, bringing rain and cloudy to overcast conditions. During the 2010 campaign an educators' protest often prevented students from gaining access to the schools, and therefore the instruments. The educators' protest extended for many weeks in which readings at certain schools either ceased or were taken irregularly.

Other obstacles, such as students having to write exams or attend classes meant that students could not always excuse themselves to take readings. Further, instrument faults or battery problems were not always reported timeously. These limitations were common during all three campaigns.

Data for the winter campaign was collected for the period from the 21st July to the 12th August 2008; for the early winter campaign from the 28th April to the 8th June 2009; and for the late winter campaign from the 21st July to the 31st August 2010. Data recovery for each campaign is presented in the following tables. The percentage of data available for each

school during each campaign is presented, showing significantly low data recovery at some of the schools (Table 3.5). Some of the datasets were excluded as a result of inconsistencies in the data collected. The data recovery is further presented per school per campaign per averaging period. The tables indicate the number of readings taken at each hour of the day (Table 3.6 to 3.8); and the number of readings taken per day per school (Table 3.9 to 3.11). These numbers are then used to calculate the percentage of data available for each hourly average and each daily average for all the schools combined. The data recovery is significantly low at times as a result of the various circumstances discussed above. These statistics are therefore included in this section in order that the data availability be well understood.

Table 3.5: Data Recovery (as percentage) is presented for each school for each campaign. Data recovery for 2010 is significantly lower for some of the schools.

Site	**2008**	**2009**	**2010**
Bob Edward High School (BE)	44	18	9
J. Gotsube High School (JG)	23	20	67
J. Mokololobatsi High School (JM)	48	40	excluded
Machadam Combined School (Mach)	29	16	7
Marikana High School (Mar)	31	32	19
Rakgatla High School (Rak)	48	68	61
St. Theresa High School (ST)	42	20	31
Thlapi Moruwe High School (TM)	36	excluded	excluded

Table 3.6: Percentage data recovery for each hour representing daylight hour variations in aerosol loadings during the 2008 campaign. The number of readings per school per hour is presented; along with the overall percentage recovery for all schools for each hour.

Hour	BE	JG	JM	Mach	Mar	Rak	ST	TM	% per hourly average
7	24	13	9	19	24	11	11	31	31.70
8	51	30	25	28	28	26	27	19	52.23
9	37	17	40	25	28	31	22	26	50.45
10	33	21	33	28	24	41	31	27	53.13
11	33	19	25	24	29	37	36	42	54.69
12	37	15	36	16	28	35	39	30	52.68
13	32	16	29	22	17	33	22	19	42.41
14	10	4	38	6	6	33	25	16	30.80
15	0	0	33	0	0	23	21	0	17.19
16	0	0	13	0	0	10	11	0	7.59
17	0	0	0	0	0	0	0	0	0.00

Table 3.7: Percentage data recovery for each hour representing daylight hour variations in aerosol loadings during the 2009 campaign. The number of readings per school per hour is presented; along with the overall percentage recovery for all schools for each hour.

Hour	BE	JG	JM	Mach	Mar	Rak	ST	TM	% per hourly average
7	18	9	28	8	20	39	17	24	28.30
8	12	13	35	25	25	58	29	28	39.06
9	12	17	32	18	28	58	13	33	36.63
10	20	11	34	17	22	56	20	21	34.90
11	16	10	29	11	19	57	17	24	31.77
12	21	23	40	14	21	59	17	24	38.02
13	13	17	26	9	25	54	11	27	31.60
14	12	17	26	10	27	54	13	21	31.25
15	7	17	30	10	32	49	6	25	30.56
16	12	21	29	4	27	40	11	14	27.43
17	4	1	3	3	10	15	4	12	9.03

Table 3.8: Percentage data recovery for each hour representing daylight hour variations in aerosol loadings during the 2010 campaign. The number of readings per school per hour is presented; along with the overall percentage recovery for all schools for each hour.

Hour	BE	JG	Mach	Mar	Rak	ST	% per hourly average
7	2	22	2	2	22	16	13.10
8	5	47	6	3	54	27	28.17
9	5	53	7	8	55	24	30.16
10	8	50	11	16	55	29	33.53
11	11	41	8	23	61	35	35.52
12	11	46	5	36	55	28	35.91
13	6	51	4	29	56	31	35.12
14	9	47	3	31	56	28	34.52
15	8	39	6	14	46	24	27.18
16	11	41	10	6	49	23	27.78
17	1	16	1	0	27	6	10.12

Table 3.9: Percentage data recovery for each day representing daily variations in aerosol loadings during the 2008 campaign. The number of readings per school per day is presented; along with the overall percentage recovery for all schools for each day.

Day	BE	JG	JM	Mach	Mar	Rak	ST	TM	% per day
July									
15	6	7	6	4	3	5	5	4	23.81
16	6	0	0	3	3	0	6	0	10.71
17	0	0	0	0	0	7	2	0	5.36
18	0	0	0	0	0	0	12	0	7.14
19	0	0	0	0	0	0	0	0	0.00
20	0	0	0	0	0	0	0	0	0.00
21	17	6	10	7	5	18	13	15	54.17
22	14	14	15	10	8	15	15	12	61.31
23	18	10	1	11	11	11	7	8	45.83
24	4	8	12	8	4	6	8	4	32.14
25	9	3	10	2	3	11	8	6	30.95
26	13	10	11	0	1	13	12	12	42.86
27	15	10	9	14	6	16	12	13	56.55
28	12	2	11	9	1	16	10	6	39.88
29	12	0	14	8	10	17	8	6	44.64
30	16	0	16	11	4	16	8	7	46.43
31	11	0	13	11	7	17	15	9	49.40
August									
1	14	3	15	7	9	12	10	2	42.86
2	5	10	18	0	11	1	11	5	36.31
3	0	6	19	9	6	4	13	2	35.12
4	5	0	8	7	14	13	10	9	39.29
5	14	8	16	8	9	14	12	14	56.55
6	18	6	9	5	14	14	14	12	54.76
7	14	8	14	8	6	10	10	16	51.19
8	13	10	14	5	13	17	13	12	57.74
9	5	2	18	10	14	9	8	8	44.05
10	13	7	17	2	15	0	0	14	40.48
11	3	5	5	4	6	15	3	12	31.55

Table 3.10.: Percentage data recovery for each day representing daily variations in aerosol loadings during the 2009 campaign. The number of readings per school per day is presented; along with the overall percentage recovery for all schools for each day.

Day	BE	JG	JM	Mach	Mar	Rak	ST	% per day
April								
28	5	6	5	4	3	6	3	21.77
May								
4	2	6	0	0	9	3	0	11.90
5	4	17	10	0	10	16	0	33.93
6	4	7	9	0	12	10	0	25
7	4	9	5	0	0	17	0	20.83
8	2	11	11	0	3	19	0	27.38
9	0	6	1	0	0	5	0	7.14
10	0	11	4	0	0	16	0	18.45
11	24	7	0	0	8	19	0	34.52
12	34	15	16	0	13	21	0	58.92
13	2	14	11	5	11	18	0	36.31
14	0	13	18	8	6	15	0	35.71
15	3	9	5	0	7	16	9	29.17
16	3	0	0	0	1	3	0	4.17
17	4	7	1	0	5	21	8	27.38
18	0	0	10	16	2	18	17	37.5
19	11	1	19	5	2	16	16	41.67
20	10	17	6	1	0	23	19	45.24
21	0	0	0	0	0	5	0	2.98
22	9	0	20	0	18	17	10	44.05
23	6	0	19	0	8	19	0	30.95
24	19	0	14	0	0	13	4	29.76
25	1	0	10	4	18	21	6	35.71
26	0	0	14	15	19	21	9	46.43
27	0	0	9	21	20	20	9	47.02
28	0	0	8	11	18	21	5	37.5
29	0	0	18	0	16	19	2	32.74
30	0	0	18	0	18	0	3	23.21
31	0	0	2	0		14	7	13.69
June								
1	0	0	5	6	10	19	2	25
2	0	0	10	0	12	17	5	26.19
3	0	0	14	0	6	18	3	24.40
4	0	0	6	9	0	13	3	18.45
5	0	0	7	11	0	17	8	25.60
6	0	0	0	0	0	12	4	9.52
7	0	0	6	0	0	7	4	10.12
8	0	0	0	4	0	4	1	5.36

Table 3.11: Percentage data recovery for each day representing daily variations in aerosol loadings during the 2010 campaign. The number of readings per school per day is presented; along with the overall percentage recovery for all schools for each day.

Day	BE	JG	Mach	Mar	Rak	ST	% per day
July							
21	11	0	0	15	0	0	20.63
22	8	4	0	0	5	0	13.49
23	1	13	16	3	13	0	36.51
24	0	15	10	0	16	0	32.54
25	0	11	1	7	12	0	24.60
26	0	10	9	6	10	0	27.78
27	12	13	9	10	12	0	44.44
28	13	14	7	9	12	0	43.65
29	0	11	6	12	20	0	38.89
30	0	0	3	10	14	0	21.43
31	0	0	0	9	15	0	19.05
August							
1	0	0	0	0	13	0	10.32
2	0	9	2	0	16	5	25.40
3	0	9	0	0	15	4	22.22
4	10	16	0	8	14	5	42.06
5	14	17	0	2	14	11	46.03
6	0	15	0	0	16	1	25.40
7	0	14	0	0	18	0	25.40
8	0	18	0	0	19	0	29.37
9	0	14	0	0	18	0	25.40
10	0	15	0	0	0	0	11.90
11	8	7	0	9	15	14	42.06
12	0	10	0	8	0	8	20.63
13	0	13	0	0	20	5	30.16
14	0	7	0	0	14	0	16.67
15	0	9	0	0	6	10	19.84
16	0	11	0	11	14	7	34.13
17	0	13	0	12	13	5	34.13
18	0	12	0	0	20	13	35.71
19	0	14	0	0	17	18	38.89
20	0	9	0	10	17	24	47.62
21	0	10	0	11	19	0	31.75
22	0	0	0	8	18	8	26.98
23	0	14	0	0	14	21	38.89
24	0	17	0	0	14	21	41.27
25	0	14	0	0	14	15	34.13
26	0	11	0	0	11	21	34.13
27	0	16	0	0	9	19	34.92
28	0	12	0	0	1	19	25.40
29	0	14	0	0	0	17	24.60
30	0	8	0	8	14	0	23.81
31	0	14	0	0	14	0	22.22

****

The methodology and instrumentation involved in the investigation into the aerosol loading over the Bojanala District have been discussed. The site description reveals that diverse sources of aerosols are prominent in the area. The meteorological background indicates that inversions and low levels of rainfall are characteristic of the area. An investigation into the calibration of the instruments reveals a successful calibration for most of the instruments. Data recovery, however, is low and inconsistent. The following chapter explores the results of each of the 2008, 2009 and 2010 campaigns, considering temporal variation of AOT and Ångstrom exponent for each campaign.

CHAPTER 4: THE PROPERTIES OF AEROSOLS OVER THE BOJANALA DISTRICT

A temporal analysis of aerosol optical thickness and Ångstrom exponent is investigated. The impact of foreign airmasses on the Bojanala District is investigated. Aerosol data is compared to that of ambient particulate matter concentrations. Flight profiles are investigated to discover the distribution of aerosols with height and whether the aerosol loadings may be related to ground-level sources.

4.1.Aerosol Optical Properties

4.1.1. Aerosol Optical Thickness and the Ångstrom Exponent

4.1.1.1. The Frequency Distribution of AOT

The percentage frequency of AOT during the three research campaigns indicates significant differences between AOT levels in early winter as opposed to middle and late winter (Figure 4.1). The 2008 winter campaign data indicates that the frequency of occurrence of AOT between 0.2 and 0.3 is the highest. This level of AOT occurs 20.10% of the time. The most common AOT levels fall between 0.1 and 0.4. Data for the 2009 early winter campaign reveals that the highest frequency of occurrence of values of AOT lie between 0.1 and 0.2 (43.15%). AOT lies most commonly within the range of 0.1 and 0.3. The most commonly occurring AOT value during the late winter 2010 campaign, lies within the range of 0.1 and 0.5. The highest frequency of occurrence of AOT during the 2010 research campaign lies within the range of 0.2 to 0.3, occurring 22.7% of the time. Concentrations of aerosols appear to be lower during the early winter months in 2009 than in the later winter months of 2008 and 2010. AOT levels reach high levels of between 0.3 and 0.5 more commonly during the late winter 2010 campaign than in the previous campaigns. The 0.4 to 0.5 AOT range is almost 8% higher in 2010 than in 2008.

AOT loadings rarely reach above 0.6, however, it is notable that these high levels are more frequent during the 2008 campaign. It is possible that these high levels are caused by the concentration of pollutants as a result of the presence of persistent inversion layers (Tyson, 1986; Tyson and Preston-Whyte, 2000) and enhanced domestic fuel burning practices during these cold winter months (Mathee and Von Schirnding, 2003). The frequency distribution for early winter 2009 is substantially different to that of winter and late winter. This is likely as a

result of domestic fuel burning practices being less pronounced during the warmer months of May and early June (consider Figure 3.5 indicating higher temperatures in May and June); as well as weaker and less frequent inversion layers. As with the early winter campaign, warmer temperatures during late August may result in inversions layers being less pronounced. Further, the high AOT levels identified during late winter may be attributed to the onset of the biomass burning season which peaks from August to October (Queface, 2013).

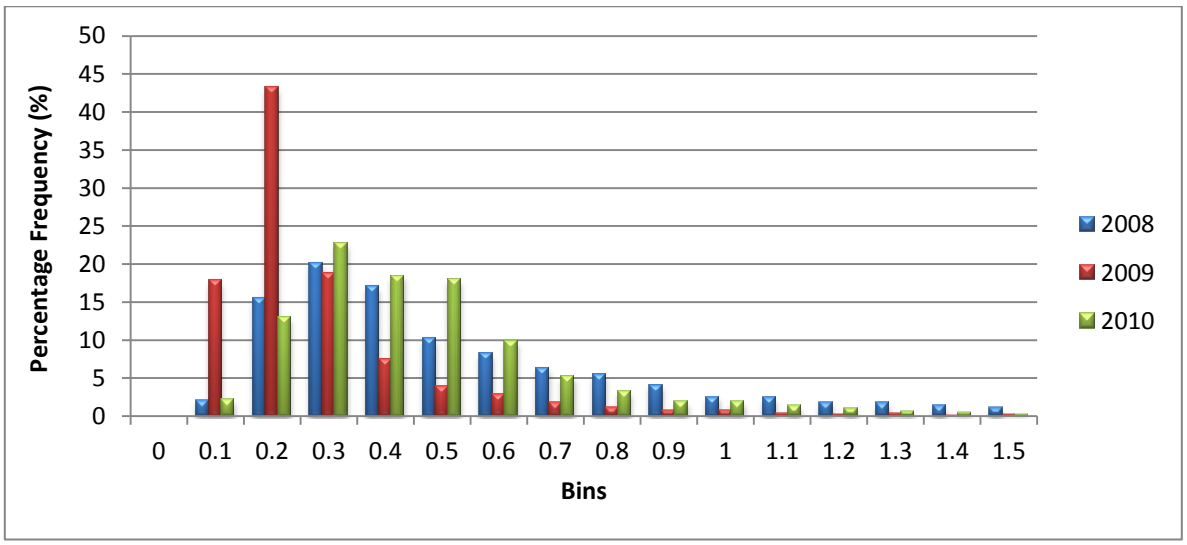

Figure 4.1: Percentage frequency of occurrence of AOT levels between 0 and 1.5 during the three study campaigns.

4.1.1.2. The Frequency Distribution of the Ångstrom Exponent

The frequency of occurrence of the Ångstrom exponent (AE) during the three campaigns indicates a greater frequency of occurrence of larger particles during early winter in comparison to the other campaigns (presented in Figure 4.2). AE values lying between 1.5 and 1.75 are identified as occurring most frequently during the 2008 winter campaign (18.77%). Particles with an AE of between 1 and 1.5 are considered to be accumulation mode particles and are found to occur 28.7% of the time (Tesfaye, 2011). These particles are very important with regard to the attenuation of solar radiation (Powers, 2007) and the quantification of their impacts in the area should be undertaken. Overall, AE's between 1 and 2 occur most commonly, indicating that fine mode particles are significant in the area. AE's below 1 occur 34.03% of the time. This indicates that fine mode (combustion origin) and coarse mode particles (non-combustion sources) are both very important throughout the district. Fine mode particles make up approximately two thirds of the particles characterising

the aerosol loading over the Bojanala District during 2008. The contribution of coarse mode particles is also significant, and this is to be expected as a result of the dust created from mining and other industries. Dirt roads are also commonly travelled by trucks and large mining vehicles resulting in a significant amount of dust entrainment into the atmosphere (AQMP, 2005).

For the duration of the early winter campaign (2009) AE above 1 once again occur most frequently. AE's between 1 and 1.75 exhibit the highest frequency of occurrence at 55.49%. Accumulation mode particles are found to occur 39.88% of the time. This is somewhat higher than that of recorded AE values for 2008. AE values between 1 and 2 occur 61.15% of the time. This indicates a dominance of fine mode, combustion particles to the aerosol loading. AE's lying below 1 (indicating coarse mode particles) occur 35.64% of the time. This is slightly higher than that of the 2008 campaign. AE's for the winter/late winter campaign of 2010 indicate that values between 1 and 1.5 occur most frequently. These values occur 24.22% of the time. This has once again decreased from the 2009 campaign and is similar to that of what is measured during the 2008 campaign. As with the 2009 campaign the most commonly occurring AE values lie within the range of 1 and 1.75 (59.94%). It is clear that both fine and coarse mode particles are important to the aerosol loadings over the Bojanala District. The emissions from the various mining activities in the area, which are in close proximity to the sights, are considered substantial through each campaign as mining activities are not seasonal.

The percentage contribution of fine-mode particles for each campaign (Figure 4.3) reveals that the relative contribution in the frequency of occurrence of fine ($\alpha>1$) particles is similar for 2008 and 2009. The occurrence of fine mode particles is 65.96% during winter 2008, decreasing slightly during early winter 2009 to 64.3%, and once again increasing significantly during late winter 2010 at 71.25%. This is higher than the previous years, when the frequency of occurrence of fine mode particles was approximately two-thirds. It is obvious that during late winter the contribution of fine mode combustion particles is significantly higher than during early winter and winter. It is expected that biomass burning aerosols increase the regional aerosol loading over the northern parts of South Africa during late winter, spring (Tesfaye, 2011). The biomass burning season (peaking during the months of August, September and October in southern Africa) is found to be associated with double the amount of fine mode particles, as coarse mode particles, compared to the other months of the year. The concentrations of fine mode and coarse mode particles are found to be

relatively equal during the other months of the year (Queface, 2013). This is consistent with these findings.

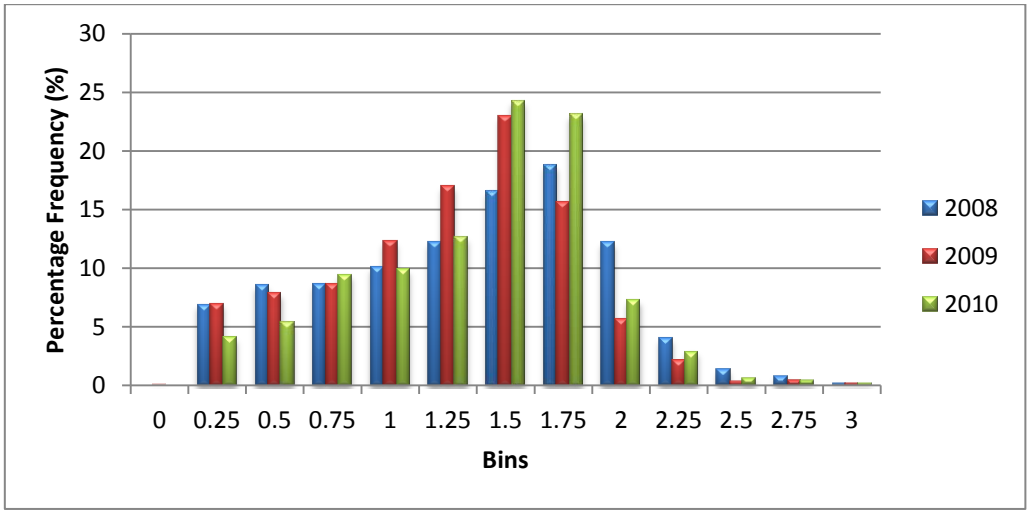

Figure 4.2: The percentage frequency of occurrence of the Ångstrom exponent for the 2008, 2009 and 2010 campaigns.

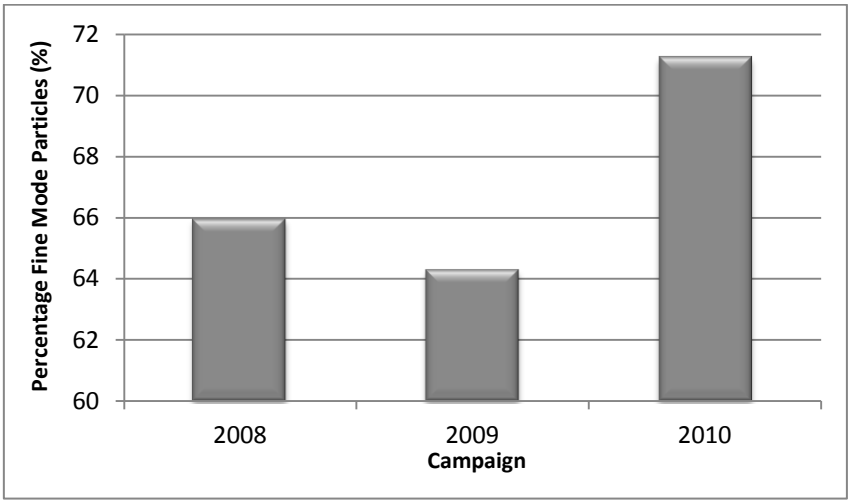

Figure 4.3: The variation in the percentage frequency of occurrence of fine mode particles from the 2008 campaign to the 2010 campaign.

4.1.1.3. Aerosol Loadings over the Bojanala District

The average AOT (Figure 4.4) for the winter 2008 and late winter 2010 research periods is much higher than early winter 2009. The exception is at Bob Edward Middle School (Bob Ed) during 2010 where the AOT was very similar to that of 2009. Studies have found that the average AOT for southern Africa is approximately 0.24 (Queface, 2013). AOT during the 2008 winter campaign ranges between 0.4 at Machadam Combined School (Mach) and 0.61 at St. Theresa High School and is therefore considered high. During the early winter

campaign AOT lies between 0.16 once again at Machadam Combined School and 0.31 at Bob Edward Middle School. The 2010 campaign reveals high aerosol loadings ranging from 0.3 at Bob Edward Middle School to 0.477 at J. Gotsube High School (JG). As mentioned before the aerosol loadings during the 2008 campaign were expected to be high as July and early August are colder months than May and early June in Rustenburg. Many lower income households cannot afford to use electricity for space heating and cooking purposes during winter. As a result many informal settlements burn coal or wood (Mdluli, 2007). As ambient temperatures fall, township households burn more coal (Mathee and Von Schirnding, 2003). As a result, the aerosol loadings on a local scale may increase significantly at this time of year. As domestic fuel burning was found to be an important source of aerosols in the area, and as all of the sites are located within informal settlements, this can be considered as a possible reason for higher aerosol loadings during the 2008 campaign (AQMP, 2005; Venter *et al.*, 2012). As mentioned previously atmospheric stability and recirculation resulting from high pressure systems which dominate the country during winter, as well as recirculation processes which occur both through anabatic and katabatic flow may result in the concentration and stagnation of aerosols from the many local mining and industrial activities and traffic in the atmosphere over the Bojanala District (Tyson et al., 1996b; Freiman and Piketh, 2003; AQMP, 2005). Once again, the high aerosol loadings during late winter 2010 may be related to the onset of the biomass burning season. Aerosol concentrations are found to increase from the non-biomass burning season (April, May, June) to the peak biomass burning season (August, September, October) (Queface, 2013).

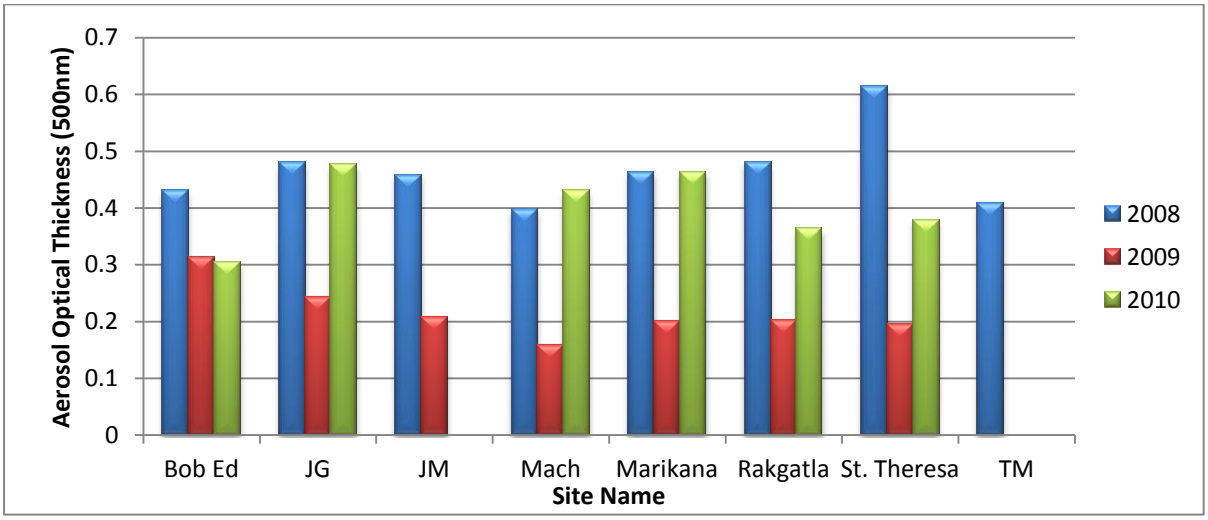

Figure 4.4: The average AOT for each site for the 2008, 2009 and 2010 campaigns.

4.1.1.4. The Variation of Aerosol Particle Sizes over the Bojanala District

The average AE for each site for each of the campaigns (Figure 4.5) reveals that the AE recorded during early winter (2009) is usually lower than that of winter (2008) and late winter (2010), except at J. Gotsube and St. Theresa. What is clear is that there may be significant variation from one site to another in terms of the size of the aerosol particles impacting on that site. It can therefore be assumed that aerosol sources within close proximity to the sites have a detectable impact on the aerosol loading of each site. During the 2008 winter campaign the AE ranges from 0.85 at St. Theresa High School (ST) to 1.6 at Rakgatla High School (Rak). These sites were identified previously to have some of the highest aerosol loadings. This indicates that significant amounts of coarse mode particles such as dust at St. Theresa are responsible for the high aerosol loadings, whereas at Rakgatla High School the aerosol loadings are attributed to the presence of fine mode particles. The higher values of AE during winter is attributed to domestic fuel burning practices as all of the sites lie within informal settlements. The average AE for all of the sites is lowest during the early winter 2009 campaign compared to the other campaigns, except at St. Theresa High School where the AE is higher during the 2009 campaign than the 2008 campaign; and at J. Gotsube High School where the average AE is higher than the 2010 late winter campaign.

At most of the sites during 2009, the AE average lies within the range of 0.9 at Johane Mokololobatsi High School to 1.26 at Rakgatla High School. Four of the eight sites exhibit an AE below or very close to 1 indicating a slightly larger contribution of coarse mode, non-combustion particles. The average AE per site during the 2010 late winter campaign is not as high as during the 2008 campaign. The AE ranges from 1.04 at J.Gotsube High School (JG) to 1.48 at Rakgatla High School. The range in the AE is much lower than in the previous campaigns and averages indicate that fine mode combustion particles are dominant. All of the sites during late winter 2010 are dominated by fine-mode particles. As discussed earlier the peak biomass burning season occurs from August to October in southern Africa. This is associated with a significant increase in the contribution of fine mode aerosols to the aerosol loadings. (Queface, 2013).

The AE at all of the sites during late winter (2010) is expected to be higher than the other two campaigns, especially when considering Figure 4.3. This is not the case however, and this may be a result of the extremes in AE recorded during winter 2008, where AE varied significantly indicating the dominance of coarse to fine particles at various sites. During

2010 the AE is above 1 for all of the sites, but the averages are not as high as those of some of the sites during winter 2008. It may also be assumed that local sources have a greater impact on aerosol loading during winter than during late winter. Biomass burning may therefore have a regional impact. The consistent importance of fine and coarse mode particles throughout the progression of winter indicates the importance of local mining and industrial sources.

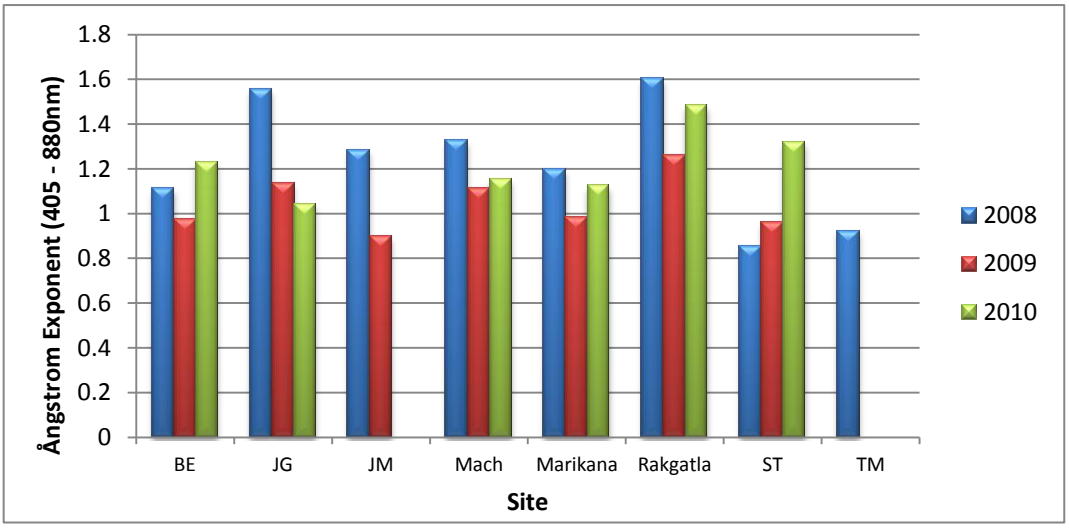

Figure 4.5: Average Ångstrom exponent for each data collection campaign.

4.1.1.5. The Hourly Evolution of Particles During the Various Stages of Winter over the Bojanala District

As a result of the nature of this project, sources of aerosols cannot be identified using variations in AOT throughout the day as AOT takes the entire atmospheric column into account and therefore aerosols aloft may have an impact on the AOT readings.

AOT varies significantly during winter (2008) throughout the day, when compared with the early winter (2009) and late winter (2010) campaigns (Figure 4.6). The AOT ranges between 0.19 and 0.304 during early winter (2009); between 0.18 and 0.99 during winter (2008); and between 0.32 and 0.469 during late winter (2010). The range in AOT is significantly greater during winter (2008) compared with the other campaigns. AOT levels in the morning during winter (2008) are found to be high (0.99) compared with that of early winter 2009 (0.19) and late winter 2010 (0.32).

This diurnal pattern where high AOT levels in the morning over the Bojanala District are identified further justifies the assumption that domestic fuel burning practices are the source of these aerosols. Further, the presence of significant inversion layers during winter serve to concentrate aerosols from domestic fuel burning, industry and traffic along the nearby roads and the N4 platinum corridor (AQMP, 2005). Particles from the local mining activities may accumulate over night under these layers as mining activities are assumed to be continuous. These sources cannot be verified as the aerosol species were not collected and studied.

Domestic fuel burning and traffic signatures also usually result in two significant peaks in ambient pollution concentrations, but due to the limitations of the hazemeters, the second peak could not be identified as readings stop at sunset. The AOT levels decrease sharply as the atmosphere is cleansed and the inversion layers, which are common in the area, deteriorate (BPDM AQMP, 2011). Once the inversion layers lift aerosol particles are dispersed and the attenuation of sunlight decreases as the concentration of particles is reduced due to the ability of the particles to disperse in all directions (Piketh, 1996). AOT levels decrease to levels lower than that recorded during the early and late winter campaigns from approximately midday.

AOT levels during early winter (2009) and late winter (2010) indicate that aerosol concentrations remain relatively stable throughout the day at these stages of winter. The hourly variation of AOT during early and late winter is very similar, however, the levels of AOT during early winter are significantly lower than those of late winter 2010. The highest levels recorded during the early winter 2009 campaign are lower than the lowest AOT levels recorded during the late winter 2010 campaign. The highest aerosol concentrations are recorded in the afternoon during the early (14h00) and late winter (13h00) campaigns.

As mentioned above, the hourly AOT averages for July and August 2010 indicate a significantly different trend in AOT, than in 2008. As data was collected during July and August for both campaigns, the trends were expected to be similar. However, the 2010 campaign extended until the end of August during 2010; whereas during 2008 the campaign ended on the 12th August. During the 2008 campaign AOT was highest during the morning, whereas during 2010 the AOT is highest at midday. The increase toward midday during

2010 is, however, not very pronounced. At 13h00, the AOT reaches its maximum at 0.49. Aerosol concentrations were expected to decrease as the day progressed, as a result of the lifting of the inversion layer, but this is not the case for late winter 2010. As discussed previously (and when considering the average temperatures in Rustenburg presented in Figure 3.4) the warmer temperatures associated with the onset of spring may result in less pronounced inversion layers and a reduction in the need for domestic fuel burning. The diurnal trend identified indicates that AOT does not reach the same levels as in 2008, however, the aerosol concentrations remain high throughout the day during late winter 2010, which leads to the conclusion that very little dispersion has taken place during late winter (2010) or perhaps more pollutants are being brought into the area or generated throughout the day. The difference between the winter and late winter diurnal trends may once again be associated with the onset of the biomass burning season. Biomass burning is usually irregular and may occur at any time of the day.

The differences between the diurnal pattern in winter compared to early and late winter are significant. The standard deviation during winter (2008) per hour (presented on the graph) indicates significant deviation; as well as a decrease in standard deviation values as the day progresses. The standard deviation, however is not such that the elevation in the AOT is doubtable. Considering the standard deviation presented, it is still clear that morning AOT is significantly higher than afternoon AOT. Further, data collection (presented in Table 3.6) indicates a reasonable spread and consistency over all the sites and over the morning and afternoon. It is clear that the high AOT during winter mornings may sway the data for the overall averages (in previous section), however, this is representative of the impacts of winter meteorological conditions and domestic fuel burning in the area.

Standard deviation varies from 0.04 to 0.17 during early winter (2009). Values decrease until midday and increase thereafter. The range in standard deviation is highest during 2010, varying from 0.05 at 8am to 1.38 at 10am. The significantly high standard deviation identified during each campaign is expected as the instruments are hand-held and the values are representative averages of hourly averages for all the schools.

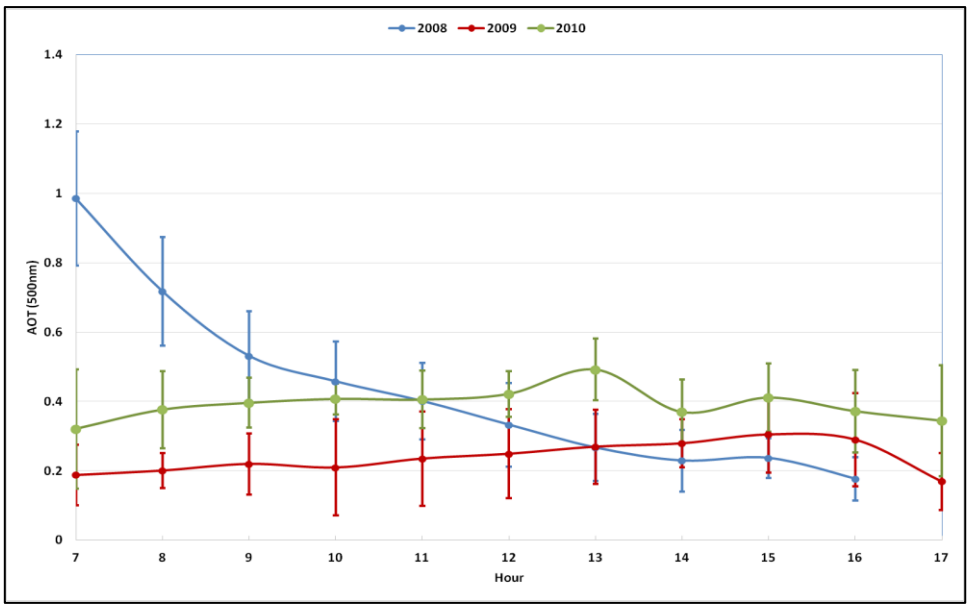

Figure 4.6: The diurnal trend in AOT presented as an average for all sites during the 2008, 2009 and 2010 campaigns. Standard deviation for each hour is indicated.

The Ångstrom Exponent

The variation of the Ångstrom exponent (AE) reveals a similar pattern to that of AOT for all three campaigns, and therefore further justifies the aerosol sources responsible for these patterns (discussed in previous sections). The range in the AE (Figure 4.7) varies from 0.62 to 1.7 during winter 2008; between 0.969 and 1.11 during early winter 2009; and between 1.11 and 1.36 during late winter 2010. The diurnal variation in the AE plotted as an hourly average for all the sites indicates that the size of particles tends to increase significantly throughout the day during the 2008 campaign (indicated by a decrease in AE). As with AOT, AE is highest at the commencement of readings during winter (2008). AE levels are at 1.7 at the commencement of data collection and continue to decrease throughout the day as with AOT. It is clear that combustion particles are resulting in the high AOT levels measured during the morning in winter 2008. At approximately 13h00 the AE decreases to below 1. It is clear that the steady decrease in the AOT measured is associated with a gradual change in aerosol source; or an increase in the dominance of a source which emitted significantly larger aerosols. Coarse mode particles, and therefore non-combustion aerosol sources become more dominant as the day matures. AE levels reduce to very low levels as AOT decreases indicating that the very large particles which become dominant at this time of the day. It is clear that these large particles do not have a significant impact on incoming solar radiation

(as indicated by Seinfeld and Pandis, 2006). Dust was found to be a significant problem in the Rustenburg area (AQMP, 2005).

As with the 2008 winter campaign, variation in AE during early and late winter exhibited a similar trend to that of AOT at these stages of winter. AE appears to have remained fairly stable throughout the day during early winter (2009), with only small variations of 0.14. AE remained slightly above 1 indicating the slight dominance of fine mode particles. While AOT increased slightly from 10am, only small increases in AE are identified after this time, indicating that the aerosol source has remained relatively consistent. As a result of the absence (or less common occurrence) of domestic fuel burning and biomass burning during early winter, it is possible that AOT and AE variations may be associated with local industrial sources which are consistent throughout the year.

As with the early winter campaign, the AE remains fairly stable during late winter 2010. Variation is somewhat more pronounced, but is still low (0.25) when compared with the range identified for winter 2008. The slight peaks identified in AOT (Figure 4.6) appear to coincide with slight decreases in AE at the same time of day. The changes are only small and this leads to the conclusion that aerosol species/sources have not changed considerably. AE remains above 1 at all times. It is evident that slightly larger particles are more abundant and result in the slightly higher AOT levels at these times of the day.

As with the standard deviation in AOT the standard deviation in the AE varies throughout the day. Standard deviation is highest at approximately midday during winter (2008) and late winter (2010), ranging from 0.15 at 5pm to 0.37 at midday; and from 0.11 at 7am to 0.38 at 1pm, respectively. Variation of standard deviation during early winter (2009) indicates the opposite trend, with a very high standard deviation at 5pm (0.424), and the lowest at midday (0.14).

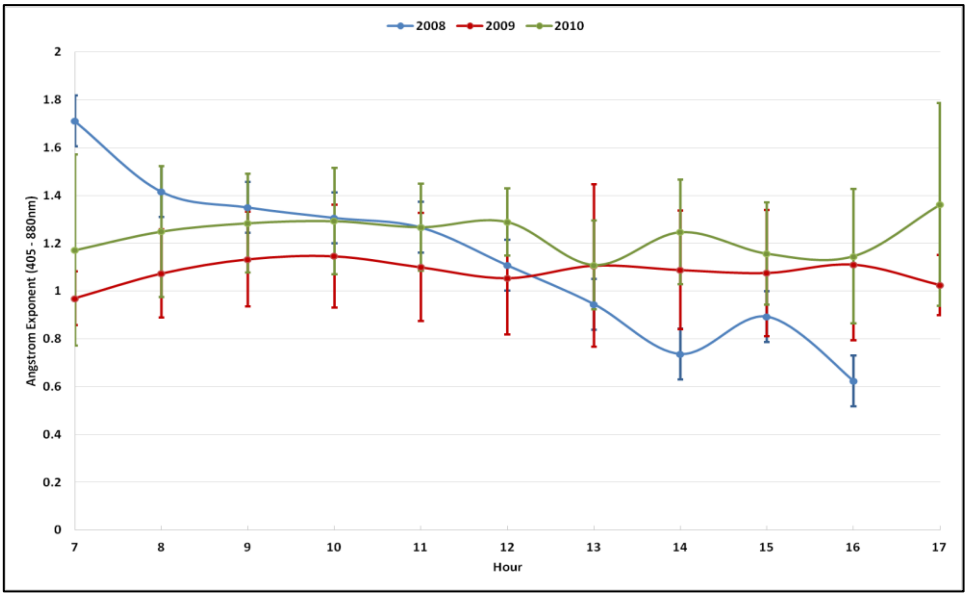

Figure 4.7: A comparison of the diurnal variation in the Ångstrom exponent for each campaign calculated as hourly averages for all sites. Standard deviation for each hour is indicated

4.1.2. Episodes of Extreme Aerosol Loadings over the Bojanala District and the Association with Foreign Airmasses

The variation in AOT during early winter 2009 (Figure 4.9); winter 2008 (Figure 4.8) and late winter 2010 (Figure 4.10) indicates that the aerosol loadings vary from day to day over the Bojanala District. The purpose of these plots is to indicate the changes in AOT which occur from one day to the next over the Bojanala District. According to Li (2007), AOT should not vary significantly from one day to the next. Daily average AOT varies between 0.26 to 0.79 during the winter 2008 campaign; between 0.087 to 0.549 during the early winter 2009 campaign; and between 0.19 to 0.67 during the late winter 2010 campaign. The highest average daily aerosol loadings were recorded during winter 2008. The minimum AOT average recorded during winter 2008 is the highest minimum AOT compared to the other stages of winter (2009 and 2010).

The temporal variation in AOT (500nm) for the winter 2008 campaign per site (top) and on average (bottom), plotted as daily averages reveals that the aerosol loadings are found to be fairly uniform throughout the district. It is clear that on certain days the AOT increases at all of the sites. The average daily AOT (Figure 4.8 – bottom) calculated for all the sites combined for winter 2008 is 0.485. AOT levels are above average 35% of the time. AOT levels often exceeded 0.5 and even reached levels of 0.79. The highest AOT daily averages

are indicated by red arrows. AOT remains high for extended periods of time; with reduced AOT levels of below 0.4 lasting for approximately two days. AOT levels, when significantly elevated, remain so for up to four to five days. The AOT levels are considered high on average. Periods of extreme aerosol loadings (indicated by arrows) last for up to three days. AOT levels above 0.4 are considered high, and it is obvious that these levels are reached frequently during winter (Queface, 2002).

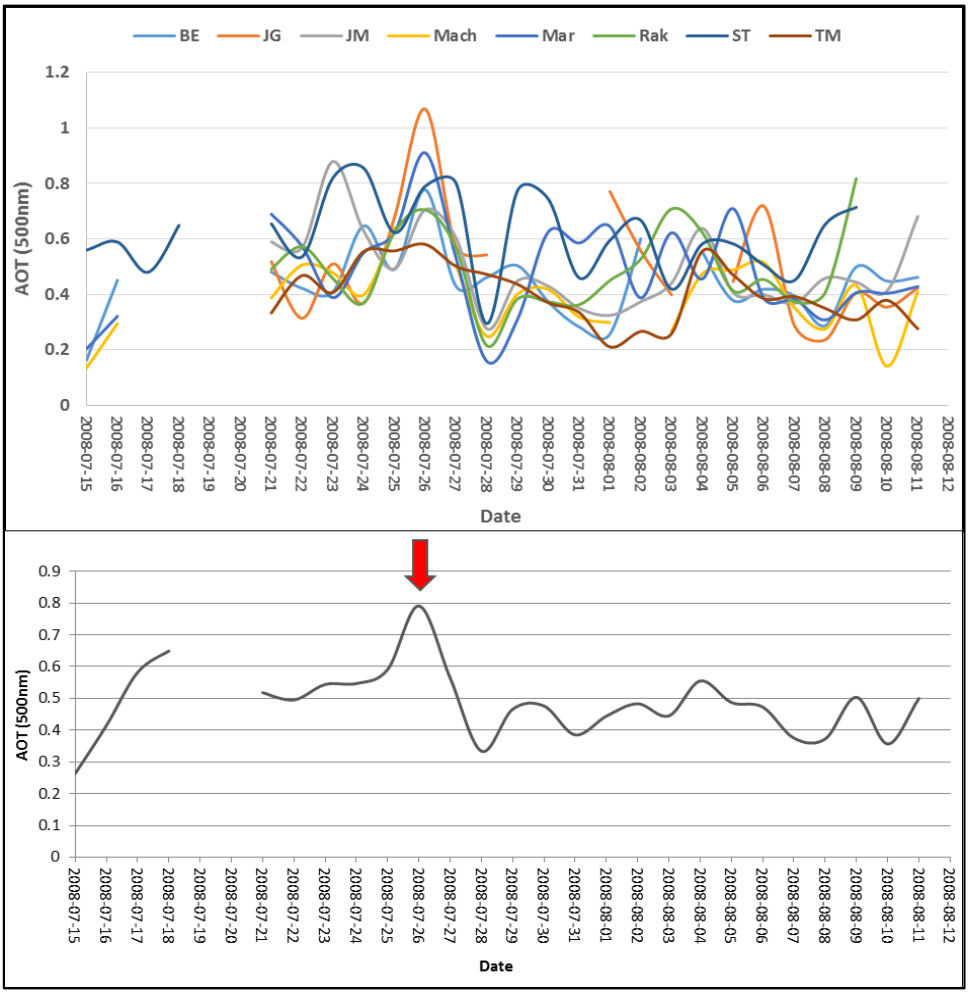

Figure 4.8: The daily average AOT for all of the research sites in the Bojanala District (above). Daily average AOT for all sites together is presented to identify overall high AOT days for the district (below). Red arrows indicate the highest daily averages recorded for the district.

The daily average variation of AOT during the early winter campaign of 2009 indicates that AOT varies significantly from one day to the next compared to the 2008 campaign (Figure 4.9). Analysis of synoptic charts has revealed that atmospheric conditions were often cloudy to overcast during the 2009 campaign, making data collection difficult. This may also be the

reason for the significant variation in the AOT; even though the data was quality controlled in this regard. The average AOT for all of the sites combined during early winter 2009 is 0.240. The highest AOT daily averages recorded (indicated by red arrows) are 0.54 and 0.55. AOT levels only reach levels above 0.4, 11% of the time during this early winter campaign. It appears that during early winter the AOT varies considerably within every two days or so. Periods of slightly elevated AOT are found to last for up to seven days, whereas significantly high peaks in AOT usually last for two to three days. The atmosphere appears to be cleansed twice during the period of data collection, reducing AOT to within 0.09 to 0.25 for up to twelve days.

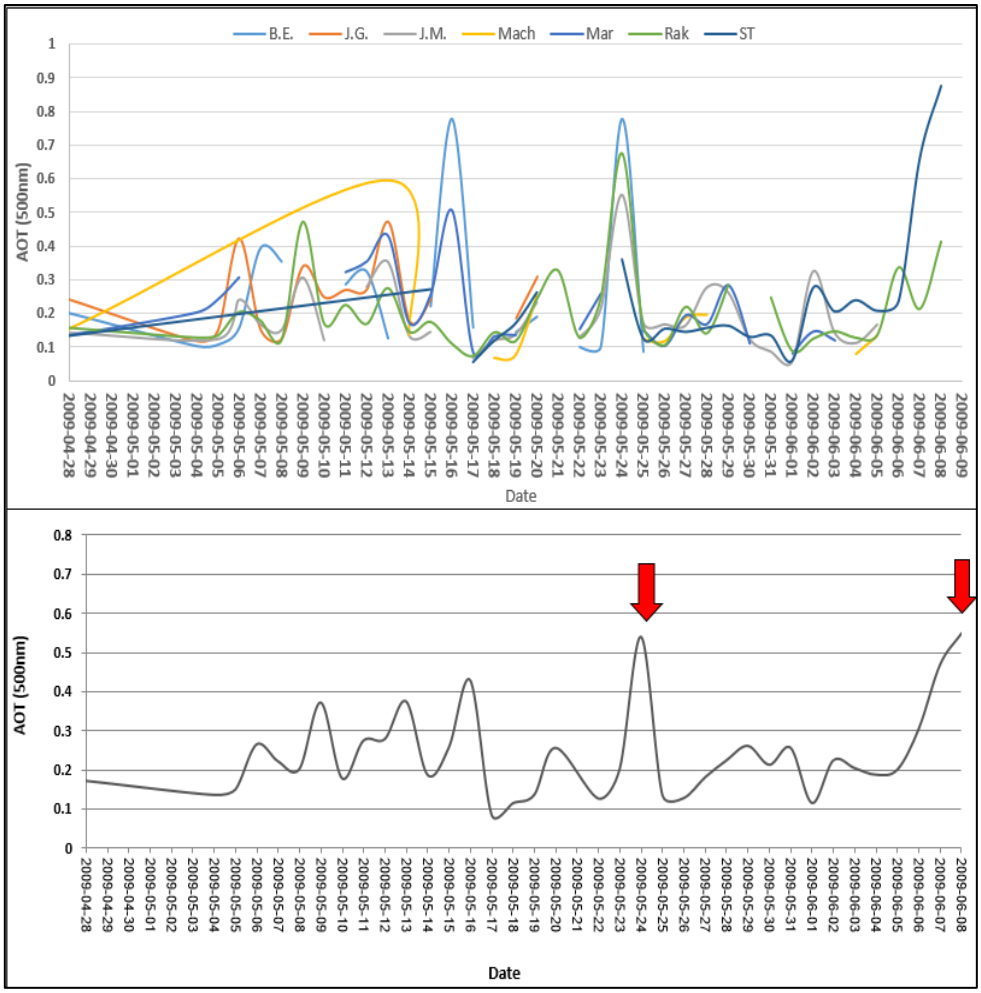

Figure 4.9: Temporal variation in AOT during the 2009 campaign. Red arrows indicate the highest daily average AOT recorded.

As with the early winter campaign, daily average AOT during the 2010 late winter campaign (Figure 4.10) indicates significant variation in AOT on occasion. Inconsistencies in data (top) are clear. The same high peaks/ periods of elevated AOT are identified in each season. These peaks (Figure 4.10 – bottom) are large and last two to three days, followed by days of

clean air and then a gradual increase. The average daily AOT for all sites combined is 0.416 during late winter 2010. AOT levels appear to remain elevated for long periods of time. Extreme peaks in AOT (red arrow) levels last for two to three days, as was also identified in early winter 2009 and winter 2008. AOT appears to remain within the range of 0.3 to 0.5 for long periods of time; with periods of reduced AOT (0.2 to 0.3) lasting up to eight days. A consistent increase in daily average AOT from the 15th August is clearly evident. It is from this point onwards that the highest AOT levels were recorded, exceeding 0.5 for seven days at the end of August (indicated by black arrows). During this period, AOT levels remain well above average. This further justifies that the high AOT measured in late winter is related to the onset of the biomass burning season which commonly has an impact in the area (AQMP, 2005).

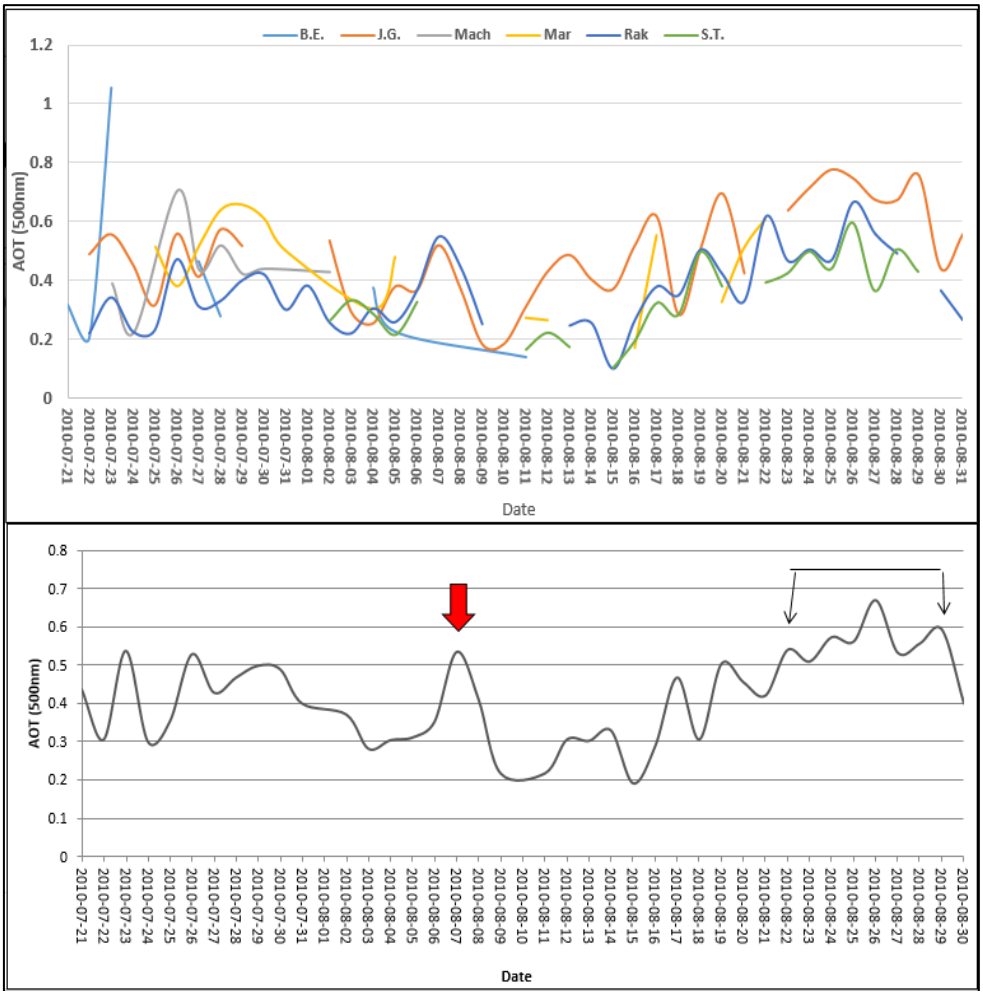

Figure 4.10: Temporal variation of AOT during the 2010 winter campaign. Arrows indicate periods of elevated AOT.

Periods of extreme AOT levels identified during the three stages of winter above may be associated with the impact of long-range transport or foreign airmasses as the aerosol loadings drop or increase significantly over the entire district.

4.1.3. The Impact of Foreign Airmasses on the Bojanala District

HYSPLIT trajectories were created for the Bojanala District to determine the impact that foreign airmasses from specific areas mentioned in Chapter 3 had on the aerosol loadings over the district during the period of data collection. The trajectories in this section were created on the Air Resources Laboratory-HYSPLIT website (www.arl.noaa.gov/HYSPLIT.php) and were set to run for a 72-hour period prior to the date of interest. Trajectories were set up to run every six hours and were plotted at arrival heights of 500, 1000 and 1500m above ground level. The purpose of selecting these heights is that the instruments detect the amount of solar radiation reaching the surface and therefore higher levels of the atmospheric column are considered.

A significant increase or decrease in AOT or Ångstrom exponent at all of the sites indicates that a foreign airmass has potentially entered the region. On a number of occasions the aerosol loadings increased significantly on average for all the sites. Inconsistencies in the data are clear for the early winter and late winter campaigns (Figure 4.9 (top) and Figure 4.10 (top). Elevated aerosol loadings are therefore not identified at all sites, and peaks in AOT in the overall average graphs (Figure 4.9 (bottom) and Figure 4.10 (bottom)) are therefore used to identify high or low AOT days. HYSPLIT trajectories were created for these high AOT days in order to identify where these aerosols are originating from; and to understand whether the airmasses resulting in these elevated levels of AOT potentially have a common origin. A number of trajectories indicate a common origin or path, originating from, or moving over, the Mpumalanga Highveld (Figure 4.11) during all three stages of winter. The trajectories (a, b and c) were created for the events which occurred on the 26th July 2008, 13th May 2009 and 7th August 2010, respectively. On each of these days an airmass which originates from, or passes over, the Mpumalanga Highveld moves into the Bojanala District. It is apparent that airmasses recirculated over the interior in all three examples.

The Mpumalanga Highveld is a highly industrialised area, home to many power stations and industries. The airmasses which originate over the Indian Ocean (a) may accumulate

significant amounts of aerosols as they move down to ground level over Mpumalanga. The trajectories (b) are shown to originate from ground-level up to 1000m above the Mpumalanga Highveld. The blue and red trajectories (b) may indicate that the recirculation of airmasses takes place in the area, which results in the build-up of pollutant concentrations and the lack of atmospheric dispersion and cleansing (Piketh, 2000). These airmasses circulate at up to 1000m above the district and may have had an impact on the aerosol loadings as AOT takes the entire atmospheric column into account. Further, an airmass originating from the same atmospheric levels toward the northern part of South Africa also had an impact on the aerosol loading of the district. Recirculation over the Mpumalanga Highveld is once again identified in the trajectory plotted for the 7th August 2010 (c). This trajectory indicates that prior to the 7th August 2010 recirculation over the interior over the country is prominent. Studies have shown that recirculation is common over southern Africa, and pollutants may be recirculated for a number of days before exiting over the oceans (Garstang *et al*., 1996; Piketh, 2000). The peaks identified in the aerosol concentrations at these times could possibly have been caused by this. The significant rise in aerosol concentrations means that aerosol particles impact significantly on direct solar radiation over the area.

A similar low-level recirculation pattern was identified toward the end of the late winter campaign of 2010 (Figure 4.11c). The biomass burning season reaches maximum intensity in South Africa in September (BPDM AQMP, 2011). It is therefore of interest to identify whether biomass burning activities could have resulted in the elevated AOT levels recorded at this time. Fire data downloaded from the Advanced Fire Information System website (southernafrica.afis.co.za) was requested from 23rd August 2010 to coincide with the HYSPLIT trajectory which was set up to run for 72 hours prior to the 26th August 2010. The figure was created using MODIS/MISR data (Figure 4.12). Airmasses originating from the Indian Ocean move over South Africa, along the northern border before changing direction and moving Southward over the Bojanala District. These airmasses, which remain within the range of ground-level up to 500m move over a significant number of fires during this time.

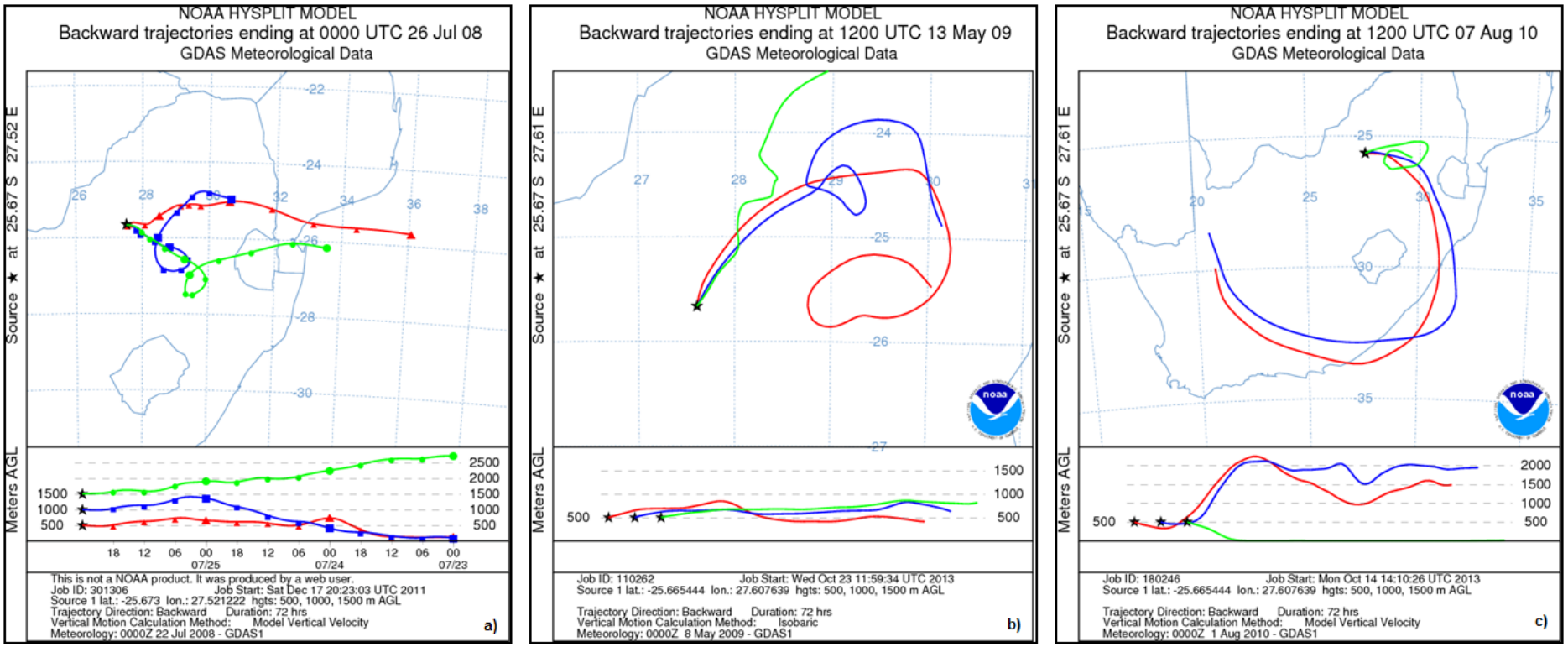

Figure 4.11: HYSPLIT trajectories indicating the movement of airmasses from over the Mpumalanga Highveld and areas east of the Bojanla District for 26 July 2008 (a), 13 May 2009 (b) and 7 August 2010 (c).

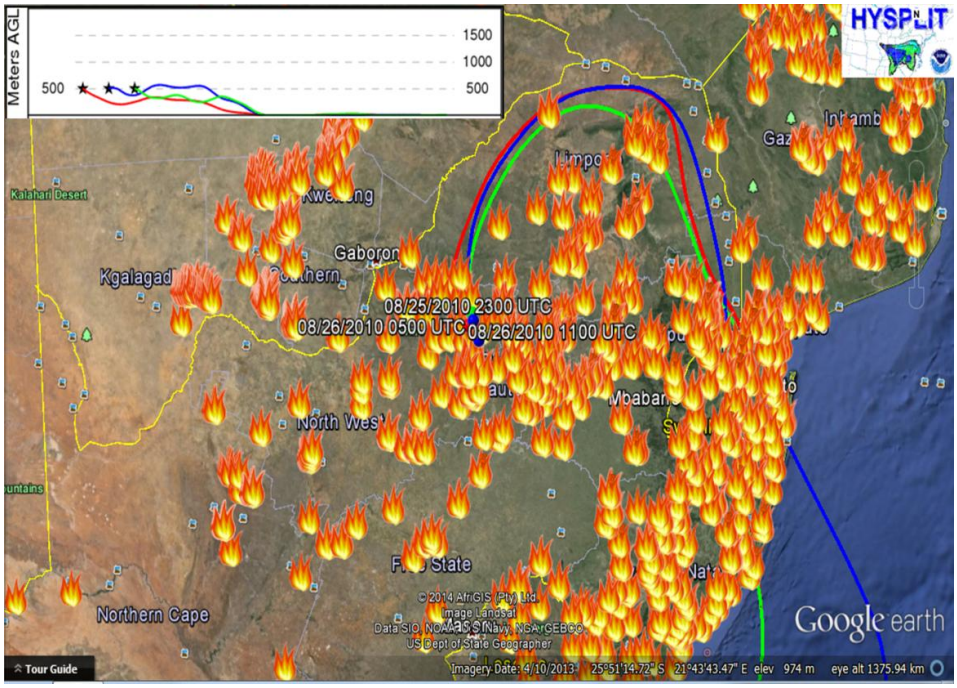

Figure 4.12: HYSPLIT trajectory for the 26th August 2010, together with AFIS data created for the time period from 23rd August 2010 to 26th August 2010. Fires are indicated by orange fire icons.

Wind roses created to understand the surface wind conditions on the high AOT days discussed above (Figure 4.13) indicate that the surface wind direction was similar to that of the indicated direction of entry of the foreign airmasses on 13 May 2009 and on 7 August 2010. The wind rose created for 26 July 2008, however, indicates a different surface wind direction, indicating the possibility of sources originating from different directions at different levels in the atmosphere. It is therefore clear that ambient particulates at various levels in the atmosphere have an impact on the aerosol loadings over the district.

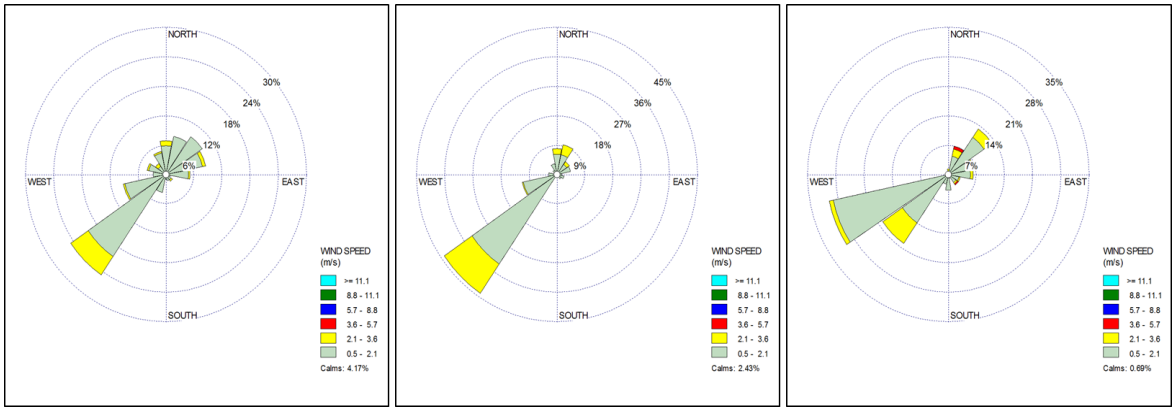

Figure 4.13. Surface wind roses created for days of high AOT recorded on 26 July 2008 (left), 13 May 2009 (middle) and 7 August 2010 (right)

Foreign airmasses appear to also have a positive impact on the aerosol loadings over the Bojanala District. A number of trajectories were plotted to coincide with days where aerosol loadings were found to be below average (Figure 4.14). These trajectories, created for the 29th July 2008 (a); the 1st June 2009 (b) and the 10th July 2010 (c) indicate that airmasses originating from over the Atlantic Ocean move into the Bojanala District on the same day as average aerosol loadings decrease significantly. These south-westerly airmasses often move over southern Africa in winter as a Low Pressure Cold Front system. Airmasses such as these transport clean air from over the ocean into the research site from high levels in the atmosphere, causing aerosol concentrations to drop. Airmasses from as high up as 6000m are identified to potentially have an impact on the aerosol loadings over the Bojanala District (a and c). According to Tesfaye (2011) the concentrations of aerosols tend to decrease with height. It can therefore be assumed that the airmasses originating from such high levels in the atmosphere carry lower concentrations of aerosols.

Occasionally, airmasses originating from the Atlantic Ocean during winter may be accompanied by rain. Studies over southern Africa reveal that rainfall serves to remove aerosols effectively through wash-out processes (Yum and Hudson, 2001). Further, these systems, which often move over the country in winter, may bring larger particles into the area, as natural aerosols such as sea salt aerosols commonly tend to be larger (with a few exceptions) than combustion aerosols (Seinfeld and Pandis, 2006; Eck *et al*., 2005). The result is that the air over the Bojanala District may be mixed well with the cleaner air originating over the oceans and therefore the concentrations of aerosols decrease. This sort of occurrence is common during the 2009 campaign and was also identified on other occasions. Overall, the aerosol loadings during the early winter campaign are significantly lower than the aerosol loadings during the winter and later winter campaigns (as discussed in the previous sections). This may be attributed to the frequency with which these south-westerly airmasses impacted on the Bojanala District.

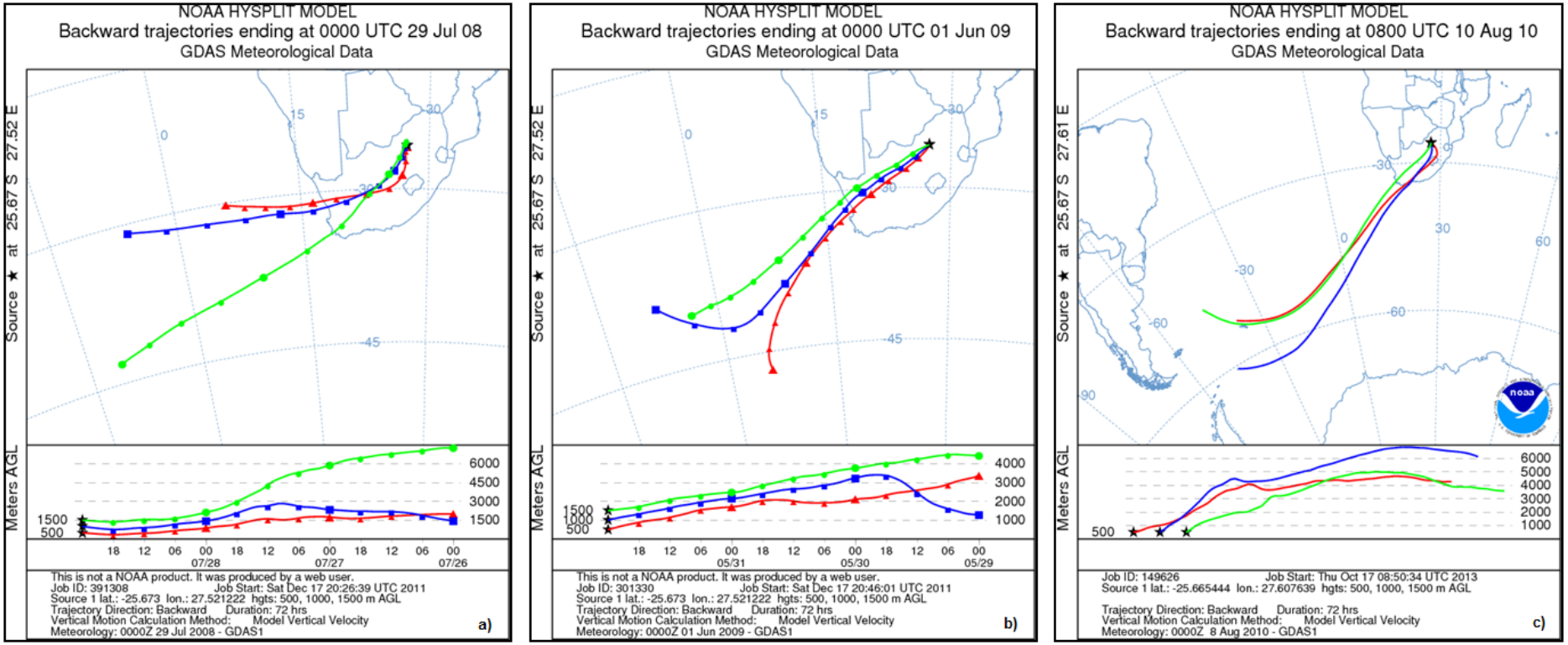

Figure 4.14: HYSPLIT trajectories indicating the movement of airmasses from high levels over the Atlantic Ocean into Bojanla Distrist for 29 July 2008 (a), 1 June 2009 (b) and 10 August 2010 (c).

A HYSPLIT trajectory was created for a day when aerosol concentrations are significantly lower than on other days during the late winter 2010 campaign (Figure 4.15). The lowest AOT daily average levels for the late winter campaign of 2010 occur on this day and trajectories were set up to coincide with this date. The AOT is recorded at 0.19 for the day over the district. The origin of clean air is found to lie to the west of the Bojanala District. This area to the west was found by Josipovic (2011) to be an area where background airmasses (clean air) originated. The airmass originating from a westerly direction possibly has the effect of reducing aerosol concentrations in August 2010.

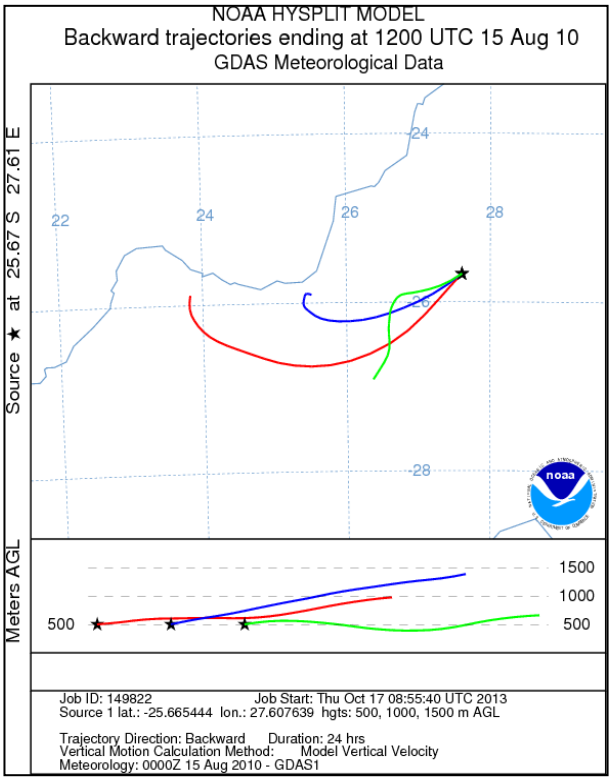

Figure 4.15: HYSPLIT trajectory indicating the movement of airmasses from areas west of the Bojanla Distrist for 15 August 2010.

4.1.4. The Relationship between Aerosol Optical Thickness and Ambient Particulate Matter Concentrations

Particulate data received from a study carried out by Paul Beukes and colleagues at the University of Potchefstroom's Unit for Environmental Science and Management is used to identify whether a correlation exists between ambient particulate matter concentrations and AOT at Marikana in the Bojanala District. In 2008 particulate matter concentrations were recorded using a Tapered Element Oscillating Microbalance (TEOM) instrument rotating between PM1, PM2.5 and PM10. Time resolution is limited as readings were only taken

every hour, alternating between the three particulate sizes, therefore data for each PM size was only recorded every three hours. During 2009 PM concentrations were measured using a Synchronized Hybrid Ambient Real-time Particulate Monitor (SHARP), model 5030, which replaced the TEOM. Only PM10 data was recorded every 15 minutes. No data is available for comparison with the 2010 aerosol data.

As the particulate matter concentrations are measured at ground level, it was uncertain as to whether any correlation between these concentrations and the aerosol loadings measured by the hazemeters would be identified. The reason for this is that aerosol loadings measured by the hazemeters measure the entire atmospheric column, whereas PM concentrations only measure ground-level (ambient) concentrations. This data is therefore used to aid in the understanding of whether a relationship exists between the aerosol loadings measured and ambient particulate matter concentrations. PM1, PM2.5 and PM10 concentrations recorded during the same period of measurements during the July and August 2008 campaign are used as a comparison; as well as PM10 concentrations recorded during the 2009 campaign. Unfortunately only a few PM values are available for comparison as a result of the poor temporal resolution of the data; and further, as a result of the limitation of AOT data, which is only available for daylight hours. The data is plotted as diurnal averages in order to observe the correlation between particulate matter concentrations and aerosol loadings at different times of the day.

It is clear from the figures that PM2.5 and PM10 diurnal trends (Figure 4.17 and 4.18 (top)) are very similar to that of the AOT diurnal trend; however, the PM1 diurnal trend is significantly different (Figure 4.16(bottom)). Further, the PM data is plotted for the full diurnal profile to indicate (Figures 4.16 (bottom) to 4.18 (bottom)), as a matter of interest, that the aerosol loadings decrease at the same time as the PM10 and PM2.5 concentrations decrease. With consideration of the close relationship between the PM10, PM2.5 and AOT throughout the day it is interesting to note the full diurnal profile of particulate matter indicates significant morning and evening peaks in data. Concentrations reach their lowest points at the warmest times of the day. These peaks and troughs in ambient data assist in the assumptions that domestic fuel burning, traffic emissions and inversion layers are important factors which affect aerosol concentrations in the area. A slight peak in PM1 at

approximately 10am reveals the importance of industrial emissions to the PM1 concentrations. This peak is not identified in the AOT, PM2.5 or PM10 data. The importance of the local mining and industrial activities to the PM1 concentrations is therefore highlighted.

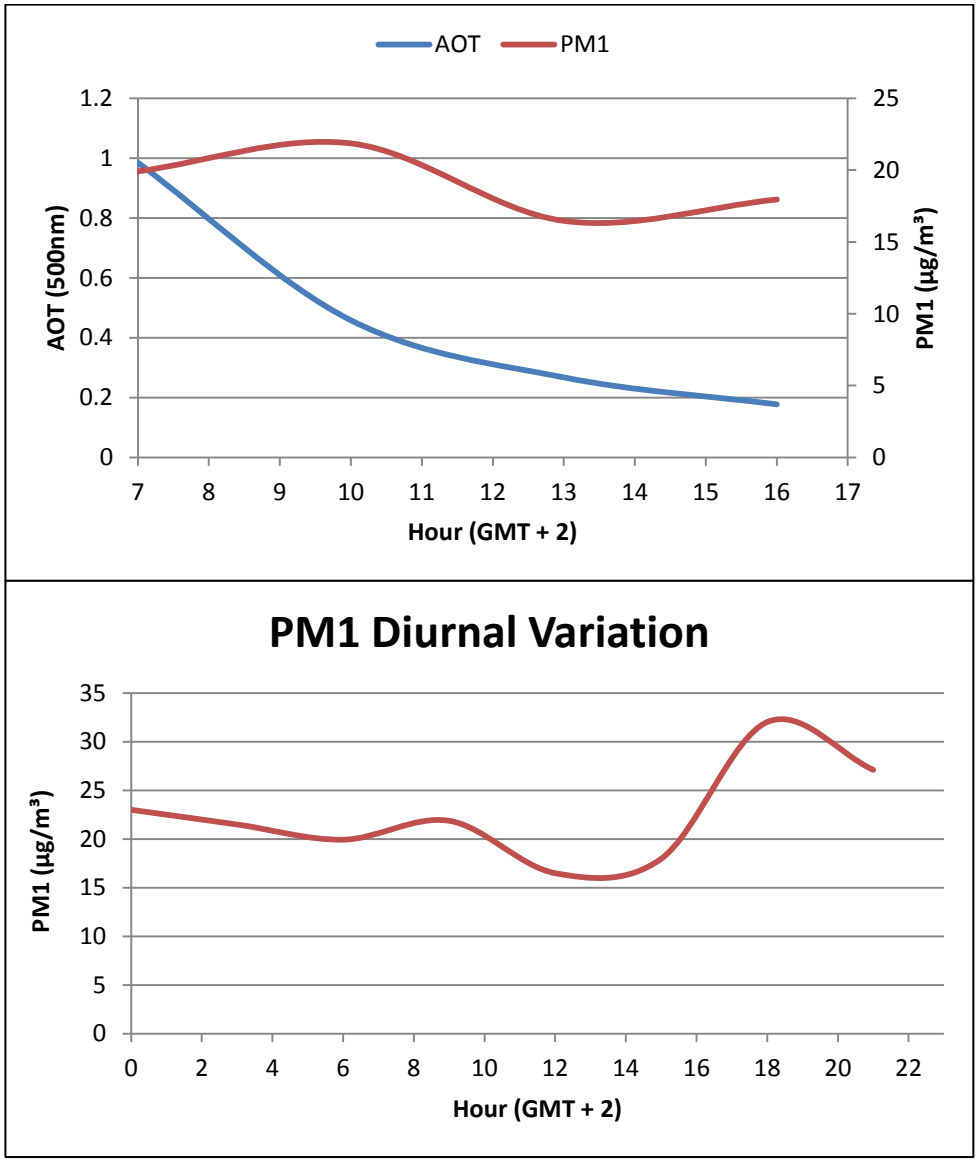

Figure 4.16: Diurnal trends in AOT and PM1 between 21 July 2008 and 12 August 2008.

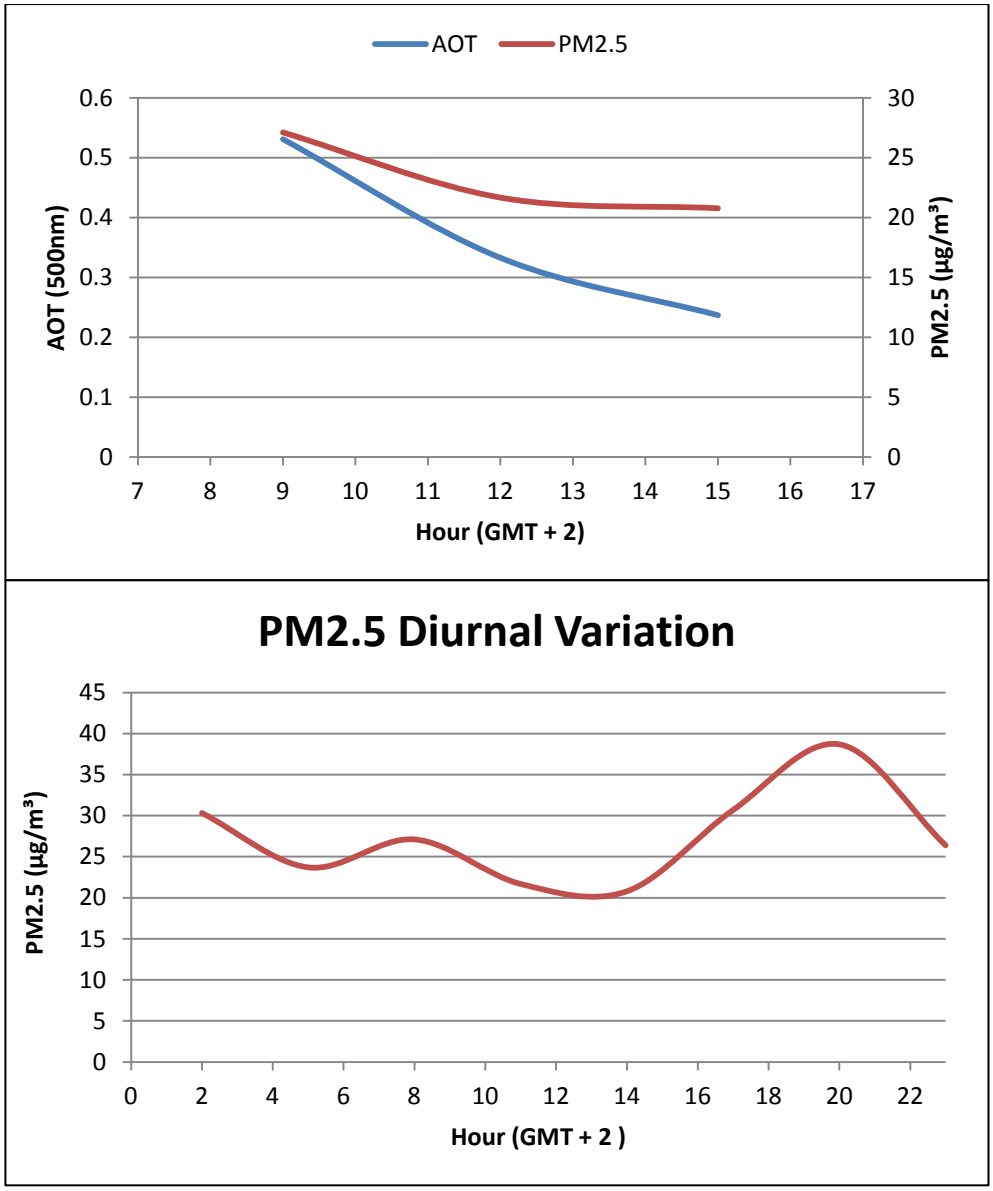

Figure 4.17: Diurnal trend in AOT and PM2.5 measured between 21 July 2008 and 12 August 2008.

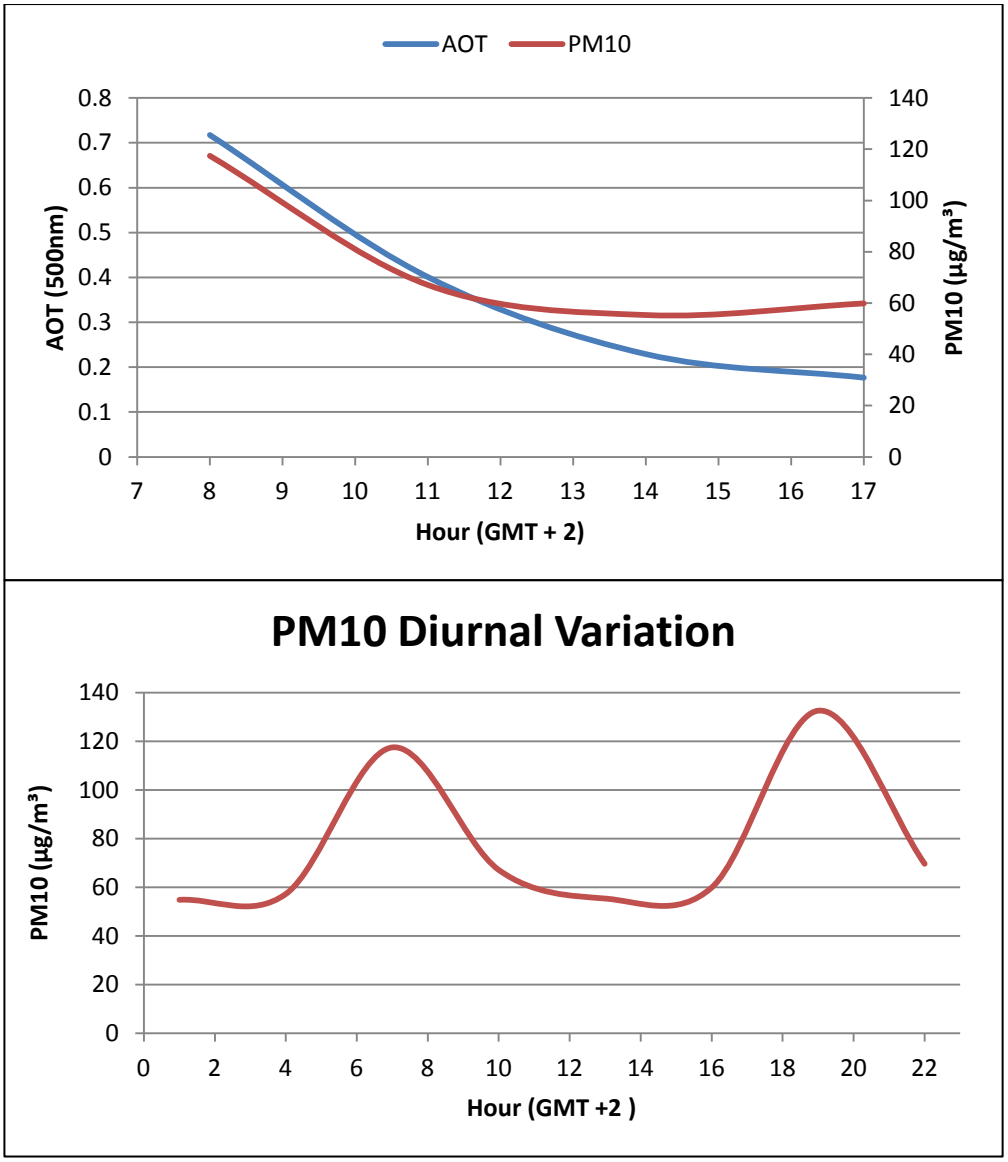

Figure 4.18: Comparison of diurnal variation in AOT and larger aerosol particles (PM10) recorded between 21 July 2008 and 12 August 2008.

The relationship between AOT and PM10 concentrations measured during the 2009 early winter campaign is poor (Figure 4.19). The diurnal variation in PM10 does not compare well with the AOT data when compared with that of the 2008 winter campaign comparison discussed above. AOT increases gradually throughout the day, while PM10 concentrations decrease. A sharp decrease in AOT at approximately 16h00 corresponds to a sharp increase in PM10 at the same time. This change further illustrates the inverse relationship identified during the preceding hours. The morning and evening peaks in PM10 are once again identified during early winter as with the 2008 winter campaign. Unfortunately PM2.5 and

PM10 data is not available for comparison to establish whether a similar correlation exists between the PM2.5 and PM1 data as identified for the 2008 winter campaign (above).

It appears that the PM10 concentrations vary from one hour to the next during the 2009 early winter campaign more than during winter 2008. The PM10 concentrations identified are significantly lower than during winter 2008. The differences in the correlation between PM10 and AOT during winter 2008 and early winter 2009 requires further investigation. It is possible that upper-air airmasses have a greater impact on the aerosol loadings during early winter, or perhaps, that the aerosol sources differ significantly.

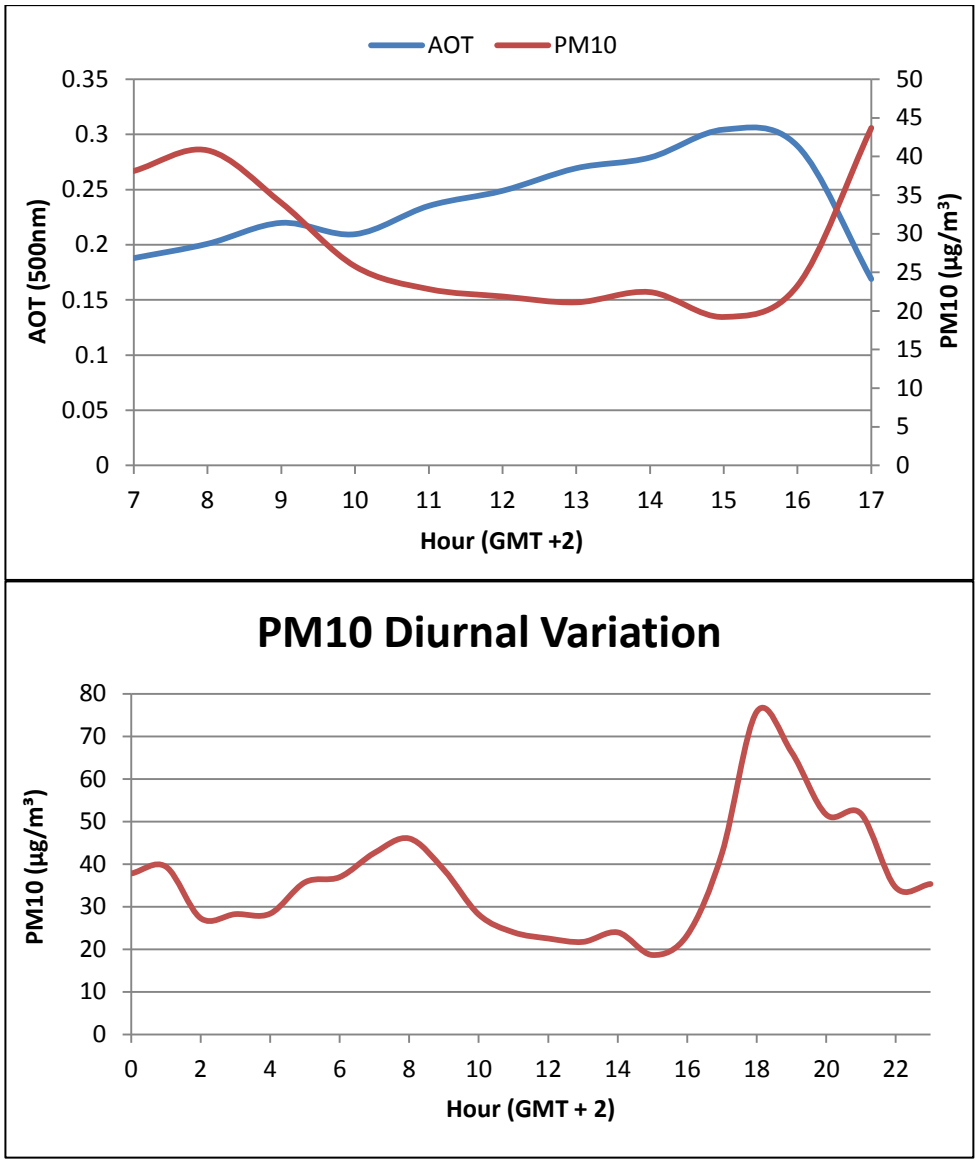

Figure 4.19: Diurnal variation in AOT compared with that of PM10 during the 2009 campaign.

4.1.4.1. The Relationship between AOT and Particulate Matter

Only the AOT and the PM10 data for the 2008 winter campaign are compared using a scatter plot as data available for comparison with the PM2.5 data is very limited as a result of the poor resolution of this PM data. PM10 concentrations and AOT are compared for both the 2008 winter campaign and the early winter 2009 campaign. A strong correlation is identified between PM10 and AOT for the 2008 winter campaign, exhibiting an R^2 value of 0.92 (Figure 4.20). AOT appears to decrease with a decrease in PM10. These results reveal that ambient PM10 particles are a significant contributor to AOT during the 2008 campaign. It was expected that a high correlation between PM2.5 and AOT would exist as a result of domestic fuel burning activities in the area. However, the continued mining activities at night, as well as the smoke from inadequate fires, rekindling of fires overnight and smouldering of fires early in the morning could contribute to larger particles. The distinct morning and evening peaks in PM10 (Figure 4.18) reveal a correlation between increased concentrations of pollutants from local mining activities, inversion layers, domestic fuel burning practices and traffic. Increased activity on nearby dust roads at the start of the day also serve to increase concentrations of course particles. Further, studies by Mdluli (2007) reveal extreme levels of PM7 (which are larger particles) during domestic fuel burning practices. Studies by Naidoo (2014) reveal that depending on the type of fuel used PM10 emissions from domestic fuel burning practices are significant. All of these possible sources/activities result in coarse particles which are trapped below the inversion layer on a cold winter morning.

The same comparison for the 2009 campaign (Figure 4.21) once again indicates a strong correlation between PM10 and AOT; however, indicating an inverse relationship where high AOT levels are associated with decreasing PM10 concentration. The range in AOT during early winter 2009, is however, significantly lower than 2008 revealing a lack of comparison to high aerosol loadings. The higher PM10 concentrations identified during winter 2008 compared with early winter 2009 is consistent with the higher levels of AOT identified for winter 2008.

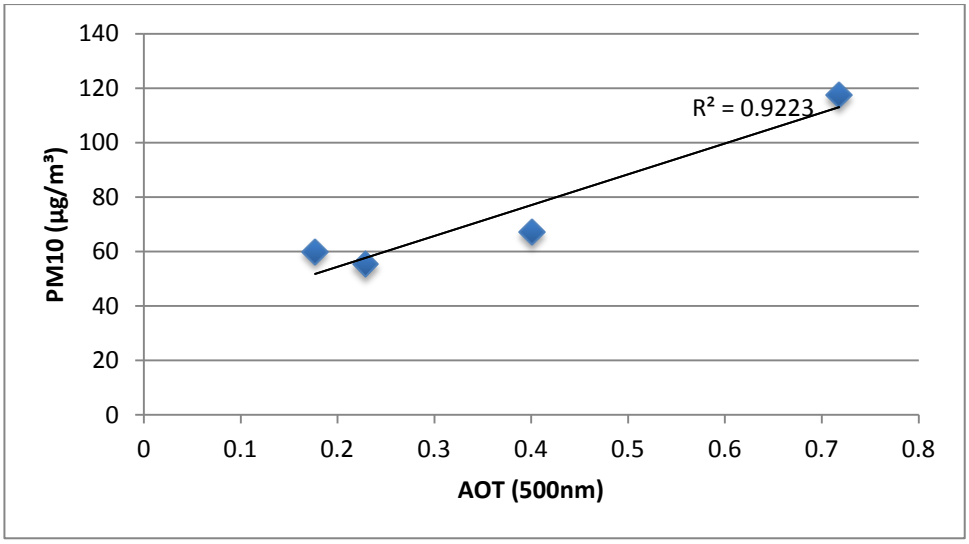

Figure 4.20: Scatter plot of AOT vs PM10 during the 2008 campaign.

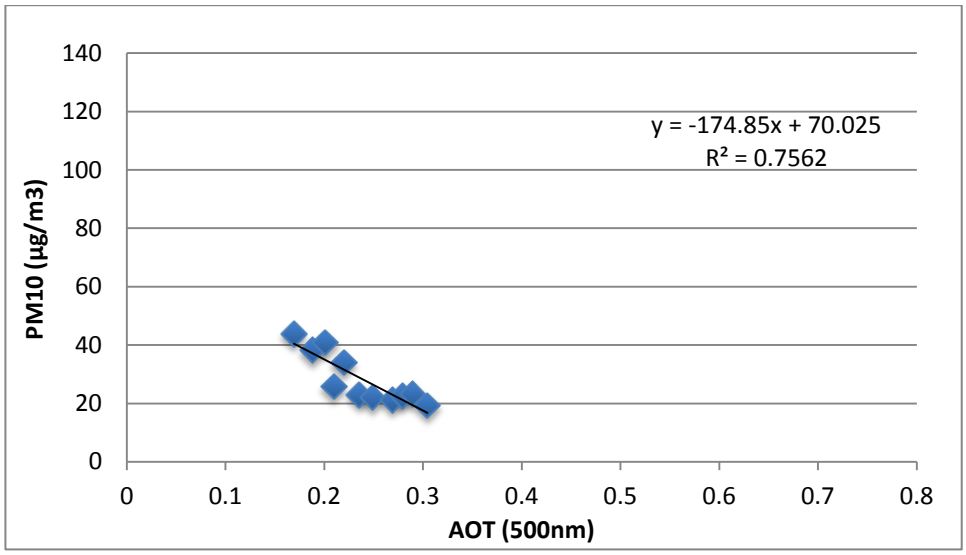

Figure 4.21: Scatter plot showing the inverse relationship between AOT and PM10 during the 2009 campaign.

4.1.5. Further Temporal Analysis

The diurnal variation in AOT as a function of the day of week reveals similar weekday patterns for early winter and winter, with a slight difference in hourly variation on Sundays. Presenting AOT loadings as a function of the day of week is particularly successful with regard to identifying traffic signatures in pollutant data. Traffic signatures can be identified by peaks in ambient air quality data during the morning and afternoon peak hour traffic. These peaks, however, usually only occur during the week when the majority of people go to and from work. These signals are usually not detected on weekends. The variation during the 2008 winter campaign (Figure 4.22) indicates a peak in AOT during the morning peak-

traffic, however, no peak is seen in the afternoon. AOT readings may cease too early in the day to pick up this signal. Data analysis for each of the campaigns does not indicate any significant difference between weekdays and the weekends, except during early winter 2009 (Figure 4.23) and winter 2008 (Figure 4.22), where AOT patterns appear to be different. On Sundays, AOT appears to be higher during the morning in early winter, while being higher during the evening during winter. For the 2010 campaign all the days of the week exhibit similar trends (Figure 4.24). While a morning peak was identified during the 2008 campaign, this peak was not identified during the other two campaigns.

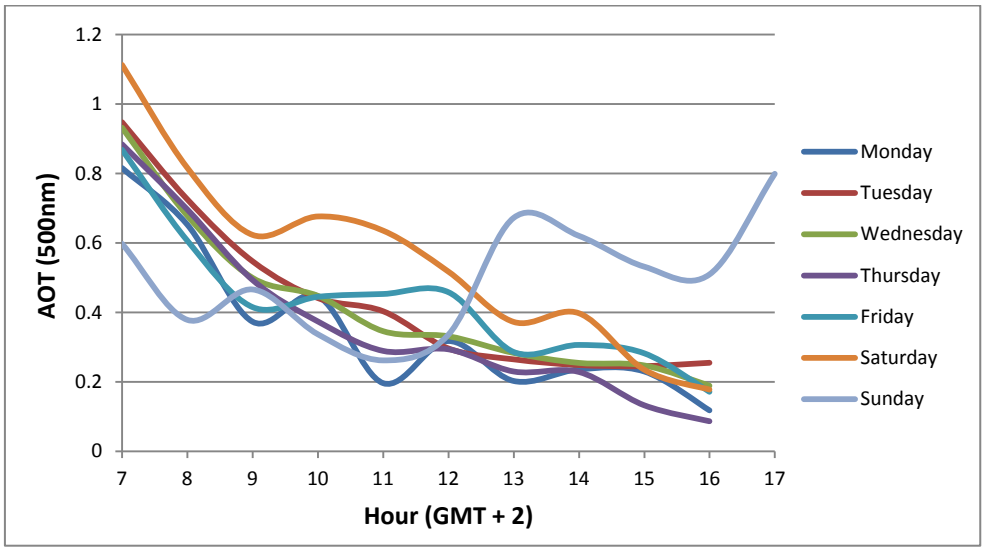

Figure 4.22: Hourly average variation in aerosol loading per day of week for the 2008 campaign.

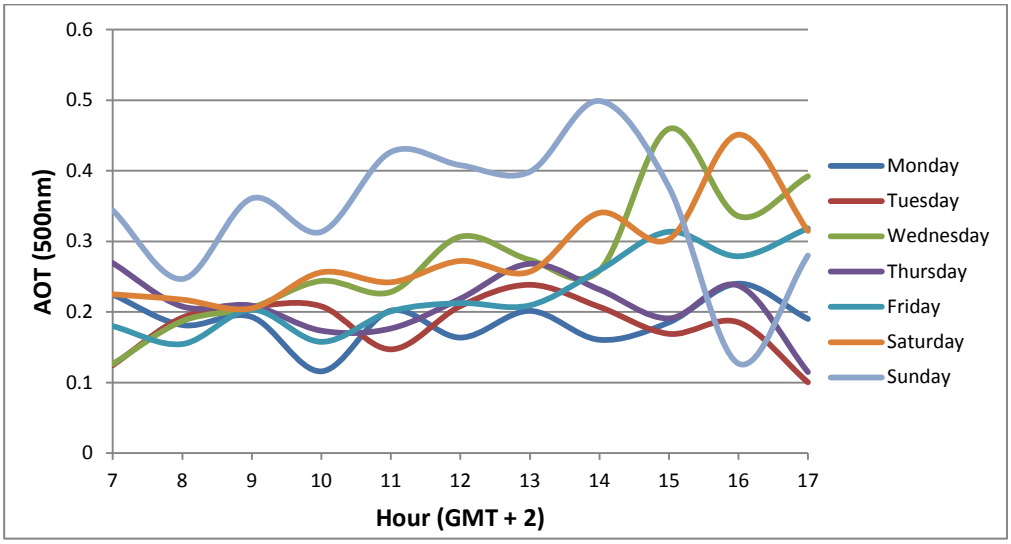

Figure 4.23: Hourly average variation in aerosol loading per day of week for the 2009 campaign.

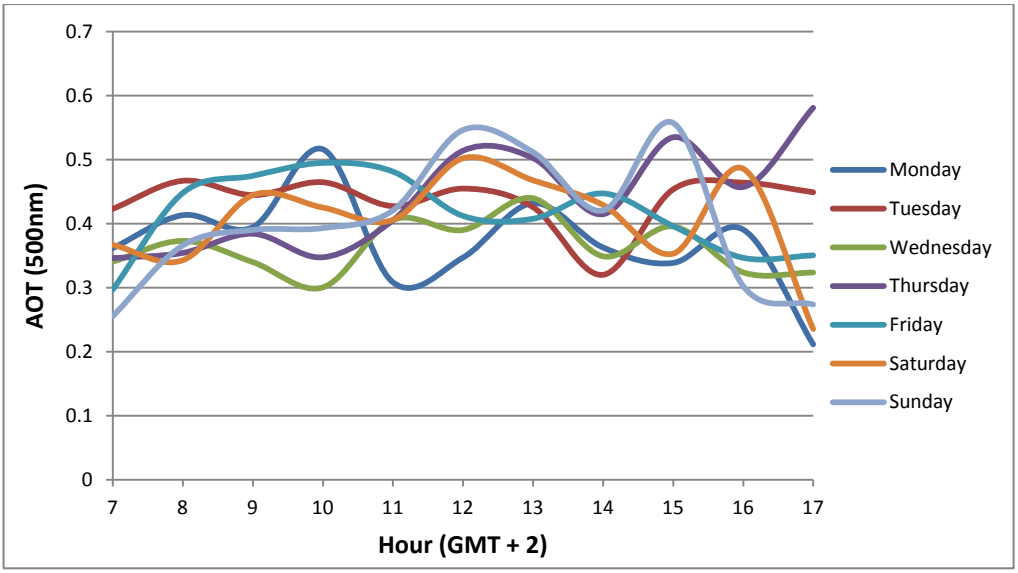

Figure 4.24: Hourly average variation in aerosol loading per day of week for the 2010 campaign.

A comparison of AOT and SANRAL traffic statistics indicates that the relationship between AOT and traffic is not clear. The aerosol optical thickness diurnal variations presented above were compared with the diurnal variation in traffic volumes in Figure 4.25; which was taken from SANRAL statistics for the Marikana Toll Plaza. The graph indicates that there is some sort of correlation between the aerosol loadings and traffic data during the 2008 campaign (SANRAL, 2009; 2010). High AOT in the morning corresponds to high traffic volumes at the same time. AOT during winter decreases toward midday, while traffic volumes decrease at the same time. There is very little correlation for the other two campaigns, and as diurnal traffic cycles do not vary from season to season or year to year, it is possible that traffic does not play a significantly large role in the area.

These findings indicate that the aerosol loadings may not be attributed to traffic, but this should not be excluded as an aerosol source.

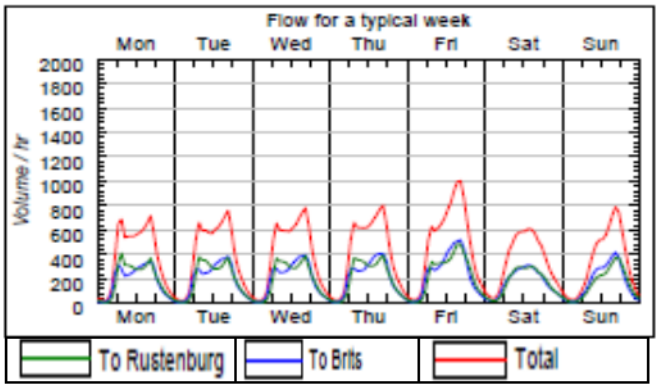

Figure 4.25: SANRAL traffic data indicating diurnal variation as a function of the day of week for the Marikana Toll Plaza (after SANRAL, 2010).

4.1.6. Rustenburg Flight Profiles – An Analysis of the Vertical Distribution of Aersosols over the Rustenburg Area

The vertical distribution of aerosols over the Bojanala District is found to vary depending on the meteorological conditions of the atmosphere. Aerosol research has revealed that the concentrations of aerosols decrease with height (Power, 2003). During the flights undertaken by the Climatology Research Group (CRG) and the Department of Environmental Affairs during 2005 over various regions in South Africa, measurements of the vertical profile of aerosol concentrations were recorded over the Rustenburg area. Flights were undertaken on the 25th July 2005 from 12:37 to 13:49 (Figure 4.26) and the 27th July 2005 from 12:29 to 14:20 (Figure 4.27). The synoptic patterns on the 27th July 2005 were identified to be common winter conditions, dominated by a high pressure system (Ncipha, 2011). All of the winter campaign days were characterised by a surface nocturnal inversion layer in the morning. Upper-level inversions were also identified at approximately 1000 to 1800 magl. Afternoons were characterised by deep mixing layers and an upper air inversion layer varying between 1200 and 1800magl. This upper level inversion layer was not present on the 27th July 2005 (Ncipha, 2011). As is evident from both figures the highest concentrations of aerosols occur closer to the ground (below 400m) on the 27th July 2005; however, on the 25th July 2005 the concentrations of aerosols are more evenly spread and the highest concentrations occurred up to approximately 600magl. These results indicate that aerosols present in the atmosphere over the Bojanala District usually originate from ground-levels sources. Vertical dispersion appears to be hindered well into the day during winter. This, however, is dependent on the atmospheric conditions and may vary significantly. It can

therefore not be predicted whether the aerosol loadings are attributed to ground-level sources or other sources as this is dependent on atmospheric conditions.

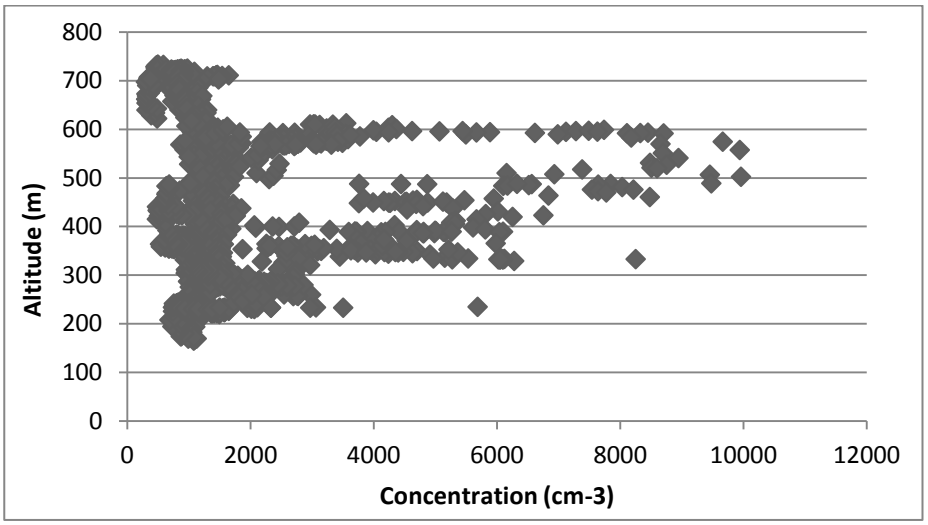

Figure 4.26: Vertical profile of aerosol concentrations measured on 25th July 2005 (12:37 to 13:49).

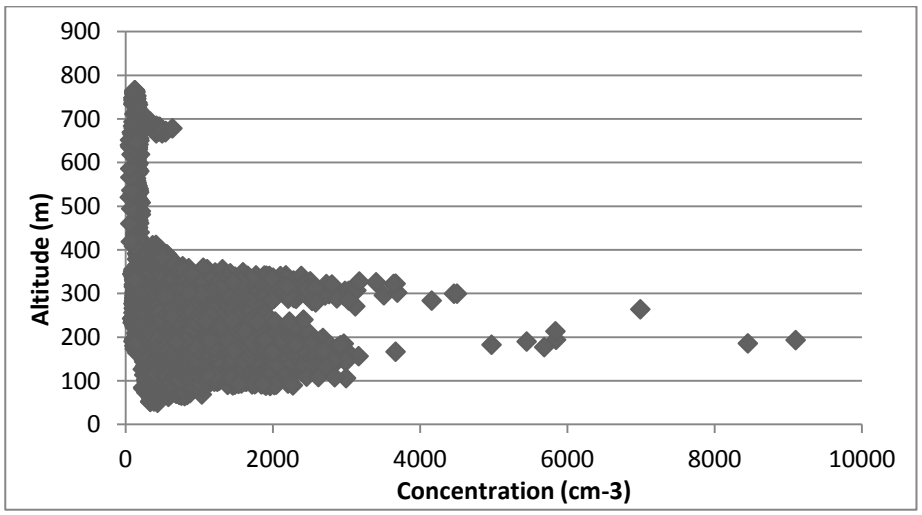

Figure 4.27: Variation of aerosol concentrations with height recorded on 27th July 2005 (12:29 to 14:20).

****

The temporal variation in aerosol optical thickness and Ångstrom exponent have been analysed in this chapter. Results reveal that AOT and AE are highest during winter and late winter. Possible reasons for the elevated levels during winter are domestic fuel burning and the concentration of pollutatns as a result of inversion layers. The relative contribution of combustion and non-combustion sources has revealed a

significant increase in fine mode particles during the biomass burning season. Diurnal variation is similar for early and late winter. The impacts of domestic fuel burning and the onset of the biomass burning season are significant. The daily variation of AOT may vary significantly. Foreign airmasses and vertical meteorology have a significant impact on the aerosol loadings over the Bojanala District. The following chapter explores the spatial distribution of aerosol optical thickness and Ångstrom exponent over the Bojanala District as well as a brief section on the climatological impacts of the aerosols in the district.

CHAPTER 5: A SPATIAL ANALYSIS OF THE AEROSOL LOADINGS OVER THE BOJANALA DISTRICT

The average aerosol optical thickness and Ångstrom exponent recorded over the Bojanala District during each of the campaigns is analysed. The data was plotted using ArcGIS software to present an idea of the spatial distribution of aerosols and the sizes of these aerosols over the Bojanala District. An analysis of the meteorological conditions prevalent during each campaign is presented.

5.1.The Spatial Distribution of Aerosols over the Bojanala District

5.1.1 Aerosol optical thickness over the Bojanala District

Maps illustrating the spatial characteristics of aerosols over the Bojanala District were generated using bi-linear interpolation. It is important to note that bi-linear interpolation may result in under or over estimation outside of observed data points.

A map illustrating the spatial distribution of the aerosol optical thickness during the 2008 research campaign indicates an increase in AOT toward the east (Figure 5.1). The AOT over the eastern area is found to range between 0.48 and 0.613. As indicated in Table 3.1 the important sources of aerosols in the eastern sector of the district are a mine dump, domestic fuel burning practices and many dust roads. The sites situated to the east of the district are situated within very large informal settlements. The aerosol optical thickness over the rest of the research site (which is home to a significant amount of mining sources – both combustion and non-combustion) lies predominantly within the range of 0.4 to 0.48. Although these areas are identified as having lower aerosol loadings, the AOT recorded at these sites are still considered high (Queface, 2002; Globe, 2002). The locations of some of the nearby mining industrial aerosol sources are indicated as black stars.

As a result of the high AOT identified during winter mornings in 2008, the morning spatial distribution of AOT is plotted (Figure 5.2). It is clear that the spatial patterns are similar to the overall average map presented. Further, it is clear that the high AOT recorded during winter mornings in 2008 ultimately results in elevated averages for winter 2008.

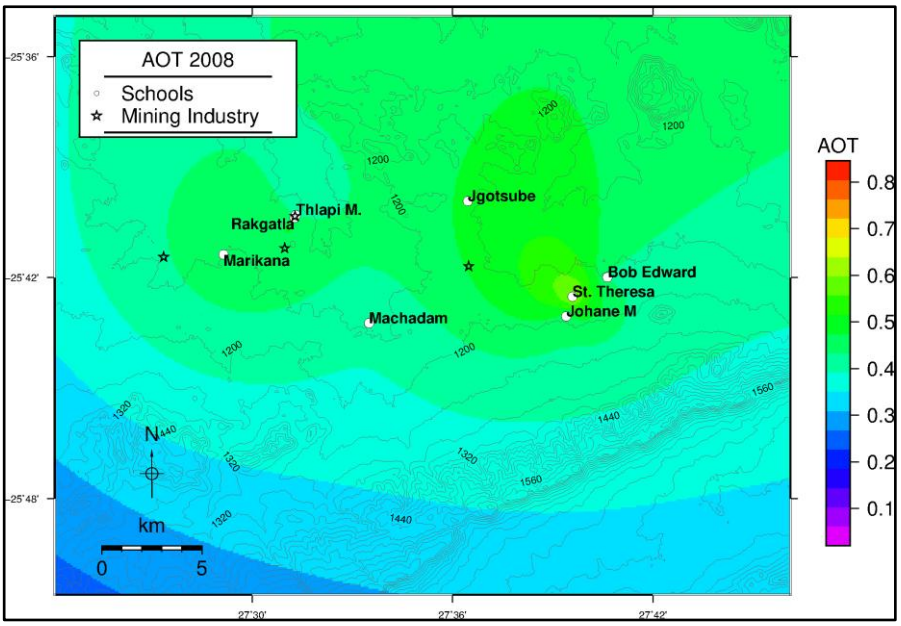

Figure 5.1. Map indicating the spatial distribution of AOT over the Bojanala District during the 2008 winter campaign.

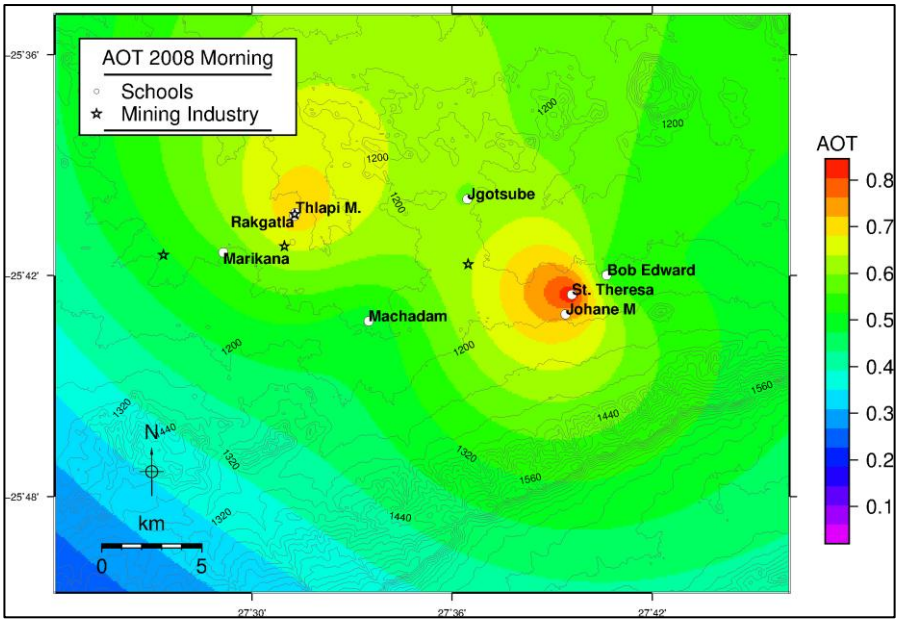

Figure 5.2. Map indicating the morning spatial distribution of AOT over the Bojanala District during the 2008 winter campaign.

The distribution of AOT during the early winter campaign of 2009 indicates a similar increase in AOT toward the eastern part of the area (Figure 5.3). During the early winter period of May and June 2009 the aerosol optical thickness over the research area is lower than that recorded during the winter months of July and August in 2008 (presented above). Aerosol concentrations are relatively low over the district (Globe, 2002), with the eastern

areas of the research site once again exhibiting the highest aerosol loadings. The AOT at the majority of the sites lies within the range of 0.159 to 0.312. Machadam Combined School was once again recorded as exhibiting the lowest aerosol loadings over the district. From the image, it is obvious that the entire research site is exposed to relatively low concentrations of aerosols at this time of year as the highest concentrations of aerosols recorded during this campaign still remain well below that of the lowest aerosol loadings recorded during the 2008 campaign discussed above.

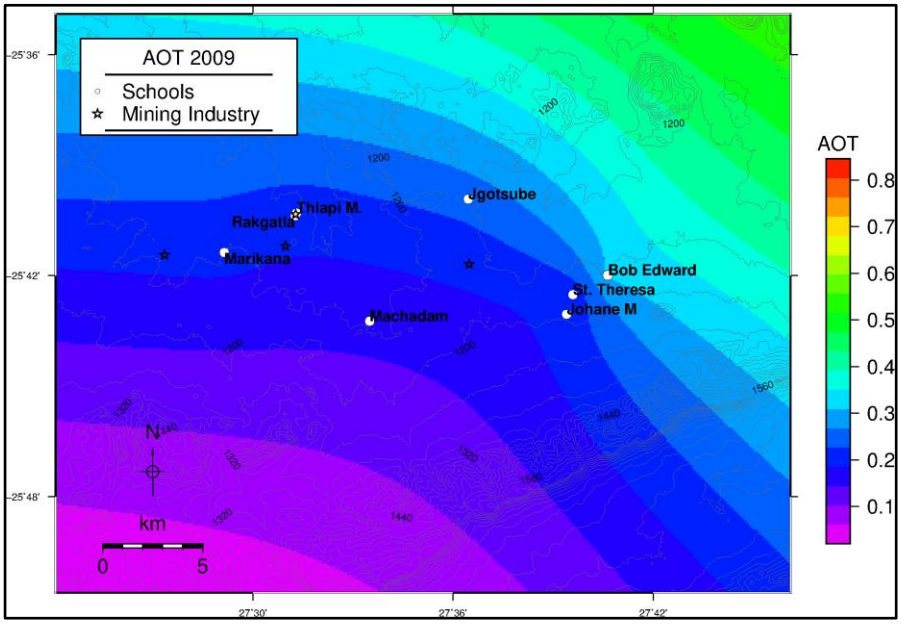

Figure 5.3: The spatial distribution of AOT during the May and June early winter 2009 campaign.

The spatial distribution of aerosol optical thickness during the winter/late winter campaign of 2010 indicates a different distribution to that of the other stages of winter (Figure 5.4). The AOT appears to be high over the entire research area, and ranges from 0.3 to 0.477. According to Globe (2002) AOT above 0.4 presents hazy conditions. Queface (2013) indicated that the average AOT for southern Africa is 0.24. The sites exhibiting the highest concentrations of aerosols were identified in the northern and western parts of the Bojanala District. The lowest concentrations of aerosols are identified at Bob Edward Middle School, Johane Mokololobatsi High School and St. Theresa High School. The reason for this change perhaps lies within the fact that data was collected until the end of August (onset of the biomass burning season). Biomass burning practices have been found to significantly enhance aerosol loadings over the area, even over clean air sites (Queface, 2002; AQMP, 2005). AOT is identified on average to be high within the area, especially when compared to

the early winter 2009 campaign. AOT levels do not reach the elevations recorded during the 2008 campaign.

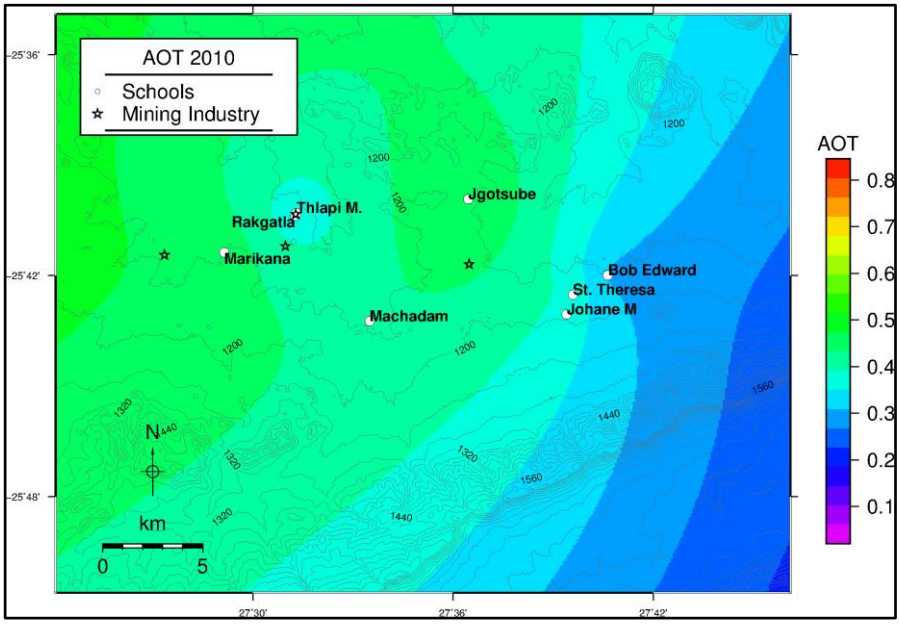

Figure 5.4: Spatial distribution of AOT for the 2010 campaign.

5.1.2 The Spatial Distribution of Fine and Coarse Mode Aerosols

The spatial variation in the Ångstrom exponent over the Bojanala District (as exhibited in Figure 5.5), reveals that larger particles, which are referred to as non-combustion particles are dominant over the eastern portion of the district, where AOT is highest. As discussed above, a mine dump, domestic fuel burning practices and many dust roads are important in the eastern part of the district. These coarse-mode particles have an Ångstrom exponent of below 1. The Ångstrom exponent at the majority of the sites lies within the range of 0.85 to 1.6, indicating the dominance of particles which may be fine to slightly coarse. At J. Gotsube, Thlapi Moruwe, Rakgatla, Machadam and Marikana High Schools particles exhibiting origins from combustion processes are identified (Ångstrom exponent above 1). The western parts of the district appear to be exposed to the finest particles. This is consistent with the local smelter identified near J.Gotsube, as well as numerous combustion sources in the area. The fine mode particles which dominate at J.Gotsube result in high AOT levels in the area. This highlights the potential impact of mining combustion sources to aerosol loadings in the area. It is obvious that both combustion and non-combustion sources impact significantly on the aerosol loadings of the area. This is particularly evident as the Ångstrom exponents lie relatively close to 1, indicating a significant coarse-mode contribution. Fine particles are

dominant over the western areas of the district where AOT was found to be lower than the eastern areas; whereas slightly coarse to slightly fine particles are identified in the eastern areas of the district where AOT loadings were identified to be the highest for the area. The majority of sites in the research area lie within the range of 1 to 1.6 and therefore a significant portion of the aerosol loading is made up of accumulation mode particles (Tesfaye, 2011).

The spatial distribution of morning AE levels (indicated in Figure 5.6) present a very similar pattern to that identified for the overall average. High levels of AE at specific sites appear to drive the high AE levels recorded on average for the area.

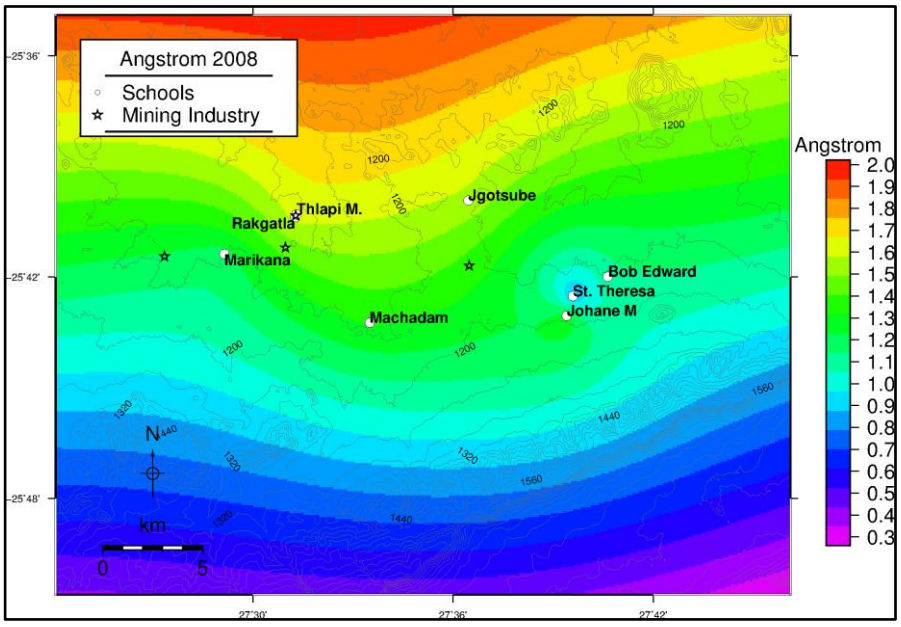

Figure 5.5: The spatial representation of the distribution of combustion and non-combustion related aerosol loadings over the district during the 2008 winter campaign.

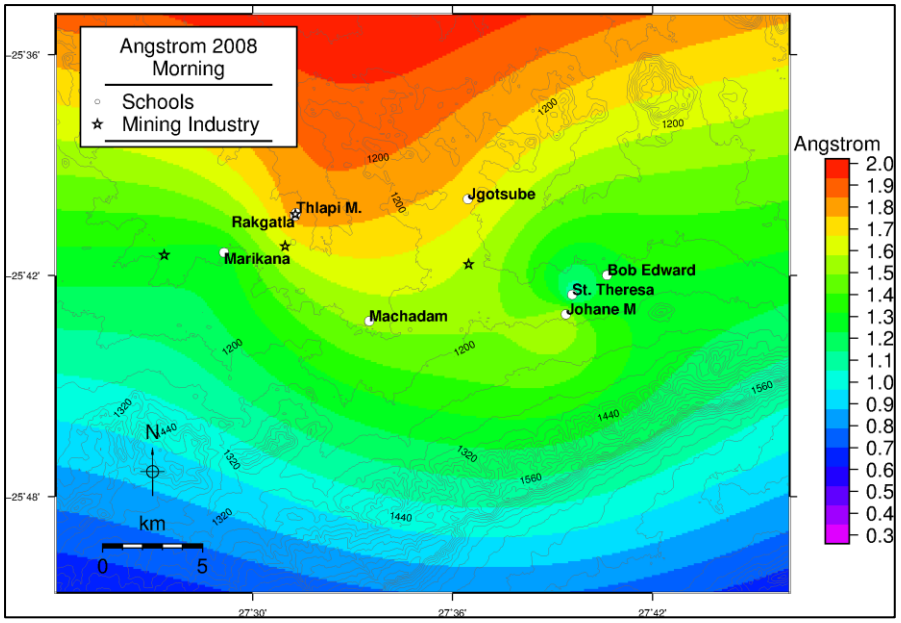

Figure 5.6. The spatial representation of the morning distribution of combustion and non-combustion related aerosol loadings over the district during the 2008 winter campaign.

The spatial variation of the Ångstrom exponent for the 2009 early winter research campaign is similar to that of winter 2008 (presented in Figure 5.7). As discussed above, the largest particles once again occur in the atmosphere over St. Theresa High School, Bob Edward Middle School and Johane Mokololobatsi. The western parts of the study area are exposed to fine mode particles, and as a result J. Gotsube High School, Thlapi Moruwe High School, Rakgatla High School and Machadam Combined School, fall within the region dominated by combustion particles. Accumulation mode particles are once again significant for the area, however, resulting in lower aerosol loadings than in 2008.

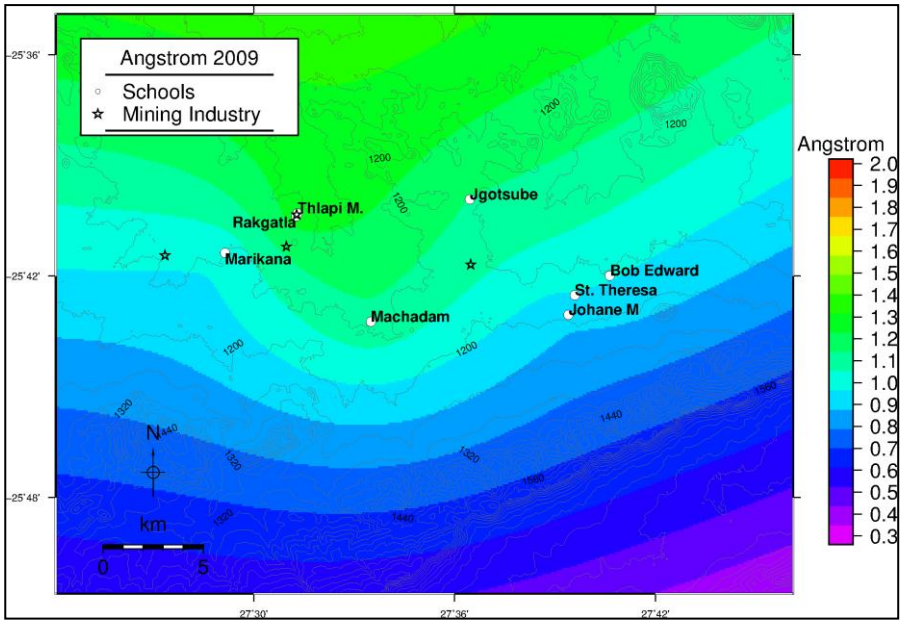

Figure 5.7: The spatial distribution of the Ångstrom exponent during May and June 2009.

Figure 5.8 represents the spatial distribution of the Ångstrom exponent over the district during the 2010 campaign. As with the AOT the variation in space of fine and coarse mode particles is different to that of the previous campaigns. As with AOT there appears to be a westward shift in high AE values. It appears that the finest particles were recorded over the eastern and western parts of the research site. The occurrence of the largest particles appears to have shifted westward. At Thlapi Moruwe and Rakgatla High Schools the finest particles once again make up the aerosol loading of the atmosphere. The entire district appears to be exposed to fine mode, combustion particles. At J. Gotsube and Machadam High Schools the Ångstrom exponent is only slightly above 1, and indicates a slightly larger contribution of coarse mode particles at these sites. The largest aerosols are found to have an impact over the central part of the study area where AOT was found to be highest. It would appear that the aerosol loading over most sites exhibit a shift toward the dominance of fine mode particles since 2008. From the map, one can see that accumulation mode aerosols are becoming increasingly more dominant. The dominance of fine mode particles at all sites, as well as the variation in the spatial distribution of aerosols may once again be associated with the onset of the biomass burning season.

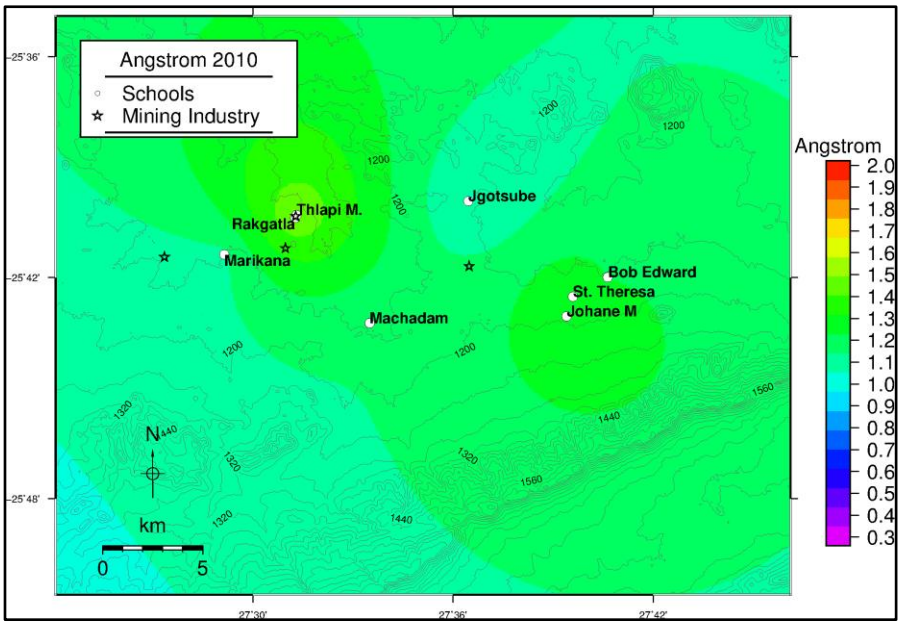

Figure 5.8: The spatial distribution of combustion and non-combustion aerosol loadings over the Bojanala District during the 2010 research campaign.

5.2.Meteorological Overview

5.2.1. Overview of Meteorological Conditions during the 2008 Campaign

By referring to the spatial maps discussed above, as well at the Google Earth image presented in Figure 5.9 one can identify aerosol sources at or near each of the sites. The Rustenburg Meteorological station and Lonmin's L2/BMR station (decommissioned since 2004) are also indicated on the image. While wind direction is an important parameter to consider when identifying the sources of aerosols and pollutants, one must bear in mind that AOT measures the entire atmospheric column. The aerosols in the path of direct solar radiation are at different levels in the atmosphere and therefore industries on the ground lying in the dominant wind path cannot be assumed to be the only sources of aerosols. Assumptions can only be made regarding dominant wind directions and the potential association to high aerosol loadings, as discussed below.

Meteorological data received from the South African Weather Service for the town of Rustenburg has been analysed to determine whether particles originating from a specific area are being carried into the research area. The location of the Rustenburg meteorological station must be considered, especially when considering the change in topography toward the research sites (Figure 5.9). Wind roses were generated using hourly wind speed and direction

recorded at Rustenburg for each study period. The wind roses which were created include those representing day (07h00 – 18h00), night (18h00 – 07h00) and overall wind regimes. A wind rose gives a graphic representation of the dominant wind directions (represented as a percentage frequency – the length of the bar) and the corresponding wind speeds (indicated as the colours of the bars).

The frequent occurrence of winds blowing over these sources may have a direct impact on the aerosol concentrations of the area. Hourly wind speed, wind direction and precipitation have been analysed using WR-Plot View, which is used to create wind rose plots for meteorological data. The programme is a freeware programme downloaded from the Lakes Environmental Software website.

The topography of the area near Rustenburg creates very dominant katabatic and anabatic flow as discussed in Chapter 3. The average wind direction during the July/August 2008 research campaign indicates a very dominant wind blowing from the South-West (Figure 5.10). Wind speeds in this direction are predominantly low, ranging from 0.5 to 3.6m/s, and occasionally increase to within the range of 3.6 to 5.7 m/s. Calm conditions are uncommon in the area. Wind speeds between 1 and 4m/s occur 72.9% of the time, while wind speeds between 4 and 7 m/s occur less frequently, 25% of the time.

As is evident in Figure 5.9 the schools which formed part of the study are largely situated in mining areas. As winds are found to dominantly originate from the south-westerly direction, J. Gotsube High School is directly impacted upon by aerosols originating from the WPL, the BMR and the Karee Mine. The BMR and Karee Mine are partial sources to the aerosol loading over Thlapi Moruwe and Rakgatla High Schools. These mining industrial sites will have a direct impact on the aerosol composition and concentrations when these dominant south-westerly winds blow. Further, all of the sites lie within a north, north-easterly direction of the aerosol sources, directly in the dominant wind path of these sources. The town of Rustenburg and various industries nearby lie west and south-west of the sites. It can therefore be assumed that emissions from these sources and areas may have a direct impact on the aerosol loading at these sites.

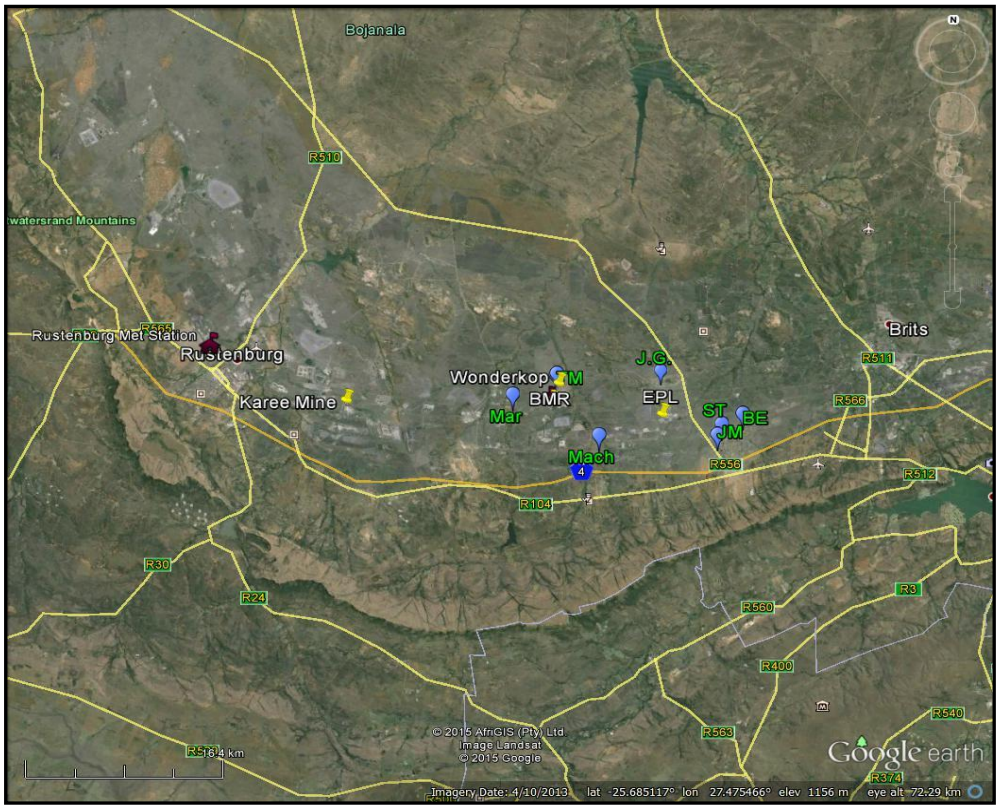

Figure 5.9: Google Earth image created for the research site indicating the schools where measurements were taken, the Rustenburg and Lonmin Meteorological stations and some coordinates of the local mining activities.

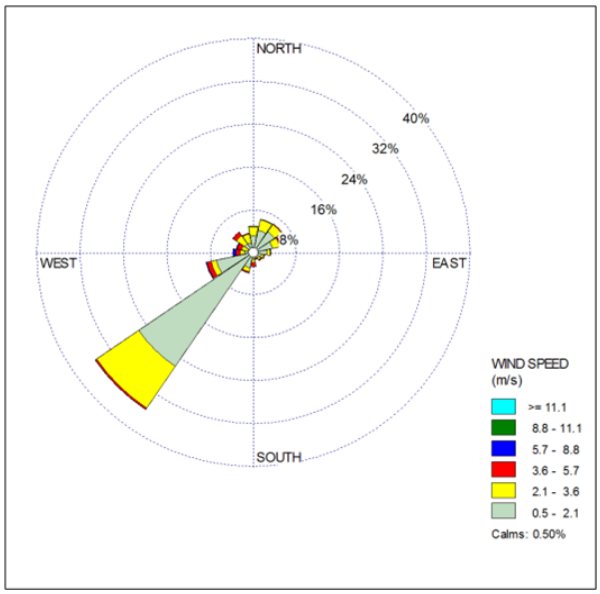

Figure 5.10: Wind rose plot for the July and August 2008 campaign for Rustenburg.

5.2.1.1. The meteorological conditions during the 2008 campaign: day vs night

Wind speed and direction from 7am until 6pm was plotted for the winter period of July and August 2008. These were plotted to coincide with the time of day when solar radiation measurements were taken. The wind rose (Figure 5.11) indicates that winds originating from the eastern to northern sectors are common during daylight hours. Wind speeds in this direction commonly reach up to 3.6m/s, with maximum speeds between 3.6 to 5.7m/s. Wind direction during the day is highly variable, with wind direction ranging from north-east to south-west. Wind speeds of 1 to 4m/s are dominant, while higher wind speeds of 4 to 7m/s are also common.

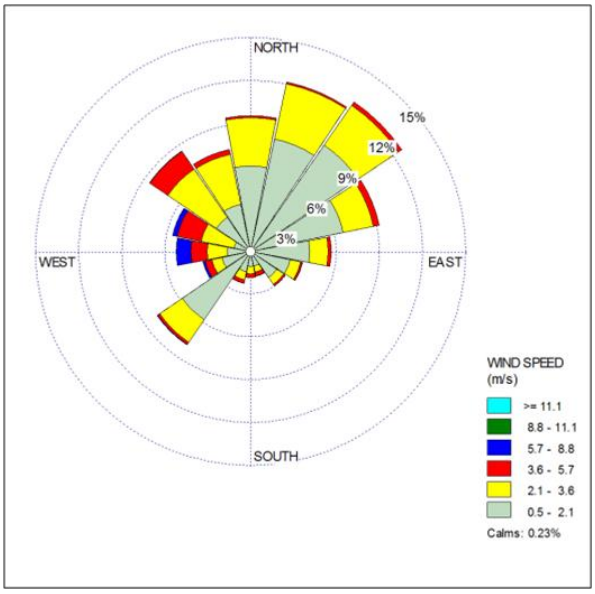

Figure 5.11: The diurnal wind rose plotted for wind data from 7am to 6pm for July and August 2008 campaign for Rustenburg.

During the day, as indicated above, wind direction is highly variable. The EPL, WPL, Wonderkop and BMR industrial sites lie within the direction of the most frequently occurring winds, and impact directly on Marikana High School. Aerosols originating from the Karee Mine, K4, BMR, WPL and EPL will move straight over Rakgatla High School and Thlapi Moruwe. J. Gotsube is impacted on by the WPL and the EPL, and Machadam by the EPL only.

Nocturnal wind directions were plotted from 7pm until 6am (Figure 5.12). The figure indicates a very dominant wind direction during these hours, originating from the South-West, this is as a result of valley winds. Wind speeds are commonly lower from this

direction, and may reach 3.6 m/s occasionally. The frequency of occurrence of the wind speeds between 1 and 4 m/s is 79.5%. The extremely dominant wind direction identified during the night time resulting from the topography of the area will move over the WPL, the BMR and the Karee Mine, carrying aerosols toward J.Gotsube High School, Thlapi Moruwe and Rakgatla High School. The presence of aerosols being emitted from these sources at night is dependent on whether these processes are scheduled for nocturnal activity.

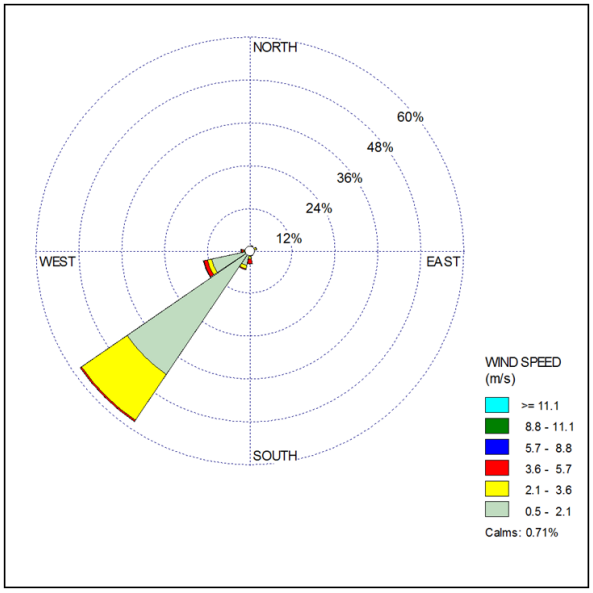

Figure 5.12: Nocturnal wind speed and direction from 7pm to 6am is plotted for the July and August 2008 campaign for Rustenburg.

The variation in AOT and Ångstrom exponent with wind direction is plotted in Figure 5.13. Each number at the bottom of the graph represents a specific wind direction class, starting at 0° and moving up to 360°. Each class represents 25°, except the final class which represents 35˚. The highest AOT and Ångstrom exponents are associated with winds from the south-western sector (200 to 250° - Class 9 and 10). Standard deviation bars (indicated on the graph as error bars) indicate high standard deviation for the AE for most of the wind classes. High standard deviation is identified for AOT and AE for the 8th and 9th wind class (170º to 225º) where significant variation in AOT and AE has occurred. The hourly variation in wind direction and wind speed is plotted in Figure 5.14 and indicates that at the time of the commencement of readings at 7am, the wind direction lies within the 200 to 250° direction, indicating that industries and sources lying south-west of the district are responsible for the extreme AOT and Ångstrom exponents identifiable early on a winter morning in the Bojanala District. The wind direction changes to approximately a northerly direction as the day progresses. This change occurs in an anticlockwise direction, indicating the variation in

aerosol sources throughout the day. As the wind direction changes (until approximately 10am) the wind speed increases slightly. This may result in the increased levels of coarse mode particles identified at this time of the day as the particles are picked up by stronger winds.

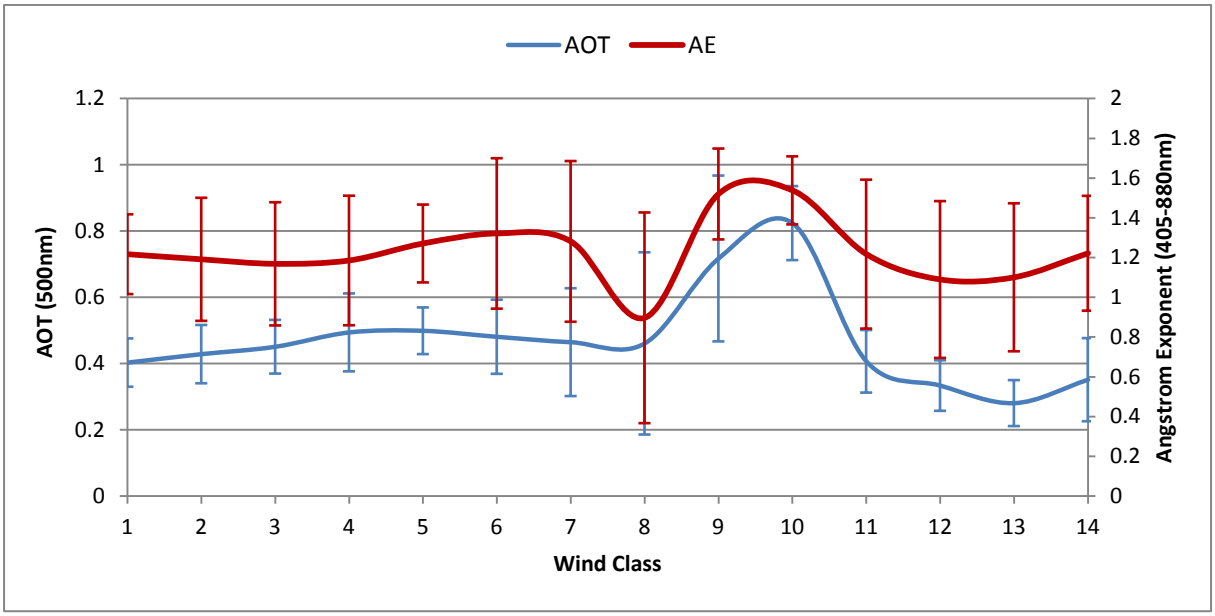

Figure 5.13: The variation in the AOT and Ångstrom exponent associated with specific wind direction classes. Each wind class is represented alphabetically and represents 25º eg. Class 1 represents 0 to 25°, Class 2 represents 26 to 50° etc. Standard deviation is represented by the error bars on the graph.

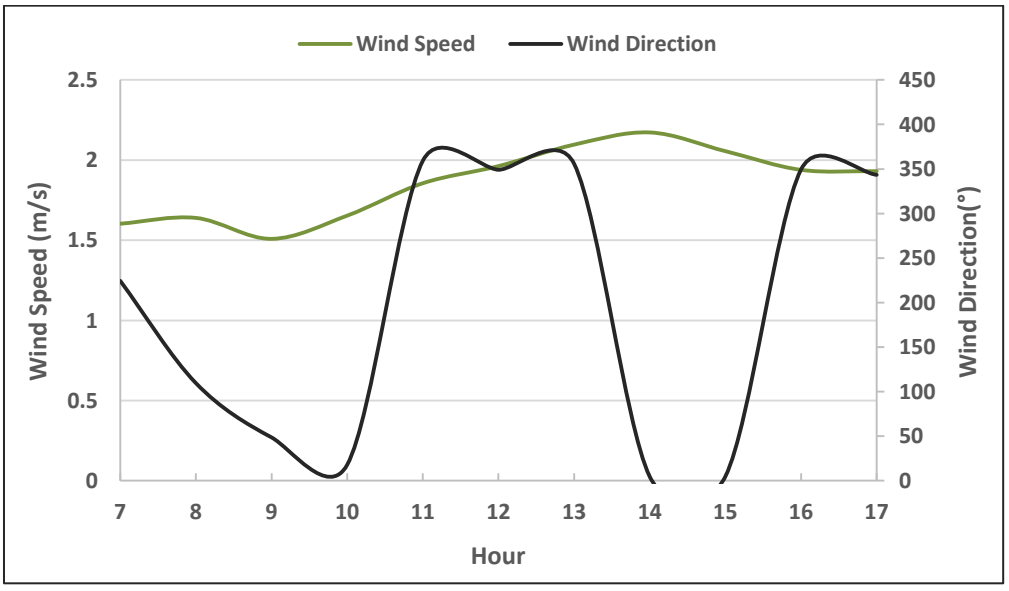

Figure 5.14: The average wind direction and wind speed per hour of the data collection period.

5.2.2. Overview of Meteorological Conditions during the 2009 campaign

Wind data was analysed to determine whether a dominant wind direction is identified in the area during early winter. The wind rose created for the early winter period of 1st May to 10th June 2009 (Figure 5.15), indicates that the dominant wind direction is that from the South-West and West-South-West. This is the same as that which was discovered for the 2008 campaign. The most dominant wind direction is South-Westerly in origin, with wind speeds rarely reaching 5.7m/s. Winds from the West-South-Westerly direction tend to reach higher velocities of up to 8.8 m/s. This is, however, uncommon. Wind speeds between 0.5 and 2.1m/s occur most frequently at 79.7% of the time.

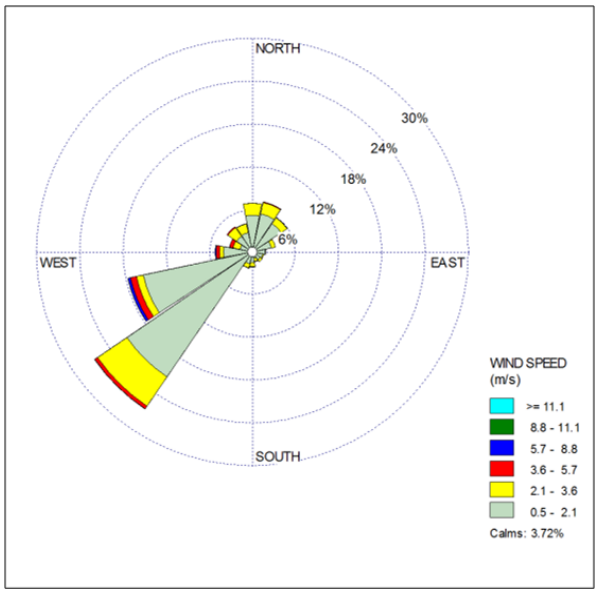

Figure 5.15: Average wind direction and wind speed for Rustenburg for May and June 2009.

The wind rose above indicates the dominant direction from which aerosols may be carried into the area. During May and June 2009 winds moving from the south-west to west-south-westerly direction would have picked up aerosols emitted from Wonderkop, WPL, BMR and Karee Mine and transported these directly over J. Gotsube High School. Aerosols emitted from industrial mining activities carried out at Karee Mine and the K4 are frequently carried in the south-west, west-south-westerly direction over Rakgatla and Thlapi Moruwe High Schools. Once again, aerosols originating from Rustenburg and other industries lying south-west of the research site should be considered as important contributors to the aerosol loading over the area.

5.2.2.1. The meteorological conditions during the 2009 campaign: day vs night

Wind directions from 7am to 6pm are highly variable in the area at this time of year. Wind direction, as exhibited in Figure 5.16, varies from the North-north-east to south-east, south-south-west to west-south-west, and less dominantly from east-south-east to south-south-west, and west to north-west. Wind speeds are commonly below 2.1 m/s, and wind speeds reach 5.7 m/s more frequently when originating from the north-west to south-east. Low wind speeds (0.5 to 2.1 m/s) occur most frequently, however, a significant percentage of winds reach 3.6 m/s.

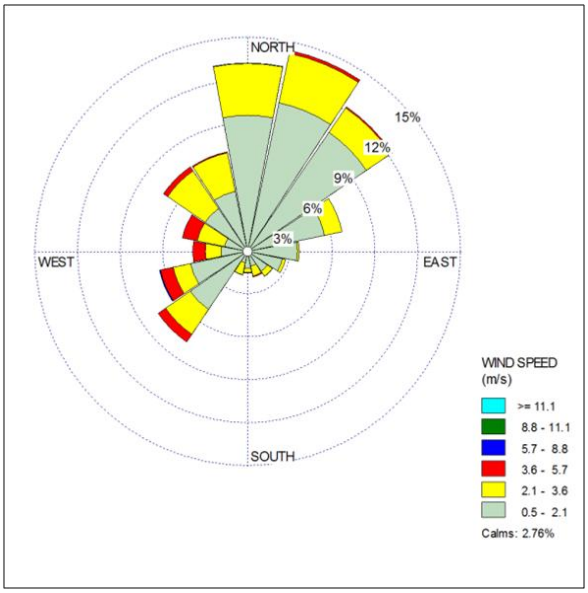

Figure 5.16: Diurnal wind rose created for Rustenburg using wind data occurring between 7am and 6pm during the 2009 early winter campaign.

Diurnal air flow carries aerosol particles from EPL and WPL to Machadam Combined School. Aerosols originating at WPL are carried toward Marikana, Rakgatla, Thlapi Moruwe and J. Gotsube High Schools. Particles from BMR, K4 and Karee Mine also impact directly on the J. Gotsube High School. Aerosol concentrations over Rakgatla High School and Thlapi Moruwe High School may be made up of aerosols originating at the BMR, K4 and the Karee Mine. Marikana High School is also directly in the wind-path of aerosols emitted from the BMR.

A very dominant nocturnal wind direction is identified in the wind rose in Figure 5.17. The wind rose exhibited was created for the time period from 7pm to 6am. Dominant wind

directions range from west-south-west to south-west. Wind speeds in these directions are predominantly below 2.1 m/s. Wind speeds occasionally reach 8.8 m/s in the west-south-west direction.

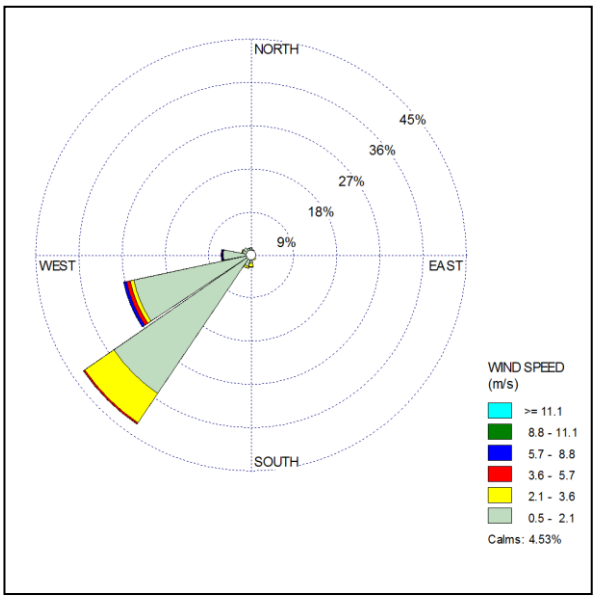

Figure 5.17: Nocturnal wind rose created for Rustenburg for the hours between 7pm and 6am during the 2009 early winter campaign.

At night, the dominant wind direction may bring aerosols from the WPL, Wonderkop, BMR and the K4 to J. Gotsube High School. Rakgatla High School and Thlapi Moruwe high School lie in the direct path of airmasses which move over and pick up pollutants at the K4 and Karee Mine.

Figure 5.18 represents the hourly variation in the average wind speed and direction. This indicates that from approximately 12pm the wind direction has a very dominant northerly component. As with the winter campaign wind speeds increase as the day progresses. Wind speeds are almost doubled by 5pm. The increase in wind speeds may be associated with an increase in the suspension of coarse particles. This change is not identified in the data, however. The possible reason for this is that early in winter conditions are not as dry as during winter. Figure 5.19 indicates the variation in the AOT and the Ångstrom exponent with wind class. The variation in AOT remains relatively stable, whereas there is a distinct decrease in the Ångstrom exponent when the wind direction lies within the 50˚ to 100° classes (Class 4). This north-easterly wind direction obviously serves to bring in coarse mode particles such as dust between 9 and 11am in the morning. As the wind direction then further approaches a northerly direction the Ångstrom exponent once again increases to be

dominated by combustion particles. The change in wind direction as the day progresses is similar to that of the winter campaign, indicating once again a variation in wind direction in an anti-clockwise direction (and therefore a variation in sources) until approximately midday. The standard deviation (indicated on the graph as error bars) is once again high as with the winter campaign. The highest standard deviation is once again identified for the 8th class.

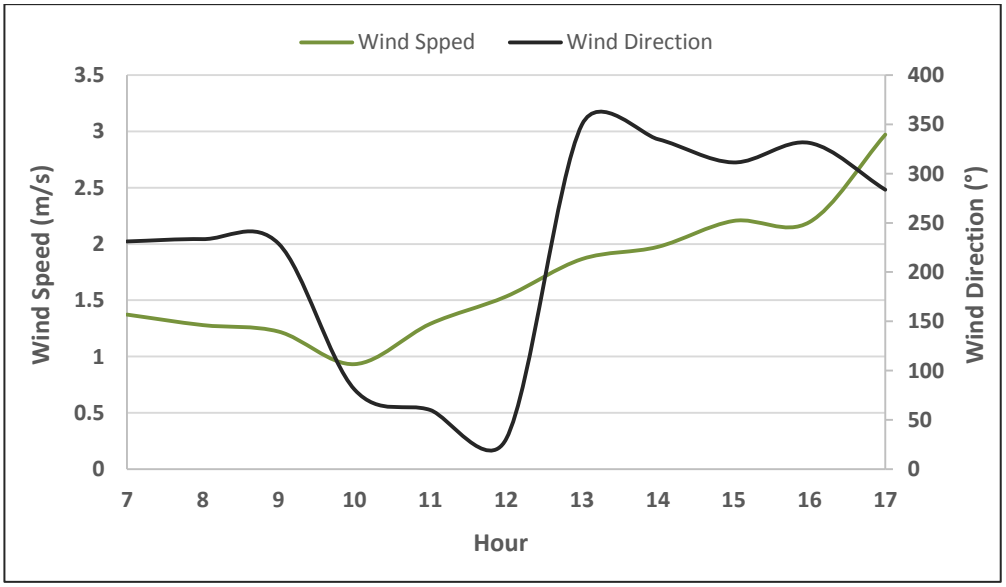

Figure 5.18: The hourly variation in the average wind speed and wind direction is presented for the 2009 early winter campaign for Rustenburg.

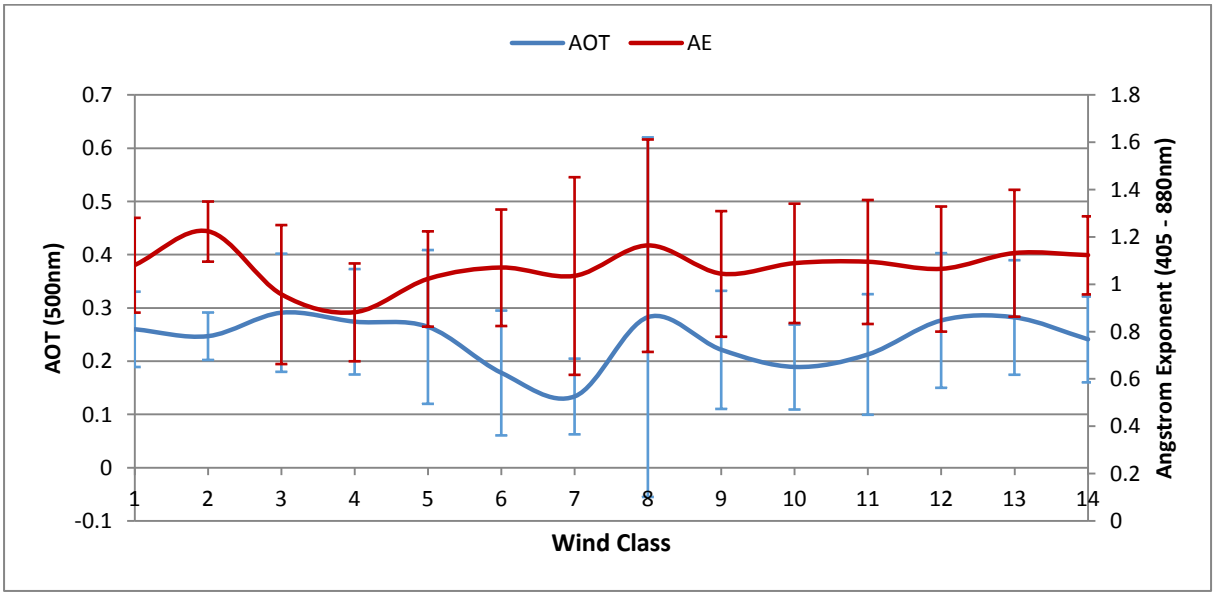

Figure 5.19: The variation in the AOT and Ångstrom exponent associated with specific wind direction classes. Each letter represents a 25° wind class. Class 1 represents 0 to 25°, Class 2 represents 26 to 50° and so on. Standard deviation is represented by error bars in the graph.

5.2.3. Overview of Meteorological Conditions during the 2010 campaign

The seasonal wind rose for the winter months of July and August 2010 is exhibited in Figure 5.20. It is evident from this wind rose that a very dominant wind impacts on the area. Winds originating from the south-west and west-south-westerly direction occur most frequently and reach speeds of between 3.6 and 5.7 m/s. As indicated in the wind classes, wind speeds between 0.5 and 2.1 m/s occur most frequently in these directions.

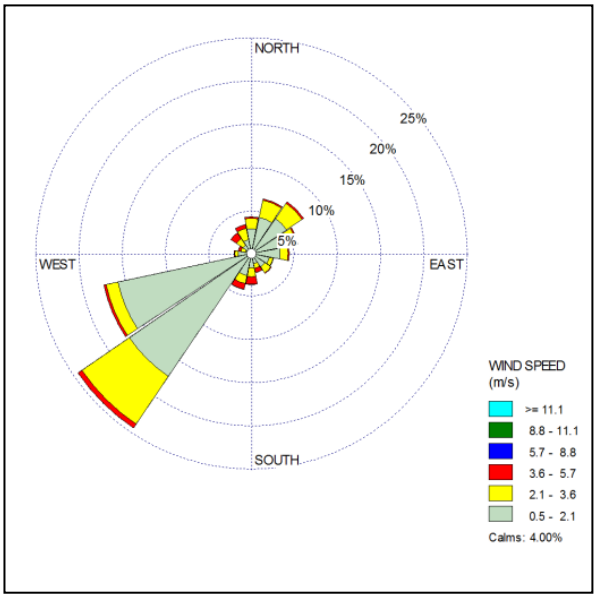

Figure 5.20: The overall average wind speed and direction at Rustenburg during the 2010 campaign.

The wind rose (above) created for the entire 2010 research period (including both day and night) indicates that J. Gotsube High School is in the direct path of airmasses which move over Wonderkop, WPL, BMR and Karee Mine. Only Rakgatla and Thlapi Moruwe High Schools are impacted on by winds originating from the west-south-west to south-westerly direction, and in line with the Karee Mine and K4. The dominant wind direction is once again the same as the previous years and once again all industries located south-west of the sites may have a significant impact on the aerosol loading.

5.2.3.1. The meteorological conditions during the 2010 campaign: day vs night

The diurnal wind rose for the winter period of July and August 2010 is exhibited in Figure 5.21. Prevailing wind directions from 7am to 6pm for July and August 2010 once again indicate a highly variable wind direction. Winds originating from the east-north-easterly and north-easterly direction occur most commonly. Wind direction appears to vary frequently

from the north-east to the south-westerly direction. The most dominant winds tend to exhibit lower wind speeds, with wind speeds frequently reaching between 2.1 and 3.6 m/s. The frequency of occurrence of wind speeds between 0.5 and 2.1m/s is 60.5%, while wind speeds between 2.1 and 3.6 m/s also commonly occur 33.6% of the time.

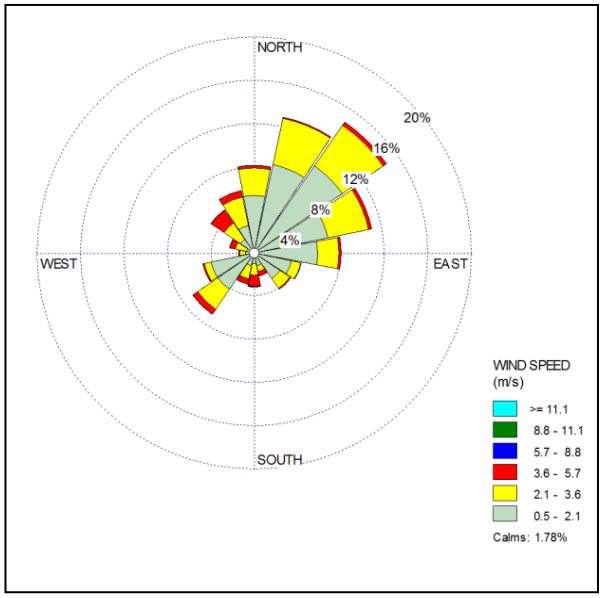

Figure 5.21: Diurnal wind rose created for hourly averaged wind data between 7am and 6pm for July and August 2010 for Rustenburg.

The highly variable wind directions identified above indicate that winds originating from the north-north-easterly direction to the west-south-westerly direction may carry aerosols from the EPL and WPL to Machadam Combined School. The WPL, BMR, K4 and Karee Mine may emit aerosols into air flow moving toward Rakgatla, Thlapi Moruwe, and J. Gotsube High Schools. Aerosols emitted from the WPL and BMR may also have an impact on the aerosol loading over Marikana High School.

The nocturnal wind rose (Figure 5.22) plotted from 7pm to 6am for the winter months of July and August 2010 exhibit a very dominant wind originating from the south-west to the west-south-west direction. Wind speeds in these directions frequently range between 0.5 and 2.1 m/s (84.1%). Wind speeds in the west-south-west and south-west direction reach speeds of 3.6 to 5.7m/s, 12.2% of the time.

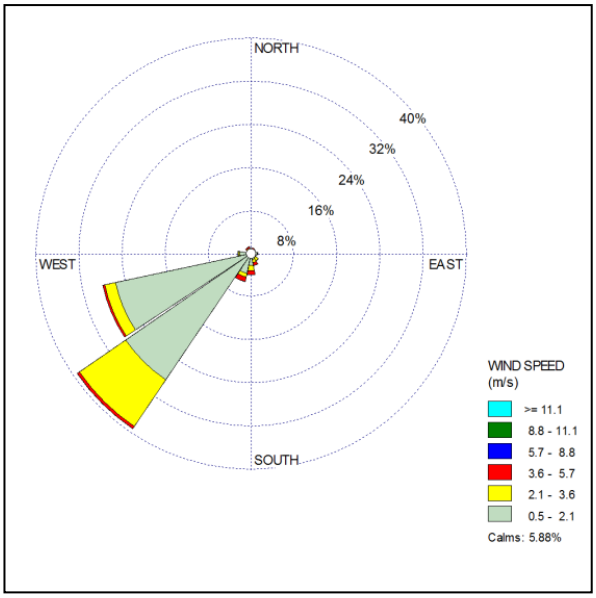

Figure 5.22: Nocturnal wind speed and direction at Rustenburg for July and August 2010 from 7pm to 6am.

The nocturnal wind rose indicates that dominant winds originate from the south-west to west-south-westerly direction. This air flow has a significant impact on J. Gotsube High School, as particles carried from the WPL, Wonderkop, the BMR and the K4 may be brought into the area. Both Rakgatla High School and Thlapi Moruwe High School may experience aerosols moving in from the direction of the K4 and the Karee Mine.

The hourly variation in the wind direction and wind speed presented in Figure 5.23 indicates the dominance of south-westerly winds until 9am, and thereafter a shifted in an anti-clockwise direction toward dominance of northerly winds from 12pm. A difference between the early winter and winter, and the late winter campaigns is not clear as the change in wind direction as the day progresses is similar. This indicates the importance of the same aerosol sources and local micrometeorology during late winter. Wind speeds once again appear to increase significantly with a change in wind direction. The variation in wind speeds is not associated with any change in particle size or concentration. The wind data presented here, therefore does not aid in the understanding of the differences in spatial distribution of aerosols identified during late winter. Figure 5.24 presents the variation in the AOT and the Ångstrom exponent with specific wind classes. There is no real relationship which may be identified in the data. The aerosol loadings appear to remain consistently high throughout the day, regardless of the origin of the winds. The spread of the data, indicated by the standard deviation bars, is high once again, as with the early winter and winter campaigns. The

standard deviation during late winter is lower, however during 2010, with a significant increase for the 7th and possibly the 8th wind class.

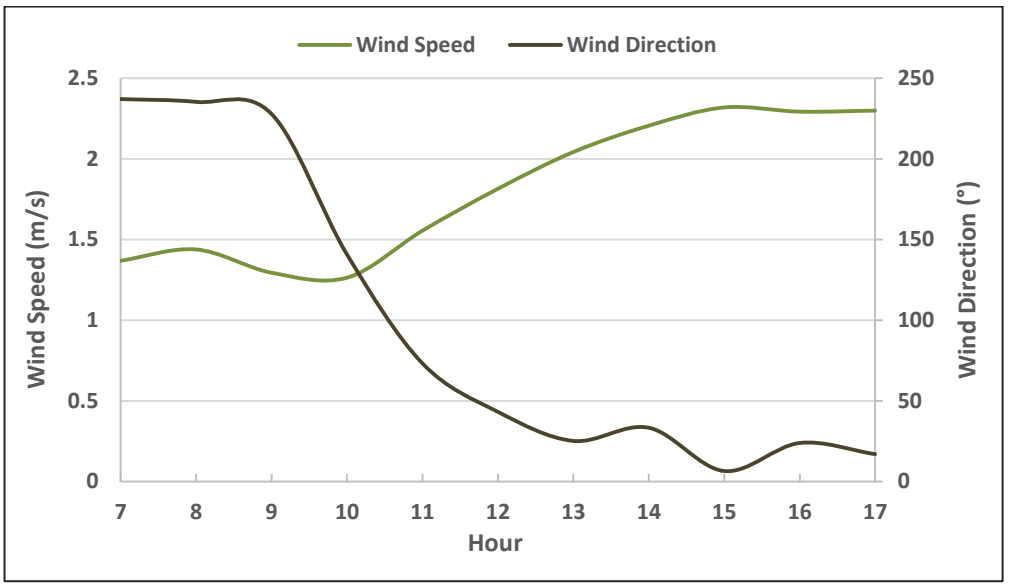

Figure 5.23: Hourly variation in wind direction and wind speed during late winter 2010.

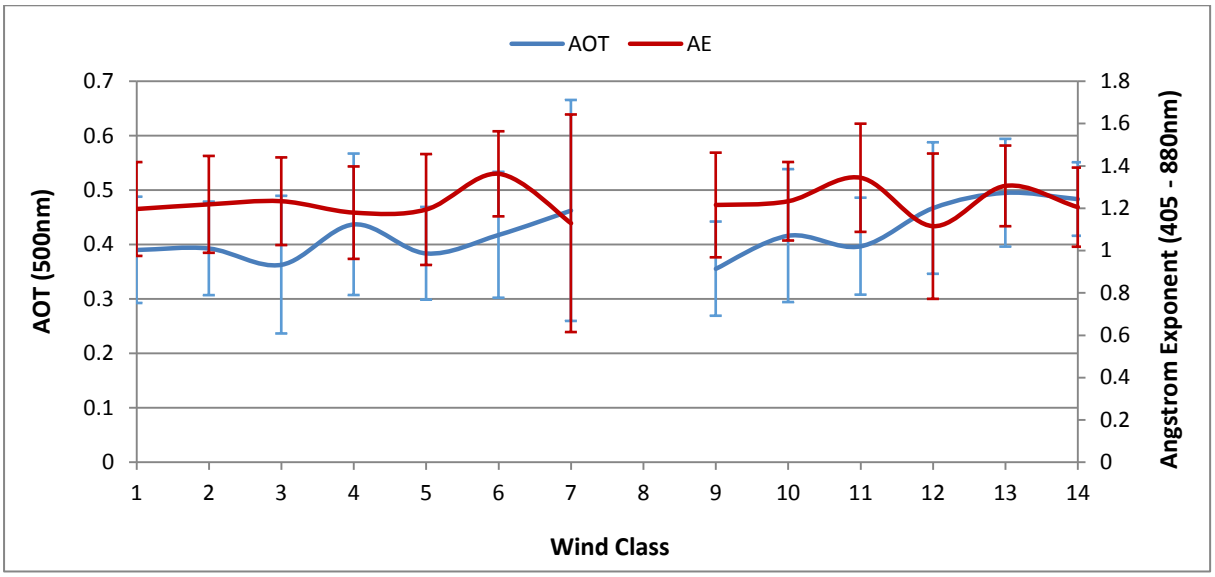

Figure 5.24: The variation in AOT and Ångstrom exponent according to various wind classes does not indicate any specific trend. Each wind class represents 25° eg. Class 1 would represent 0 to 25°, Class 2 would represent 26 to 50° and so on. Standard deviation is represented by the error bars in the graph.

The sources mentioned above cannot be regarded as the only contributors to the aerosol loading over the district as AOT is a measure of the aerosol loading of the entire atmospheric column. It is clear that the wind direction data presented for all three campaigns is driven by

local topography and therefore the micrometeorology of the area. This indicates the importance of local aerosols. However, as presented in the section on trajectory analysis, and the associated wind roses, foreign aerosols may play a significant role at various levels in the atmosphere.

5.2.4. Rainfall

Aerosols cannot remain in the atmosphere forever as there are various mechanisms by which these particulates may be removed. Aerosols may either fall out of the atmosphere as a result of gravity or, one of the most effective of these mechanisms, the washout which occurs through the occurrence of rainfall. This is known as wet deposition (Yum and Hudson, 2001). Analysis of synoptic data and meteorological data requested from the South African Weather Service and Lonmin Platinum reveals that very little rain occurred at the research site during winter 2008 (Table 5.1). The impact of this lack of rain cannot be quantified, however, it can be assumed that the aerosol loading over the Bojanala District remained significantly elevated throughout this time as a result. The impact of this, together with the presence of the Continental High Pressure, recirculation, and inversions, is that of the concentration and build-up of aerosols in the area (Piketh, 2000; Tyson and Preston-Whyte, 2000). The long-term presence of aerosols in the atmosphere results in coagulation, amongst other processes, which eventually results in aerosol growth (Formenti, 2003; Haywood et al., 2003a).

A slightly larger amount of rainfall was recorded over two separate days during the early winter 2009 research campaign than the winter (2008) and late winter (2010) campaigns. The amount of rainfall recorded during early winter is not significant enough to allow for the assumption that aerosol levels were low during 2009 as a result of precipitation scavenging. The cloudy to overcast conditions recorded for 2009 may have resulted in the scavenging of aerosols by raindrops, and so atmospheric cleansing occurred more frequently.

Table 5.1: Meteorological conditions for each of the research campaigns

Campaign	Rainfall (mm)	Atmospheric Conditions
2008	1.4	Fine
2009	4.2	Cloud-Overcast
2010	no rain	Fine

5.3.The Climatological Implications of the Nature of Aerosols over the Bojanala District

The types and sources of aerosols in this research project are not identified. The concentration of aerosols has also not been quantified and thus conclusions drawn regarding the climatological impacts of the aerosols over the research site are only estimations of the type of impact which these particles may have. Aerosols may absorb or scatter solar radiation, depending on their composition. This would mean that energy is either absorbed into the atmosphere and the atmosphere heated, or energy may be scattered back to space, resulting in the cooling of the atmosphere (Seinfeld and Pandis, 2006; Queface, 2002).

The aerosols which are responsible for the aerosol loading over the research site during 2008 resulted in high aerosol optical thickness compared to that of 2009, as discussed in Chapter 4. A high aerosol optical thickness would result from a high level of interference with incoming solar radiation by aerosol particles. This interference was significantly less during the 2009 campaign as AOT on average was revealed to be lower than that those recorded during 2008. The average AOT recorded for the 2010 campaign does not reach the high levels that it did in 2008, however, the AOT is still consistent with hazy conditions (Globe, 2002).

The diurnal variation of AOT and Ångstrom exponent presented in Chapter 4 exhibit a significantly elevated AOT and Ångstrom exponent during the morning hours during the 2008 campaign. These levels are significantly higher than the AOT and Ångstrom exponents recorded during the morning hours of the 2009 and 2010 campaigns. It can therefore be assumed that the impact on solar radiation and potentially climate during the 2008 campaign was significantly higher during the morning hours of July and August 2008 than during the corresponding times during the other campaigns. As discussed previously the AOT during the 2009 campaign was recorded to be lower than during the other two campaigns. This is further revealed in the diurnal variation. The AOT remains relatively consistent throughout the day (as with the 2010 AOT), however, the values of AOT are somewhat lower than during the 2010 campaign. The elevated levels of AOT during the 2010 campaign are concerning for the climatology of the area as these values recorded during the afternoon are well above those of the 2008 and 2009 campaigns. The aerosol loadings remain elevated throughout the day and do not decrease as expected. At midday the airmass is at its smallest

and the amount of sunlight reaching the surface of the earth is higher as a result of the fact that there is less air to travel through, and thus, less particle interference. High levels of fine particles at this time of day could possibly mean that radiative forcing is significantly intensified. The impact on the climate of the area during 2009 may be assumed to be significantly less, however, the presence of fine-mode particles remains considerable.

Ångstrom exponents recorded during each campaign reveal a dominance of fine mode particles to the aerosol loading during all three campaigns. The Ångstrom exponent calculated for each of the sites during the 2009 campaign indicates a dominance of fine mode particles. The frequency of occurrence of Ångstrom exponents revealed that slightly lower Ångstrom exponents were recorded during May and June 2009. These particles, however, do not occur in the atmosphere at significantly high concentrations when compared with the other campaigns and therefore will cause little impact on the climate of the area. Ångstrom exponents were revealed to be above 1 for all sites during 2010, whereas in the previous campaigns some sites were impacted on more dominantly by non-combustion aerosols. This research project has found that the percentage contribution of fine mode particles has increased significantly from 2008 to 2010. The 2010 campaign presents a problem for the climatology of the area. Results discussed in Chapter 4 reveal a contribution of 71.26% by fine mode combustion particles to the aerosol loadings during the 2010 campaign. The impact which high levels of fine mode particles will have on the climate of the area may be considered to be significantly high. The concentration of fine mode particles during this campaign appears to be slightly higher around midday. Particles of this size react more readily to incoming solar radiation of the visible wavelengths, where the incoming solar flux is highest (Seinfeld and Pandis, 2006; Charlson, 1992). The amount of solar radiation at this time of day reaching the earth is highest and therefore the impact may have been considerable.

Spatial analysis indicates that the highest aerosol loadings were recorded toward the eastern and central parts of the district. Larger particles were recorded in these areas, however, since the interference with solar radiation (revealed by higher AOT) was higher than in the areas where the finest particles were measured, it can be assumed that these particles would have a greater impact on the climatology of the area. During the 2010 campaign the Ångstrom

exponent was found to be above 1 for all of the sites indicating that the spatial extent of this radiative forcing may be substantial. Depending on the nature and source of these aerosols, they may have had a very significant impact on regional climate of the area.

The area should be monitored and the nature and sources of these aerosols established in order to discover the magnitude of radiative forcing which has resulted from these aerosols. This is particularly important in light of the increasing concentrations of fine mode particles to the aerosol loading. A large portion of these fine mode particles were found to be accumulation mode aerosols. These particles are highly effective at interacting with incoming solar radiation and because of their size remain in the atmosphere for longer amounts of time (Power, 2003). From the percentage frequency of the Ångstrom exponent indicated in Figure 4.8, it is obvious that accumulation mode aerosols are important in the atmosphere over the Bojanala District. It is therefore very important to continue to monitor the concentrations of these aerosols and the impact which they may have on climate. Finally, the possibility of the elevation of AOT on occasion with the onset of the biomass burning requires significant focus as aerosol loadings appear to increase toward the end of August. Cluster analysis, trajectory analysis and fire information data indicate that biomass burning could significantly elevate aerosol loadings and may therefore have a large impact on the climate of the Bojanala District.

****

The spatial distribution of aerosols and the distribution of fine and coarse particles have been presented in this chapter. The spatial variation in AOT and AE varies significantly over a small area, indicating the importance of local aerosol sources. The highest concentrations of aerosols are identified toward the eastern part of Bojanala District, together with the largest particles recorded. This pattern is different during late winter. This is associated with the irregular and unpredictable location of biomass burning. Analysis of wind data indicates that high AOT and AE are associated with specific wind directions and so may be associated with specific aerosol sources. The higher recordings of rainfall during early winter 2009 are not sufficiently different to indicate that washout may be a significant contributor to the cleansing of the atmosphere in the district. The conclusions of the study are drawn in Chapter 6.

CHAPTER 6: CONCLUSION

Particles exist in the atmosphere which originate from natural and anthropogenic sources. These particles, referred to as aerosols, undergo various changes in the atmosphere and may have a significant impact on climate as well as the hydrological cycle. The understanding of the nature and distribution of these particles is dependent on a large number of factors.

The increase in mining and other industrial activities in the Bojanala Platinum District has had a significant impact on the environment. Direct solar radiation readings taken over the Bojanala District revealed the following regarding the temporal distribution of aerosols over the district; as well as the relative importance of combustion and non-combustion sources:

- During the winter 2008 and late winter 2010 campaigns AOT was most frequently within the range of 0.2 to 0.3. The frequency of occurrence of AOT between 0.3 and 0.4 was also significant for both campaigns. During the 2010 campaign the frequency of occurrence of AOT between 0.4 and 0.5 was 17.9%. The highest percentage frequency of occurrence of AOT during the 2009 campaign was for the 0.1 to 0.2 range (43.15%). This is significantly lower than the winter and late winter campaigns.

- Average AOT per site per campaign reveals that the highest aerosol loadings were recorded during the 2008 and 2010 campaigns. AOT ranged between 0.39 at Machadam Combined School to 0.614 at St. Theresa High School during the 2008 campaign; between 0.158 at Machadam Combined School to 0.313 at Bob Edward Middle School during the 2009 campaign; and between 0.304 at Bob Edward Middle School and 0.477 at J. Gotsube High School during the 2010 campaign. AOT over the district is considered high to very high especially when compared with the average of 0.24 for southern Africa. It is clear that the highest aerosol loadings recorded during the 2009 campaign were on the level of the lowest readings during the other two campaigns.

- Diurnal variation in AOT indicates a similar trend for the 2009 and 2010 campaigns. The trend during 2008 which indicates elevated levels of AOT during the morning followed by a decrease in AOT throughout the day was expected to be identified during the 2010 campaign as both these campaigns recorded solar radiation measurements during the months of July and August. The trends during 2009 and

2010 indicate little variation throughout the day with AOT levels during 2010 being well above those recorded during the 2009 campaign.

- The occurrence of Ångstrom exponent within the range of 1.25 and 1.75 was most common during 2008 and 2010. During 2009 Ångstrom exponents between 1 and 1.5 were most commonly recorded. Even though coarse mode non-combustion particles were recorded less frequently, these particles played a significant role in the aerosol loading, especially during the 2008 campaign where some of the highest aerosol loadings were associated with coarse mode particles. The contribution of fine mode particles remained dominant throughout each campaign. Fine mode particles were recorded 65.97% of the time during the 2008 campaign; 64.38% of the time during the 2009 campaign and 71.26% of the time during the 2010 campaign. Fine mode particles are associated with domestic fuel burning, traffic and mine processing activities in the district. Traffic and mine processing sources continued throughout the year. The higher concentrations of fine mode combustion particles could potentially be related to the fact that readings were taking until the end of August (early spring), when biomass burning becomes important in the area.

- Average Ångstrom exponents revealed that slightly coarse mode to fine mode particles dominated at different sites. This range is attributed to sources within close proximity to each site. The highest range in the Ångstrom exponent was recorded during the 2008 campaign where an Ångstrom exponent of 0.85 was recorded at St. Theresa High School and of 1.6 at Rakgatla High School. During the 2009 campaign the Ångstrom exponents ranged from 0.897 at Johane Mokololobatsi High School to 1.26 at Rakgatla High School; and from 1.04 at J. Gotsube High School to 1.484 at Rakgatla High School. Rakgatla High School exhibited the finest particles during each of the campaigns. None of the sites were dominated by coarse mode particles during 2010.

- Diurnal plots indicated a similar variation to that of AOT. The same trend identified during the 2008 campaign for both AOT and Ångstrom exponents indicates that the highest aerosol loadings are related to fine mode combustion particles. The high AOT and Ångstrom exponents identified during winter 2008 could potentially be related to domestic fuel burning and traffic sources. The same trend, however, was not

identified in the 2010 data. The variation in Ångstrom exponent during the early witner 2009 and late winter 2010 campaigns was very similar, with little variation occurring during the day. This is a similar pattern to that of the AOT diurnal trend. Diurnal trends indicated that the Ångstrom exponent on average remained above 1 throughout the day. It is apparent that combustion sources remained the dominant sources throughout the day during 2009 and 2010, whereas combustion sources became less dominant during the 2008 winter campaign as the day progressed.

- The variation in the frequency of occurrence of various AOT levels and the associated AE, together with the diurnal patterns and overall averages presented for each stage of winter indicates the dominance of various sources during each stage of winter. It is clear that the aerosol loadings may be dominated by emissions from domestic fuel burning during winter 2008. The colder winter months of 2008 are associated with the significant enhancement of domestic fuel burning activities, as well as the strengthening and persistence of inversion layers at various layers which concentrate pollutants such as those emitted from domestic fuel burning, traffic and mining activities in the area. The differences in the impact of coarse mode particles (from mine dumps and dirt roads); and that of fine mode particles from smelters and other mining combustion activities reveal the significantly different impact that fine and coarse mode particles may have on AOT. This variation is clear during winter 2008. The absence (or reduced levels of) domestic fuel burning and biomass burning and domestic fuel burning); as well as warmer temperatures and the related reduction in strength and persistence of inversion layers may indicate that the diurnal profiles presented are indicative of the local, mining activities in the area. It is unclear, however, as to the obvious similarity between early winter and late winter diurnal patterns. As temperatures increase toward the end of August, domestic fuel burning activities are assumed to decrease significantly (as identified in diurnal variations of AOT and AE); this together with a reduction in the strength and persistence of inversion layers reveals an alternative source to the aerosol loading during late winter (as AOT levels are significantly higher than early winter). These differences, both spatially and temporally indicate that biomass burning becomes a dominant aerosol source at this time of the year. August falls within the peak period of biomass burning in the area.

- Daily average AOT values and Ångstrom exponents, averaged for all of the sites and plotted for each campaign, revealed peaks and depressions in the data where AOT and Ångstrom exponents were either elevated or below average. These peaks and depressions occurring at all of the sites indicated that foreign airmasses were potentially impacting on the aerosol burden over the district. HYSPLIT trajectories were created which indicate the importance of airmasses originating from polluted regions (Mpumalanga Highveld) and clean air regions (Atlantic Ocean). Airmasses from polluted regions such as the Mpumalanga Highveld were associated with an increase in AOT and Ångstrom exponent. Airmasses originating from the Atlantic Ocean may be associated with cold fronts which often cleanse the air over the interior during winter. Comparison of trajectories to ambient wind data reveals the importance of aerosols at different levels in the atmosphere.

- Comparisons of AOT with ambient particulate matter concentrations measured during the 2008 and 2009 campaigns at Marikana indicate a significant relationship between the diurnal trend in PM10 compared to AOT. A further significant relationship was established through a scatter plot of PM10 and AOT. Comparison with PM2.5 and PM1 did not reveal any significant relationships. Particulate matter concentrations measured during the 2009 campaign indicated an inverse relationship between AOT and PM10. Industrial signatures identified in the diurnal trend in PM1 were not identified in the AOT data, therefore further substantiating the impact and importance of upper levels of aerosols over the Bojanala District.

- Weekday analysis of AOT diurnal variation revealed no significant variation between week days and weekends. The diurnal variation in AOT and Ångstrom exponent during the 2008 campaign may be related to traffic as similar patterns were identified to that of traffic trends identified. Traffic patterns are not seasonal, however, so this is unlikely.

- Aerosol concentrations measured over the Rustenburg area on-board the AeroCommander aircraft during 2005 indicated that the majority of aerosols were concentrated in the lower levels of the atmosphere and could therefore be related to ambient emissions. This distribution with altitude may vary depending on the dynamics of the atmosphere over the area. The possibility of aerosols at elevated

levels impacting on the aerosol loadings remains to be investigated and should be taken into account as AOT measured on the ground by hazemeters takes into account the entire atmospheric column.

- Analysis of meteorological data indicated a very dominant south-westerly wind direction overall. Further analysis which separated wind data into day and night indicated a dominant south-westerly wind direction at night; whereas during the day the winds were observed to be more variable. Diurnal variation of wind direction during all three campaigns revealed that local micrometeorology and the variation of aerosol sources throughout the day are similar during each stage of winter. During 2008 high AOT and Ångstrom exponent values were recorded commonly when the wind originated from the 200 to 250º wind sector. This usually occurred at 07h00. During the 2009 campaign a northerly wind commonly occurred at approximately 12h00. Ångstrom exponents were found to decrease when the winds originated from the 50 to 100º wind directions. This usually occurred between 09h00 and 11h00. During the 2010 campaign the AOT and Ångstrom exponents remained elevated regardless of wind direction. Nearby mining activities as well as industrial activities, traffic and domestic fuel burning, as well as emissions from the Rustenburg area may have a direct impact on the aerosol loading at each site.

- Recorded rainfall indicated little to no rainfall during the 2008 and 2010 campaigns; whereas during the 2009 May and June campaign rainfall recorded was significantly higher. This could possibly have resulted in precipitation scavenging of aerosols and therefore be one of the potential reasons for the lower aerosol loadings recorded during this campaign.

Spatial analysis of the distribution of aerosols over the Bojanala District indicated the following:

- Aerosol loadings were higher over the eastern parts of the district during the 2008 and 2009 campaigns. These areas were usually associated with lower Ångstrom exponents, some of which were attributed to coarse mode particles. The sites toward the east lie in close proximity to a mind dump and are essentially large townships. There are many dirt roads in the area. It is clear that the eastern sector of the Bojanala District is dominated by larger particles which have a significant impact on AOT

levels. The AOT levels over the western sector are significantly high but dominated by fine mode particles which may be associated with various mine-related processes, such as smelters. The 2010 campaign indicates a slight shift in the areas of higher aerosol loadings westward, with the lower Ångstrom exponents being recorded in these areas as well. The Ångstrom exponent was above 1 indicating fine-mode combustion aerosols were significantly dominant over the entire district during this July and August period of 2010. The shift toward aerosols from combustion sources in 2010 is significant and requires further investigation. This could potentially be associated with the onset of the biomass burning season. It is clear that local aerosol sources had a significant impact on the aerosol loadings at each of the sites.

- The understanding of the climatological impacts of the nature and distribution of aerosols over the Bojanala District is very limited. Ångstrom exponents reveal that the fine mode particles are only slightly dominant, especially during early winter and winter. The percentage contribution of these particles increases significantly during late winter. These fine mode particles interact readily with incoming solar radiation and may have a significant impact on the climatology of the area. As the AOT and Ångstrom exponent values remain relatively stable throughout the day during late winter, it is probable that the impact which aerosols have on the climate of the area is substantial at this time of year. It was often recorded that the highest aerosol loadings were associated with slightly larger particles. The type of effect which these particles would have on solar radiation and clouds is out of the scope of this research as the nature and types of these aerosols cannot be identified using hazemeter readings. This provides difficulty in understanding whether the forcing would be positive or negative.

    - Further, spatial analysis indicates that the highest aerosol loadings are recorded toward the eastern and central parts of the district. Larger particles are recorded in these areas, however, since the interference with solar radiation (revealed by higher AOT) is higher than in the areas where the finest particles were measured, it can be assumed that these particles would have a greater impact on the climatology of the area. Accumulation mode particles are found to be of significant importance in the area, and as these particles are regarded as highly efficient at interacting with solar radiation this area should be

monitored in this regard. Aerosol loadings remain relatively the same throughout the day during the 2010 campaign. Further investigation is required as to the impact which aerosols will have during the morning when the path-length of solar radiation is longest and at midday when the path-length is shorter and the amount of interference due to particles in the atmosphere would be less.

The properties of aerosols over the Bojanala District have been analysed in terms of their spatial and temporal characteristics; as well as their potential impact on the regional climate of the area. Clear differences in aerosol loadings during early winter, winter and late winter are identified. As a result of the nature of AOT, the sources of aerosols could not be identified with certainty, however, considering various temporal and spatial analysis assumptions are made. Further investigation into the sources and possible reasons for variations in aerosol loadings during the different stages of winter are required.

CHAPTER 7: REFERENCES

Ackerman, A.S., O.B. Toon, J.P. Taylor, D.W. Johnson, P.V. Hobbs, and R.J. Ferek, 2000: Effects of Aerosols on Cloud Albedo: Evaluation of Twomey's Parameterization of Cloud Susceptibility Using Measurements of Ship Tracks, *Journal of Atmospheric Science*, **57**, 8,2684-8,2695

Albrecht, B.A., 1989: Aerosols, Cloud Microphysics and Fractional Cloudiness, *Science*, **245**,1227-1230

Andreae, M.O., 1991: *Biomass Burning: It's History, Use and Distribution and it's Impact on Environmental Quality and Global Climate, In: Global Biomass Burning*, p3-21, edited by J.S. Levine, The MIT Press, Cambridge, MA

Andreae, M.O., Atlas, E., Cachier, H., Cofer, W.R., Harris, G.W., Helas, G., Koppman, R., Lacaux, J. and Ward, D.E., 1996a: *Trace Gas and Aerosol Emissions from Savannah Fires*, J.S. Levine (ed) Biomass Burning and Global Change, MIT press, Cambridge, 278-294

Andreae, M.O., T.W. Andreae, H. Annegarn, J. Beer, H. Cachier, P. Le Canut, W. Albert, W. Maenhaut, I. Salma, F.G. Wienhold, T. Zinker, 1998: Airborne Studies of Aerosol Emissions from Savanna Fires in Southern Africa: 2. Aerosol Chemical Composition, *Journal of Geophysical Research*, **103**, 32,119-32,128.

Ångstrom, A., 1929: On the Atmospheric Transmission of Sun Radiation and on Dust in the Air, *Geographical. Annals*, **12**, 130-159

Annegarn, H.J., Leslie A.C.D., Winchester, J.W., Sellschop, J.P.F., 1983: Particle Size and Temporal Characteristics of Aerosol Composition near Coal-fired Electric Power Plants of the Eastern Transvaal, *Aerosol Science and Technology*, **2**, 489-498.

Annegarn, H.J., Kneen, M.A., Piketh, S.J., Horne, A.R., Hlapolosa, H.S.P., Kirkman, G.A., 1996: Evidence for Large Scale Circulation of Anthropogenic Sulphur over Southern Africa, National Association for Clean Air Conference, Brits, 11-13 November.

(AQMP) Piketh, S.J., M. van Nierop, C. Rautenbach, N. Walton, K. Ross, S. Holmes, T. Richards, 2005: *Rustenburg Local Municipality Air Quality Management Plan,* Environmental Science Projects

ARM Climate Research Facility: *Instrument: CIMEL Sun Photometer*, http://www.arm.gov/instruments/csphot, Date accessed: 2014/01/10

Barenbrug, M., 2003: *The Transport of Aerosol and their Effects on Direct Solar Radiation over Southern Africa*, MSc Dissertation, University of the Witwatersrand, Johannesburg

Bergstrom, R.W., Pilewskie, P., Schmid, B, and Russell. P.B., 2003: Estimates of the Spectral Aerosol Single Scattering Albedo and Aerosol Radiative Effects during SAFARI 2000, *Journal of Geophysical Research*, **108**,D13,8474,doi:10.1029/2002JD002435

Bigala, T., 2008: *The Haze over the Highveld*, MSc Dissertation, University of the Witwatersrand

Bodhaine, B.A., Wood, N.B., Dutton, E.G., Slusser, J.R., 1999: On Rayleigh Optical Depth Calculations, *Journal of Atmospheric and Oceanic Technology*, **16**, 1854-1861

Boucher, O., D. Randall, P. Artaxo, C. Bretherton, G. Feingold, P. Forster, V.-M. Kerminen, Y. Kondo, H. Liao, U. Lohmann, P. Rasch, S.K. Satheesh, S. Sherwood, B. Stevens and X.Y. Zhang, 2013: Clouds and Aerosols Supplementary Material. In: Climate Change 2013: The Physical Science Basis. Contribution of Working Group I to the Fifth Assessment Report of the Intergovernmental Panel on Climate Change [Stocker, T.F., D. Qin, G.-K. Plattner, M. Tignor, S.K. Allen, J. Boschung, A. Nauels, Y. Xia, V. Bex and P.M. Midgley (eds.)]. vailable from www.climatechange2013.org and www.ipcc.ch.

Cardell, J., 2007: Buildings and Energy from the Sun: Course, http://www.science.smith.edu/~jcardell/Courses/EGR100/protect/slides/L18.pdf, Date accessed: 2014/01/10

Campbell, J.R., Welton, E.J., Spinhirne, J.D., Qiang, J., Tsay, S., Piketh, S.J., Barenbrug, M., and Holben, B.N., 2003: Micropulse Lidar Observations of Tropospheric Aerosols over North-Eastern South Africa during the ARREX and SAFARI 2000 Dry Season experiments, *Journal of Geophysical Research*, **108**, SAF 33-1 – SAF33-19 (DOI 10.1029/2002JD002563)

Charlson, R.J., Lovelock, J.E., Andreae, M.O., Warren, S.G., 1989: Sulfate Aerosols and Climate (A Reply), *Nature*, **340**, 437-438

Charlson R.J., Longer, J. and Rodhe, H., 1990: Sulfate Aerosol and Climate, *Nature*, **326**, 655-661

Charlson, R.J., Schwartz, S.E., Hales, J.M., Cess, R.D., Coakley, J.A., Jnr, Hansen, J.E. and Hoffman, D.J., 1992: Climate Forcing by Anthropogenic Aerosols, *Science*,**255**, 423-430

Chin, M., P. Ginoux, S. Kinne,O. Torres, B.N. Holben, B.N. Duncan, R.V.Martin, J.A. Logan, Higurashi, T. Nakajima, 2002: Tropospheric Aerosol Optical Thickness from GOCART Model and Comparisons with Satellite and Sun Photometer Measurements, *American Meteorological Society*, **59**, 461-483

Chu, D.A., Y.J. Kaufman, C. Ichoku, L.A. Remer, D. Tanre and B.N. Holben, 2002: Validation of MODIS Aerosol Optical Depth Retrieval over land, *Geophysical Research Letters*, **29 (12) 8007**, (DOI: 10.1029/2001GL013205)

Chylek, P., and Wong, J., 1995: Effect of Absorbing Aerosols on Global Radiation Budget, *Geophysical Research Letters*, **22**, 929-931

Coakley, J.A. Jr., R.L. Bernstein, and P.A. Durrae, 1987: Effects of Ship Stack Effluents on Cloud Reflectance, *Science*, **237**, 953-956

Cosijn, C. and Tyson, P.D., 1996: Stable Discontinuities in the Atmosphere over South Africa, *South African Journal of Science*, **92**, 381-386

Croft, B., U. Lohmann, R.V. Martin, P. Stier, S.Wurzler, J. Feichter, R. Posselt and S. Ferrachat, 2009: Aerosol Size-Dependent Below-Cloud Scavenging by Rain and Snow in the ECHAM5-HAM, *Atmospheric Chemistry and Physics*, **9**, 4653-4675

De Graaf, M., L. G. Tilstra, P. Wang, and P. Stammes (2012), Retrieval of the aerosol direct radiative effect over clouds from spaceborne spectrometry, *J. Geophys. Res.*, *117*, D07207, doi:10.1029/2011JD017160.

De Graaf, M., N. Bellouin, L.G. Tilstra, J. Haywood, P. Stammes, 2014: Aerosol Direct Radiative Effect of Smoke Over Clouds over the SouthEast Atlantic Ocean from 2006 to 2009, *Geophysical Research Letters*, **41**, 7723-7730

Dubovik, O, A. Smirnov, B. Holben, M. King, Y. Kaufman, T. Eck, I. Slutsker, 2000: Accuracy Assessments of Aerosol Optical Properties retrieved from Aerosol Robotic Network (AERONET) Sun and Sky Radiance Measurements, *Journal of Geophysical Research*, **105**, 9791-9806

Eck, T.F., Holben, B.N., Reid, J.S., Dubovik, O., Smirnov, A., O'Neil, N.T., Slutsker, I. and Kinne, S., 1999: Wavelength Dependence of the Optical Depth of Biomass Burning, Urban, and Desert Dust Aerosols, *Journal of Geophysical Research*, **104**, 315333-31349

Eck T.F., B.N. Holben, O. Dubovik, A. Smirnov, I. Slutsker, J.M. Lober,V. Ramanathan, 2001: Column Integrated Aerosol Optical Properties over Maldives during NE Monsoon for 1998-2000, *Journal of Geophysical Research*,**106**, 28,555-28,566

Eck, T.F., B.N. Holben, J.S. Reid, N.T. O'Neill, J.S. Schafer, O. Dubovik, A. Smirnov, M.A. Yamasoe, and P. Artaxo, 2003: High Aerosol Optical Depth Biomass Burning Events: A Comparison of Optical Properties for Different Source Regions, *Geophysical Research Letters*, **30(20),** 2035, (DOI:10.1029/2003GLO17861

Eck, T.F., B.N. Holben, O. Dubovik, A. Smirnov, P. Goloub, H.B. Chen, B. Chatonet, L. Gomes, X.Y. Zhang, S. C. Tsay, Q. Ji, D. Giles, and I. Slutsker., 2005: Columnar Aerosol Optical Properties at AERONET sites in Central Eastern Asia and Aerosol Transport to the Tropical Mid-Pacific, *Journal of Geophysical Research*, **110** (DOI:10.1029/2004JD005274)

Elias, T., Piketh, S.J., Burger, R., and Silva, A.M., 2003: Exploring the Potential of Combining Column-Integrated Atmospheric Polarization with Airborne in situ Size Distribution Measurements for the Retrieval of an Aerosol Model: A Case Study of a Biomass Burning Plume During SAFARI 2000, *Journal of Geophysical Research*, **108**, (DOI 10.1029/2002JD002426)

Elias, T., A.M. Silva, N. Belo, S. Pereira, P. Formenti, G. Helas, and F. Wagner, 2006: Aerosol Extinction in a Remote Continental Region of the Iberian Peninsula During Summer, *Journal of Geophysical Research*, **11**, D14204, (DOI: 10.1029/2005JD006610)

Elsom, 1987: *Atmospheric Pollution: Causes, Effects and Control Policies*, Basil Blackwell, NewYork

Fallah-ADL, H., J. Jaja, S. Liang, 1997: Fast Algorithms for Estimating Aerosol Optical Depth and Correcting Thematic Mapper Imagery, *Journal of Supercomputing*, **10**, 315-329

Folini, D., and M. Wild, 2011: Aerosol Emissions and Dimming/Brightening in Europe: Sensitivity Studies with ECHAM5-HAM, *Journal of Geophysical Research*, **116**, (DOI 10.1029/2011JD016227)

Formenti, P., Elbert, W., Maenhout, W., Haywood, J., Osborne,S., and Andreae, M.O., 2003: Inorganic and Carbonaceous aerosols during the Southern African Regional Science Initiative (SAFARI 2000) experiment: Chemical Characteristics, Physical Properties, and Emission Data for Smoke from African Biomass Burning, *Journal of Geophysical Research*, **108**, (DOI 10.1029/2002JD002408)

Forster, P., V. Ramaswamy, P. Artaxo, T. Berntsen, R. Betts, D.W. Fahey, J. Haywood, J. Lean, D.C. Lowe, G. Myhre, J. Nganga, R. Prinn, G. Raga, M. Schulz and R. Van Dorland, 2007: Changes in Atmospheric Constituents and in Radiative Forcing. *In: Climate Change 2007: The Physical Science Basis. Contribution of Working Group I to the Fourth Assessment Report of the Intergovernmental Panel on Climate Change* [Solomon, S., D. Qin, M. Manning, Z. Chen, M. Marquis, K.B. Averyt, M.Tignor and H.L. Miller (eds.)]. Cambridge University Press, Cambridge, United Kingdom and New York, NY, USA.

Freiman, M.T. and S.J. Piketh, 2003: Air Transport Into and Out of the Industrial Highveld Region of South Africa, *Journal of Applied Meteorology*, **42**, 994-1002

Garstang, M., Tyson, P.D., Swap, R., Edwards, M., Kallberg, P., and Lindesay, J.A., 1996a: Horizontal and Vertical Transport of Air over Southern Africa, *Journal of Geophysical Research*, **101**, 23777-23791

Gobbi, G.P., Kaufman, Y.J., Koren, I., and Eck, T.F., 2007: Classification of Aerosol Properties derived from AERONET direct Sun Data, *Atmospheric Chemistry and Physics*, **7**, 453-458

Globe, 2002: *7th Biennial Conference and Trade Fair on Developing the Business of the Environment*, March 13-15, 2002, Vancouver, British Columbia

http://www.globe2002.com

Greenfield, S.M., 1957: Rain Scavenging of Radioactive Particulate Matter from the Atmosphere, *Journal of Meteorology*, **14**, 115-125

Guoyong, W., S. Tsay, R.F. Cahalan, and L. Oreopoulus, 1999: Path Radiance Technique for Retrieving Aerosol Optical Thickness over Land, *Journal of Geophysical Research*, **104** (D24), 31,321-31,332

Hansen, J., Sato, M., Ruedy, R., Caeis, A., Asanoah, K., Beckford, K., Barenstein, S., Brown, E., Cairns, B., Carlson, B., Curron, B., de Castro, S., Drayen, S., Etwarrow, L., Ferede, T., Fox, M., Gaffen, D., Glasco, J., Gordon, H., Hollandsworth, S., Jiang, X., Johnson, C., Lawrence, N., Lean, J., Lerner, J., Lo, K., Logan, J., Luckett, A., McCormick, M.P., McPeters, R., Miller, R.L., Minnis, P., Ramberron, I., Russell, G., Russell, P., Stone, P., Tegen, I., Thomas, S., Thomason, L., Thompson, A., Wilder, J., Willson, R., and Zawodny, J., 1997: Forcings and Chaos in Interannual to Decadal Climate Change, *Journal of Geophysical Research*, **102**, 25679-25720

Hansen, J.E., Sato, M, 2001: Trends of measured climate forcing agents, *Proceedings of the National Academy of Sciences of the United States of America*, **98**, 14778-14783

Hao, W.M., Ward, D.E., Susott, R.A., Bubbitt, R.E., Nordgren, B.C., Kaufman, Y.J., Holben, B.N., Giles, D.M., 2000: Comparison of Aerosol Optical Thickness Measurements by MODIS, AERONET Sun Photometers, and Forestry Service Handheld Sun Photometers in Southern Africa during the SAFARI 2000 campaign, *International Journal of Remote Sensing*, **26**, 4169-4183

Hao, W.M., D.E. Ward, R.A. Sasott, R.E. Babbitt, B.L. Nordgren, Y.J. Kaufman, B.N. Holben, and D.M. Giles, 2005: Comparison of Aerosol Optical Thickness Measurements by MODIS, AERONET Sun Photometers and Forest Service Handheld Sun Photometers in Southern Africa during the SAFARI 2000 Campaign, *International Journal of Remote Sensing*, **26**, 4169-4183

Haywood, J.M. and Boucher, O., 2000: Estimates of the direct and indirect radiative forcing due to tropospheric aerosols: A review, *Review of Geophysics*, ***38***, 513-543

Haywood, J., Francis, P., Dubovik, O., Glew, M., and Holben,B., 2003: Comparison of Aerosol Size Distributions, Radiative, and Optical Depths determined by Aircraft Observations and Sun Photometers during SAFARI 2000, Journal of Geographical Research, **108**, D13, Doi:10.1029/2002JD002250

Heald, C.L., D.A. Ridley, J.H. Kroll, S.R.H. Barrett, K.E. Cady-Perreira, M.J. Alverado and C.D. Holmes, 2014: Contrasting the Direct Radiative Effect and Direct Radiative Forcing of Aerosols, *Atmospheric Chemistry and Physics*, **14**, 5513-5527

Helas, G., Andreae, M.O., Schebeske, G. and LeCanut, P., 1995: SA'ARI-94: A preliminary View of results, *South African Journal of Science*, **91**, in press.

Held, G. And Snyman, G.M., 1994: *Accumulation and Recirculation of Pollutants in the Atmosphere of the Highveld*, Eskom report no. TRR/593174, Johannesburg, 90pp

Held, G., Scheifinger, H. and Snyman, G.M., 1996: Recirculation of pollutants in the atmosphere of the South African Highveld, *South African Journal of Science*, **90**, 91-97.

Holben, B.N., Eck, T.F. and Fraser, R.S., 1991: Temporal and Spatial variability of aerosol optical depth in the Sahel region in relation to vegetation remote sensing, *International Journal of Remote Sensing*, **12**, 1147-1163

Holben, B.N., T. F. Eck, I. Slutsker, D. Tanre, J.P. Buis, A. Setzer, E. Vermote, J.A. Reagan, Y.J. Kaufman, T. Nakajima, F. Lavenu, I. Jankowiak, A. Smirnov, 1998: AERONET – A Federated Instrument Network and Data Archive for Aerosol Characterization, *Remote Sensing of the Environment*, **66**, 1-16

Holben, B.N., D. Tanre, A. Smirnov, T.F. Eck, I. Slutsker, N. Abuhassan, W.W. Newcomb, J.S. Schafer, B. Chatenet, F. Lavenu, Y.J. Kaufman, J.Vande Castle, A. Setzer, B. Markham, D. Clark, R. Frouin, R. Halthore, A. Karneli, N.T. O'Neill, C. Pietras, R.T. Pinker, K. Voss, G. Zibordi, 2001: An Emerging Ground-Based Aerosol Climatology: Aerosol Optical Depth from AERONET, *Journal of Geophysical Research*, **106**, 12,067-12,097

Ichoku, C., Levy, R., Kaufman, Y.J., Remer, L.A., Li, R., Martins, V.J., Holben, B.N., Abuhassan,N., Slutsker, I., Eck, T.F., and Pietras, C.,2002: Analysis of the performance characteristics Of the five-channel Microtops II Sun Photometer for

measuring Aerosol Optical Thickness And the Precipitable Water Vapour, *Journal of Geophysical Research*, **17**, D13, doi:10/1029/2001JD001302

Ignatov, A., J. Shapper, S. Cox, I. Laszlo, N.R. Nalli, K.B. Kidwell, 2004: Operational Aerosol Observations (AEROBS) from AVHRR/3 on Board NOAA-KLM Satellites, *Journal of Atmosphere and Oceanic Technology*, **21**, 3-26

IPCC Report, 2014: *Climate Change 2013: The Physical Science Basis, Contribution of Working Group I to The Fifth Assessment Report of the Intergovernmental Panel on Climate Change*,

www.climatechange2013.org

Website accessed: June 2015

Iqbal, M., 1983: *An Introduction to Solar Radiation*, Academic Press, Toronto

Jacob, D.J., Andreae, M.O., Bigg, E.K., Duce, R.A., Fung, I., Hidy, G.M., Legrend, M., Prospero, J.M., Raes, F., Warren, S.G., and Wiedenschler, A., 1995: *Group Report: What Factors Influence Atmospheric Aerosols, How Have they Changed in the past and how might they change in the future, in Aerosol Forcing of Climate*, edited by R.J. Charlson and J. Heintzenburg, John Wiley &Sons, 183-195

Kahn, R.A., 2012: Reducing the Uncertainties in Direct Aerosol Radiative Forcing, *Surveys in Geophysics*, **33**, 701-721

Kaufman, Y.J., Setzer, A., Ward, D., Tanre, D., Holben, B.N., Menzel, P., Pereira, M.C., and Rasmussen, R., 1992: Biomass burning airborne and spaceborne experiment in the Amazonas (BASE-A), *Journal of Geophysical Research*, **97**, 14581-14599

Kaufman, J.B., Cummings, D.L., Ward, D.E., 1994: Relationship of Fire, Biomass and Nutrient Dynamics Along a Vegetation Gradient in the Brazilian Cerrado, *Journal of Ecology*, **82**, 519-531

Kaufman, Y.J., D. Tanre, L.A. Remer, E.F. Vermote, A. Chu, and B.N. Holben, 1997: Operational Remote Sensing of Tropospheric Aerosol over Land from EOS Moderate Resolution Imaging Spectroradiometer, *Journal of Geophysical Research*, **102 (D14)**, 17051-17067

Kaufman, Y.J., D. Tanre and O. Boucher, 2002: A Satellite View of Aerosols in the Climate System, *Nature*, **419**, 215-223

Kay, M.J., and Box, M., 2000: The Radiative Effects of Absorbing Aerosols and the Impact of Water Vapour, *Journal of Geophysical Research*, **105**, 12,221-12,234

Kemp, D.D., 1994: *Global Environmental Issues: A Climatological Approach (2nd Edition)*, Routledge, London

Kemp, D.D., 2004: *Exploring Environmental Issues: An Integrated Approach*, Routledge, London

King, M.D., Kaufman, Y.J., Tanre, D. And Nakajima, T., 1999: Remote Sensing of Tropospheric Aerosols from Space: Past, Present and Future, *Bulletin of American Meteorological Society*, **80**, 2229-2259

Kirkman, G.A., 1998: *Aerosol and trace gas distribution over southern Africa*, MSc dissertation, University of the Witwatersrand, Johannesburg, South Africa.

Kirkman, G.A., Piketh, S.J., Helas, G., Annegarn, H.J. and Andreae, M.O., 1998(a): Seasonal Tropospheric aerosol characterisation over southern Africa, *Journal of Aerosol Science*, **29**, Conference proceedings, S555-S556.

Knobelspiesse, K.D., Pietras, C., Fargion, G.S., Wang, M., Frouin, R., Miller, M.A., Subramaniam, A., Balch, W.M., 2004: Maritime Aerosol Optical Thickness Measured by Handheld Sun Photometers, *Remote Sensing of the Environment*, **93**, 87-106

Komhyr, W.D., R.D. Grass, and R.K. Leonard, 1989: Dobson Spectrophotometer 83: A Standard for Total Ozone Measurements, *Journal of Geophysical Research*, **94**, 9847-9861

Leaitch, W.R., J.W. Strapp, G.A. Isaac, 1986: Cloud Droplet Nucleation and Cloud Scavenging of Aerosol Sulphate in Polluted Atmospheres, *Tellus*, **38B**, 328-344,

Levy, R.C., L.A. Remer, S. Mattoo, E.F. Vermote, and Y.J. Kaufman, 2007: Second-Generation Operational Algorithm: Retrieval of Aerosol Properties Over Land from Inversion of Moderate Resolution Imaging Spectroradiometer Spectral Reflectance, *Journal of Geophysical Research*, **112**, D13211, (DOI: 10.1029/2006JD007811)

Levy, R.C., L.A. Remer, O. Dubovik, 2007: Global Aerosol Optical Properties and Applications to MODIS Aerosol Retrieval Over Land, Journal of Geophysical Research, 112, D13210, (DOI: 10.1029/2006JD007815)

Li, Z., Nui, F., Lee, K., Xin, J., Hao, W., Nordgren, B., Wang, Y., Wong, P., 2007: Validation and Understanding of Moderate Resolution Imaging Spectroradiometer Aerosol Products (C5) Using Ground-based Measurements from the Handheld Sun Photometer Network in China, *Journal of Geophysical Research*, **112**, doi: 10.1029/2007JD008479,207

Lohmann, U., and J. Feichter, 2005: Global Indirect Aerosol Effects: A Review, *Atmospheric Chemistry and Physics*, **5**, 715-737

Mallett, M., J.C. Reger, S. Despidu, O. Dubovik, and J.P. Putaud, 2003: Microphysical and Optical Properties of Aerosol Particles in Urban Zone during ESCOMPTE, *Atmospheric Research*, **69**, 73-97

Mathee, A. and Y.E.R. von Schirnding, 2003: "Air quality and health in Greater Johannesburg". In: G. McGranahan and F. Murray (eds), *Air pollution and health in developing countries*. Earthscan Publications, London, 206-219.

Mdluli, T.N., 2007: *The Societal Dimensions of Domestic Coal Combustion: People's Perceptions and Indoor Aerosol Monitoring*, Phd Dissertation, University of the Witwatersrand, Johannesburg

Meter, S., F. Formenti, S.J. Piketh, H.J. Annegarn and M.A. Kneen, 1999: PIXE Investigation of Aerosol Composition over the Zambian Copperbelt, *Nuclear Instrumentation Methods in Physics- Research B*, **150**, 433-438

Myhre, G., and Stordal, F., 2001: On the Tradeoff of the Solar and Thermal Infrared Radiative Impacts of Contrails, *Geophysical Research Letters*, **28**, 3119-3122

Myhre, G., B.H. Samset, M. Schulz, Y. Balkanski, S. Bauer,T.K. Berntsen, H. Bian, N. Bellouin, M. Chin, T. Diehl, R.C. Easter, J. Feichter, S.J. Ghan, D. Hauglustaine, T. Iversen, S. Kinne, A. Kirkevag, J.F. Lamarque, G. Lin, X. Liu, M.T. Lund, G. Luo, X. Ma, T. van Noije, J.E. Penner, P.J. Rasch, A. Ruiz, O. Seland, R.B, Skeie, P. Stier, T. Takemura, K. Tsigaridis, P. Wang, Z. Wang, L. Xu, H. Yu, F. Yu, J.H. Yoon, K. Zhang, H. Zhang, and C. Zhou, 2013: Radiative Forcing of the Direct

Aerosol Effect From AeroCom hase II Simulations, *Atmospheric Chemistry and Physics*, **13**, 1853–1877

Naidoo, S., 2014: *Quantification of Emissions Generated from Domestic Burning Activities from Townships in Johannesburg*, MSc Dissertation, University of the Witwatersrand, Johannesburg

Nakajima, T., and Higurashi, A., 1998: A use of 2-Channel Radiances on Aerosol Characterization from Space, *Geophysical Research Letters*, **25**, 3815-3818

Nicolet, M., 1981: The Solar Spectral Irradiance and its Action in the Atmospheric Photo-Dissociation Process, *Planetary and Space Science*, **29**, 951-974

Ncipha, X.G., 2011: *Comparison of Air Pollution Hotspots in the Highveld using Airborne Data*, MSc Dissertation, University of the Witwatersrand, Johannesburg

Ocko, I.B., V. Ramaswamy, P. Ginoux, Y. Ming and L.W. Horowitz, Sensitivity of Scattering and Absorbing Aerosol Direct Radiative Forcing to Physical Climate Factors, *Journal of Geophysical Research* , **117**, DOI: 10.1029/2012JD018019

O'Neill, N., T.F. Eck, and O. Dubovik, 2001a: A Modified Ångstrom Exponent Coefficient for the Characterization of Sub-micron Aerosols, *Applied Optics*, **40**, 2368-2376

O'Neill, N.J., T.F. Eck, A. Smirnov, B.N. Holben, and S. Thulasirman, 2003: Spectral Discriminations of Coarse and Fine Mode Optical Depth, *Journal of Geophysical Research*, **108(D17)**, 4559, (DOI: 10.1029/2002JD002975)

Paramonov, M., T. Gronholm and A. Virkkula, 2011: Below-Cloud Scavenging of Aerosol Particles by Snow at an Urban Site in Finland, *Boreal Environment Research*, **16**, 304-320

Philipona, R., Behrens, K., Ruckstuhl, C., 2009: How Declining Aerosols and Rising Greenhouse Gases Forced Rapid Warming in Europe Since the 1980's, *Geophysical Research Letters*, **36**, (DOI: 10.1029/20089L036350,2009)

Piketh, S.J., Annegarn, H.J. and Kneen, M.A., 1996: *Regional Scale Impacts of Biomass Burning Emissions over Southern Africa*, in J.S. Levine (ed), Biomass Burning and Global Change, MIT Press, Cambridge, 320-326

Piketh, S.J., P. Formenti, P.M.T. Frieman, W. Maenhaut, H.J. Annegarn and P.D. Tyson, 1998: Industrial Pollutants at a Remote Site in South Africa, *Proceedings of the 11th World Clean Air and Environment Congress (IUAPPA 6)*, Durban, South Africa

Piketh, S.J., H.J. Annegarn, and P.D. Tyson, 1999: Lower Tropospheric Aerosol Loadings over South Africa: The Relative Contribution of Aeolian Dust, Industrial Emissions and Biomass Burning, *Journal of Geophysical Research*, **104**, 1597-1607

Piketh, S.J., 2000: *Transport of Aerosols and Trace Gases over Southern Africa,* Phd Dissertation, University of the Witwatersrand, Johannesburg

Piketh, S.J., R.J. Swap, W. Maenhaut, H.J. Annegarn, and P. Formenti, 2002: Chemical Evidence of Long-Range Atmospheric Transport over Southern Africa, *Journal of Geophysical Research*, **07 (D24)**, 4817, (DOI: 10.1029/2002JD002056)

Pilinis, C., S.N. Pandis and J.H. Seinfeld, 1995: Sensitivity of Direct Climate Forcing by Atmospheric Aerosols to Aerosol Size and Composition, *Journal of Geophysical Research*, **100 (D9)**, 18739-18754

Pincus, R., and M.A. Barker, 1994: Effect of Precipitation on the Albedo Susceptibility of Clouds in the Marine Boundary Layer, *Nature*, **372**, 250-252

Power, H.C., 2003: The Geography and Climatology of Aerosols, *Progress in Physical Geography*, **27**, 4,502-547

Queface, A.J., 2002: *Atmospheric Aerosol Loading off the East Coast of Southern Africa*, MSc Dissertation, University of the Witwatersrand, Johannesburg

Queface, A.J., 2013: Direct Radiative Forcing by Aerosols Over Southern Africa, Phd Dissertation, University of the Witwatersrand, Johannesburg

Ramanathan, V., Crutzen, P.J., Kiehl, J.T., Rosenfeld, D., 2001: Aerosols, climate and the hydrological cycle, *Science*, **294**, 2119-2124

Ramanathan, V., Bates, T.S., Hansen, J.E., Jacob, D.J., Kaufman, Y.J., Penner, J.E., Prather, M.J., Schwartz, S.E., and Seinfeld, J.H., 2002: National Aerosol-Climate

Interactions Program(NACIP) A National Research Imperative, white paper, 11 pp

Ramaswamy, V., O. Boucher, J. Haigh, D. Hauglustaine, J.M. Haywood, G. Myhre, T. Nakajima, G.Y. Shi, and S. Solomon, 2001: *Radiative Forcing of Climate Change, in Climate Change 2001: The Scientific Basis – Contribution of WGI to the Third Assessment Report of the IPCC*, edited by J.T. Houghten et al., Cambridge University Press, New York

Reck, R.A., 1975: Aerosols and Polar Temperature Changes, *Science*, **188**, 728-730

Regayre, L.A., K.J. Pringle, B.B.B. Booth, L.A. Lee, G.W. Mann, J. Browse, M.T. Woodhouse, A. Rap, C.L. Reddington and K.S. Carslaw, 2014: Uncertainty in the Magnitude of Aerosol-Cloud Radiative Forcing over Recent Decades, *Geophysical Research Letters*, **41**, 9040-9049

Reid, J.S., P.V. Hobbs, R.J. Ferek, D.R. Blake, J.V. Martins, M.R. Dunlap, C. Liousse, 1998: Physical, Chemical and Optical Properties of Regional Hazes dominated by smoke in Brazil, *Journal of Geophysical Research*, **103**, 32,059-31,080.

Remer, L.A., D. Tanre, Y.J. Kaufman, C. Ichoku, S. Mattoo, R. Levy, D.A. Chu, B. Holben, O. Dubovik, A. Smirnov, J.V. Martins, R.-R. Li, Z. Ahmad., 2002: Validation of MODIS Aerosol Retrieval over Ocean, *Geophysical Research Letters*, **29(12)**, 8008, (DOI: 10.1029/2001GL013204)

Rosenfeld, D., 2000: Suppression of Rain and Snow by Urban and Industrial Air Pollution, *Science*, **287**, 1793-1796

Rosenfeld, D., and W. Woodley, 2001: Pollution and Clouds, *Physics World*, 33-37

Rosenfeld, D., 2006: Aerosol, Clouds and Climate, *Science*, **312**, 10.1126/Science.1128972

Ross, J.L., P.V. Hobbs, and B. Holben, 1998: Radiative Characteristics of Regional Hazes Dominated by Smoke from Biomass Burning in Brazil: Closure Tests and Direct Radiative Forcing, *Journal of Geophysical Research*, **103** (D24), 31,925-31,941

Ross, K.E., 2003: *Aerosol Cloud Interactions over Southern Africa*, Phd Dissertaion, University of the Witwatersrand, Johannesburg

Ross, K.E., Piketh, S.J., Bruintjes, R.J., Burger, R.P, Swap, R.J.and Annegarn, H.J., 2003: Spatial and Seasonal Variations in CCN relationship over Southern Africa, *Journal of Geophysical Research*, **108**

Satheesh, S.K., and Ramanathan, V., 2000: Larger Differences in Tropical Aerosol Forcing at the Top of the atmosphere and Earth's Surface, *Nature*, **405**, 60-63

Sato, M., Hansen, J., Koch, D., Lacis, A., Ruedy, R., Dubovik, O., Holben, B.N., Chin, M., Novakov, T.: 2003, Global Atmospheric Black Carbon Inferred from AERONET, *Proceedings of the National Academy of Sciences of the USA*, **100**, 6319-6324

SANRAL, Botha, H., 2009: South African National Roads Agency Limited: Traffic Count Information Mega Yearbook

SANRAL, Botha, H., 2010: South African National Roads Agency Limited: Traffic Count Information Mega Yearbook

Schmid, B., D.A. Hegg, J. Wang, D. Bates, J. Redemann, P.B. Russell, J.M. Livingstone, H.H. Jonsson, E.J. Welton, J.H. Seinfeld, R.C. Flagan, D.S. Covert, O. Dubovik, A. Jefferson, 2003: Column Closure Studies of Lower Tropospheric Aerosol and Water Vapour During ACE-Asia using Airborne Sun Photometery and Airborne and in Situ and Ship-based Lidar Measurements, *Journal of Geophysical Research*, **108 (D23)**, 8656, (DOI:10.1029/2002JD003361)

Seinfeld, J.H. and Pandis, S.N., 2006: *Atmospheric Chemistry and Physics: From Air Pollution to Climate Change*, John Wiley and Sons, New Jersey

Shindell, D., and Faluvegi, G., 2009: Climate Response to Regional Radiative Forcing during the 20th Century, Nature Geoscience, 2, 294-300

Smirnov, A., B.N. Holben, O. Dubovik, N.T. O'Neill, L.A. Remer, T.F. Eck, I. Slutsker, and D. Savoie, 2000a: Measurement of Atmospheric Optical Parameters in US Atlantic Coast Sites, Ships and Bermuda during TARFOX, *Journal of Geophysical Research*, **105 (D8)**, 9887-9901

Stein, D.C., Swap, R.J., Greco, S., Piketh, S.J., Macko, S.J., Doddridge, B.G., Elias, T., and Bruintjes, R.T., 2003: Haze Layer Characterization and Associated

Meteorological Controls Along the Eastern Coastal Region of Southern Africa, Journal of Geophysical Research, **108** (DOI 10.1029/2002JD003237)

Sullivan, R.C., R.C. Levy, S.C. Pryor, 2015: Spatiotemporal Coherence of Mean and Extreme Aerosol Particle Events Over Eastern North America as Observed from Satellite, *Atmospheric Environment*, **112**, 126-135

Swap, R.J., H.J. Annegarn, J.T. Suttles, M.D. King, S. Platnick, J.L. Privette, and R.J. Scholes, 2003: Africa Burning: A Thematic Analysis of the Southern African Regional Science Initiative (SAFARI-2000), *Journal of Geophysical Research*, **108 (D13)**, 8465, (DOI:10.1029/2003JD003747)

Terblanche, A.P.S., Nel, C.M.E., Opperman,L., and Nyikos, H., 1993a: Exposure to air pollution from transitional household fuels in a South African Population. *Journal of Exposure Analysis and Environmental Epidemiology,* 3 (1): 15-22.

Tesfaye, M., V. Sivakumar, J. Botai, and G. Mengistu Tsidu, 2011: Aerosol Climatology over South Africa Based on 10 Years of Multiangle Imaging Spectroradiometer (MISR) data, *Journal of Geophysical Research*, **116**, D20216, (DOI: 10.1029/2011JD016023)

Twomey, S.A., 1974: Pollution and the Planetary Albedo, *Atmospheric Environments*, **8**, 1251-1256, Pergamon Press, Great Britain

Twomey, S.A., 1977: *Atmospheric Aerosols*, Elsevier Scientific Publication Company, Amsterdam

Twomey, S.A., M. Piepgrass, and T.L. Wolfe, 1984: An Assessment of the Impact of Pollution on Global Cloud Albedo, *Tellus*, **36**, 356-366

Tyson, P.D., 1986: Climate Change and Variability in southern Africa, Oxford University Press, Cape Town

Tyson, P.D., Garstang, M., Swap, R.J., Kallberg, P. and Edwards, M., 1996: An air transport climatology for subtropical Southern Africa, *International Journal of Climatology*, **16**, 265-291

Tyson. P.D., Garstang, M., Swap, R.J., Browell, E.V., Diab, R.D. and Thompson, A.M., 1996b: *Transport and Vertical Structure of Ozone and Aerosol Distributions Over*

southern Africa, J.S. Levine (ed.), Biomass Burning and Global Change, MIT Press, Cambridge, 403-421.

Tyson, P.D., 1997: Atmospheric Transport of Aerosols and Trace Gases Over Southern Africa, *Progress in Physical Geography*, **21**, 79-101.

Tyson, P.D. and D'Abreton, P.C., 1998: Transport and Recirculation of Aerosols off Southern Africa-Macroscale Plume Structure, *Atmospheric Environment*, **32,** 1511-1524

Tyson, P.D. and Preston-Whyte, R.A., 2000: *The Weather and Climate of Southern Africa*, Oxford University Press, South Africa

Van de Hulst, H.C., 1957: *Light Scattering by Small Particles*, John Wiley & Sons, Inc., New York

Venter, A.D., V. Vakkari, J.P. Beukes, P.G. van Zyl, H. Laakso, D. Mabaso, P. Tiitta, M. Josipovik, M. Kulmala, J.J. Piennaar, L. Laakso, 2012: An Air Quality Assessment in the Industrialised Western Bushveld Igneous Complex, South Africa, South African Journal of Science, 108 (9/10).

Wang, K., Dickinson, R.E., Liang, S., 2009: Clear Sky Visibility Has Decreased Over Land Globally from 1973 to 2007, *Science*, **323**, 1468, (DOI:10.1126/Science.1167549)

Watson, J.G., and Chow, J.C., 1994: Clear Sky Visibility as a Challenge for Society, *Annua. Rev. Energy Environment*, **19**, 241-266

Wilson, D., 2011: *Aerosol Optical Properties in the South Atlantic Ocean*, MSc Dissertation, University of the Witwatersrand

Xin, J., S. Wang, Y. Wang, J. Yuan, W. Zhang, and Y. Sun, 2005: Optical Properties and Size Distribution of Dust Aerosol over the Tengger Desert in Northern China, *Atmospheric Environment*, **39**, 5971-5978

Yum, S.S. and J.G. Hudson, 2001: Vertical Distribution of Cloud Condensation Nuclei Spectra Over the Springtime Arctic Ocean, *Journal of Geophysical Research*, **106**, 15045-15052